Microglial Signaling in the Spinal Cord after Peripheral Nerve Injury

Brendan Smith

Submitted in partial fulfillment of the
requirements for the degree of
Doctor of Philosophy
in the Graduate School of Arts and Sciences

COLUMBIA UNIVERSITY

2019

ABSTRACT

Microglial Signaling in the Spinal Cord after Peripheral Nerve Injury

Brendan Smith

Injuries to the peripheral nervous system rank among the most common causes of chronic neuropathic pain. Afflicting millions of people for months or even years, symptoms of this condition have proven difficult to treat clinically. A thorough understanding of the pathophysiological changes induced by such nerve lesions is essential to the development of more efficient therapeutic options.

Peripheral nerve injury induces a robust and tightly regulated innate immune response in the dorsal horn of the spinal cord. The precise molecular mechanisms regulating the spatiotemporal dynamics and functional impact of the response remain incompletely understood. Preclinical evidence suggests mitigating this immune response can have a significant therapeutic benefit in the treatment of neuropathic pain, however these findings have yet to be clinically validated.

To elucidate the mechanisms regulating the spinal immune response, we used a mouse model of partial sciatic nerve injury exclusively in male adult (2-3-month-old) mice. The spared nerve injury (SNI) model employed throughout our studies induces robust, persistent neuropathic pain-like behavior.

We established a time course for the spinal immune response to SNI and used mRNA extracted from the ipsilateral dorsal horn of lumbar spinal cord segments L4 and L5 to analyze changes in the transcriptome at the peak of the immune reaction 7 days after nerve lesion. We

discovered upregulation of multiple elements of the triggering receptor expressed on myeloid cells 2 (Trem2) pathway. Trem2 is considered a regulator of toll-like receptor signaling in innate immune cells. It also promotes microglia-mediated phagocytosis in the central nervous system. Recent work from our lab has established neuronal apoptosis in the ipsilateral dorsal horn after SNI as an essential mechanism leading to the development of chronic neuropathic pain-like behavior. We used TUNEL staining of L4 spinal cord sections to compare the clearance of apoptotic cell profiles in $Trem2^{-/-}$ mice to wild-type littermates and discovered a key role for Trem2 in the clearance of apoptotic cells after SNI.

We further used genetic deletion of Trem2 as well as administration of a Trem2 agonist in C57Bl/6 mice to assess the impact of Trem2 signaling on both the spinal immune response and neuropathic pain-like behavior after SNI. Neither removal nor augmentation of Trem2 signaling significantly affected the development of neuropathic pain-like behavior.

Utilizing flow cytometry, we also evaluated the cellular composition of the spinal immune response. We found no evidence that monocytes from the peripheral circulation invade the spinal cord after SNI, as has been previously suggested. These findings were corroborated by immunohistochemical analysis of spinal cord sections from transgenic mice that express distinct fluorescent proteins in their monocyte and microglia cell populations.

To better understand the different mechanisms modulating the spinal immune response, we further examined several transcriptionally regulated signaling pathways. We achieved the greatest reduction of mechanical allodynia in nerve-lesioned mice treated with a P2x4r antagonist. Surprisingly, the removal of fractalkine (Cx3cl1) signaling, another prominent chemokine signaling pathway in microglia, had no significant impact on either the spinal immune response or

mechanical allodynia after SNI. Reducing the number of spinal microglia by blocking Csf1r activation did not prevent the development of mechanical allodynia after SNI either.

Our findings reveal a more nuanced concept of microglial activation after nerve injury. The impact on neuropathic pain-like behavior and phagocytosis appear to be regulated by pathways that differ from those controlling immune cell recruitment and global activation. These findings provide a greater understanding of the complex mechanisms governing microglial function and offer new insight into molecular targets essential to the development of more efficient treatment options for neuropathic pain.

TABLE of CONTENTS

List of Tables and Figures……..iii

Abbreviations…..……....vi

Acknowledgements…….ix

Dedication…….xiii

Chapter 1: Introduction……1

Neuropathic pain……...1

Experimental models of neuropathic pain……...2

The immune response to peripheral nerve injury……4

Chapter 2: Trem2-mediated phagocytosis in the spinal cord after peripheral nerve injury

Background and Significance…….9

Nerve injury-induced apoptosis in the spinal cord……12

Trem2 in neurodegenerative disease…….16

Results……...18

Indicators of cell damage and phagocytosis……..22

Trem2-dependent clearance of apoptotic cells after SNI……...27

Trem2 activation does not modulate neuropathic pain-like behavior……...29

Discussion…….33

Chapter 3: Cellular components and chemokine regulation of the spinal immune response to SNI

Background and Significance……...36

Results……...40

The spinal immune response consists primarily of resident microglia…….40

Fractalkine signaling is not a critical modulator of neuropathic pain…….…..43

Reducing microglia does not prevent the development of neuropathic pain……46

Blockade of microglial P2x4r signaling mitigates neuropathic pain……49

Discussion…….51

Chapter 4: Conclusions and Research Outlook……...56

Materials and Methods……..62

References…….77

LIST of TABLES and FIGURES

CHAPTER 1

Table 1: Efficacy of commonly used pharmacotherapies for the treatment of neuropathic pain (Binder et al, 2016)……...2

Figure 1.1: Schematic of the spared nerve injury (SNI) model of neuropathic pain (Inquimbert et al, 2018)……3

Figure 1.2: Nerve injury-induced microglial activation in the mouse spinal cord ……..…...5

Figure 1.3: Impact of decreased Kcc2 expression on neuronal inhibition (Kahle et al, 2014)……6

Figure 1.4: Proposed mechanism of enhanced Kcc2-mediated chloride extrusion (Kahle et al, 2014)……7

CHAPTER 2

Figure 2.1: Trem2 forms a signaling complex with Dap12 at the plasma membrane (Ulrich et al, 2017)……..….10

Figure 2.2: Trem2-Dap12 mediated inhibition of Tlr signaling (Turnbull and Colonna, 2007)……11

Figure 2.3: NMDAR-mediated glutamatergic transmission causes nerve injury-induced apoptosis (Inquimbert et al, 2018)……..13

Figure 2.4: Eliminating functional NMDARs in the dorsal horn blocks the transition from acute to chronic neuropathic pain (Inquimbert et al, 2018)…….15

Figure 2.5: Time course of the spinal immune response to SNI……19

Figure 2.6: SNI induces a marked upregulation of genes associated with microglial activity…..20

Figure 2.7: Pathway analysis of SNI-induced transcriptional changes……..21

Figure 2.8: Upregulation of toll-like receptor signaling molecules……..….22

Figure 2.9: SNI induces the upregulation of Trem2 and associated signaling molecules……..24

Figure 2.10: Trem2 is expressed in microglia…….……...26

Figure 2.11: Trem2 mediates the clearance of apoptotic cell profiles……....28

Figure 2.12: Time course of the spinal immune response to SNI in $Trem2^{-/-}$ mice…….……...30

Figure 2.13: Trem2 deletion does not affect SNI-induced mechanical allodynia……...31

Figure 2.14: Trem2 activation does not prevent the development of neuropathic pain-like behavior after SNI……..32

CHAPTER 3

Figure 3.1: Schematic representation of ATP-induced CatS release, resulting in the cleavage of membrane-bound FKN (Clark et al, 2012)……..38

Figure 3.2: SNI does not lead to invasion of $Ccr2^{+}$ monocytes into the ipsilateral dorsal horn in *Cx3cr1*$^{+/GFP}$-*Ccr2*$^{+/RFP}$ mice……40

Figure 3.3: Differentiation of spinal immune cells by flow cytometry…….……42

Figure 3.4: Upregulation of chemokine signaling molecules…….43

Figure 3.5: Disruption of fractalkine signaling does not alter the spinal immune response……44

Figure 3.6 Mechanical allodynia after SNI develops independently of fractalkine signaling…….45

Figure 3.7: PLX5622 depletes resident microglia in the spinal cord of uninjured mice……..46

Figure 3.8: PLX5622 prevents microglial activation after SNI……..……47

Figure 3.9: Depletion of microglia via PLX5622 does not reduce mechanical allodynia after SNI…….48

Figure 3.10: Blocking P2x4r signaling mitigates neuropathic pain-like behavior……....50

ABBREVIATIONS

Aβ	amyloid beta
AD	Alzheimer's disease
AMPAR	α-amino-3-hydroxy-5-methyl-4-isoxazolepropionic acid receptor
ApoE	apolipoprotein E
ATP	adenosine triphosphate
Bdnf	brain-derived neurotrophic factor
BSCB	blood-spinal cord barrier
C/EBP-α	CCAAT/enhancer-binding protein-α
CatS	cathepsin S
Cd11b	cluster of differentiation molecule 11b (also integrin alpha M, Itgam, macrophage-1 antigen, Mac-1, OX-42)
Clec5a	C-type lectin receptor 5a (also myeloid Dap12-associating lectin 1, Mdl-1)
CNS	central nervous system
Csf1	colony stimulating factor 1
Csf1r	colony stimulating factor 1 receptor
DAMPs	damage-associated molecular patterns
Dap12	DNAX-activating protein of 12 kDa (also tyrosine kinase-binding protein, Tyrobp)
DAPI	4',6-diamidino-2-phenylindole
DTR	diphtheria toxin receptor
EAE	experimental autoimmune encephalitis
FC	fold change

FKN	fractalkine
GABA	γ-aminobutyric acid
GFP	green fluorescent protein
GO	gene ontology
HSP	heat shock protein
IASP	International Association for the Study of Pain
Iba1	ionized calcium binding adaptor molecule 1 (also allograft inflammatory factor 1, Aif1)
IL	interleukin
Irf8	interferon regulatory factor 8
ITAM	immunoreceptor tyrosine activation motif
KO	knockout
LPS	lipopolysaccharide
LTP	long-term potentiation
mRNA	messenger ribonucleic acid
MyD88	myeloid differentiation primary response 88
NF-κB	nuclear factor κB
NMDAR	N-methyl-D-aspartate receptor
NNT	number needed to treat
NO	nitric oxide
P2x4r	P2x purinoceptor 4
p38 MAPK	p38 mitogen-activated protein kinase
PAMPs	pathogen-associated molecule patterns
PNL	partial nerve ligation

PSNL	partial sciatic nerve ligation
RFP	red fluorescent protein
sEPSCs	spontaneous excitatory post-synaptic currents
sFKN	soluble fractalkine
SNI	spared nerve injury
SNT	spinal nerve transection
Syk	spleen tyrosine kinase
TGF-β	transforming growth factor beta
Tlr	toll-like receptor
TM	tamoxifen
TNF-α	tumor necrosis factor α
Trem2	triggering receptor expressed on myeloid cells 2
TRIF	TIR-domain-containing adaptor-inducing interferon-β
TrkB	tyrosine receptor kinase B

ACKNOWLEDGEMENTS

As anyone who has gone through graduate school can tell you, it truly takes a village. There are many people to whom I owe my sincerest thanks and deepest gratitude for making this endeavor possible.

First and foremost, I must thank my mentor, Joachim Scholz. I can genuinely say that I have never been more intellectually challenged and motivated than during my years under his tutelage. The countless hours spent discussing all the different ways to approach science and the research we have undertaken over the years have been invaluable, both professionally and personally. I feel that my appreciation for neuroscience, immunology and the vast overlapping space in between these research realms has not only amplified, but really changed the way I see the world around me. I have always appreciated other people who enjoy rigorous, fact-based debate and for this, Joachim's office door was (literally) always open. His expertise and guidance over the years have been essential to my development as a scientist and my growth as a person and for that I am extremely grateful.

I must also thank all the members of the Scholz lab who have made this research possible and my time at Columbia so memorable. John Whang is not only a brilliant colleague and coworker, but also an incredible friend and one of the best people I have ever had the good fortune of working alongside. Martin Moll, Chi-Kun Tong, Fang Yang, Zafeer Baber, Jon Shintaku, Samuel Mouyal and Anisa Seenauth have all been integral to the success of the Scholz lab and I want to thank them all for their contributions to this work and the field of neuropathic pain research in general.

As a student in the Department of Pharmacology, I must also thank everyone in the department for making my time in graduate school the life-changing experience that it has been. Karen Allis is an administrative force to be reckoned with and every student who has come through the department owes her an enormous debt of gratitude. Thank you to Susan Steinberg, Michael Rosen, Neil Harrison, Rich Robinson, Robert Kass and Dan Goldberg for developing, directing and maintaining this program.

In the same vein, I must also acknowledge the incredible support I have received from the Department of Anesthesiology at the Columbia University Medical Center. Drs. Margaret Wood, Ansgar Brambrink and Charles Emala have given me a second home at Columbia and I could not be more grateful for their continual guidance and assistance throughout my time in graduate school.

I must also thank the members of my thesis advisory committee: Alice Prince, David Sulzer and Neil Harrison. Thesis committee meetings can be an incredibly stressful and difficult experience for many graduate students, but all three members of my committee have been nothing but enormously supportive from the very beginning. Our discussions at every juncture were invaluable, exciting and really helped shape this research into what it has become.

Additionally, I need to thank Nigel Bunnett and the members of his lab, particularly Dane Jensen and Rocco Latorre for opening their doors and taking me in during my final months at Columbia. They are all exceptional scientists, but the welcome I have received in just the few months I have worked closely with them has shown me what great people they are as well and for that, I am most grateful.

I also want to thank Amy McDermott and Damian Williams for the countless hours during my first few years with the Scholz lab spent discussing and analyzing all kinds of scientific data

during our lab meetings. Neither of them had any kind of professional obligation to partake in our discussions but did so anyway and brought their wealth of experience and expertise to our group in a way few others have.

Ira Schieren and Theresa Swayne also deserve my utmost gratitude for their help over the years. Ira knows more about flow cytometry than anyone I have ever met and taught me everything I know about the process and equipment involved. Theresa Swayne is a microscopy magician and has never hesitated to help anyone with anything, no matter how many times she has been asked the same question in the past. For all of their hard work and dedication, I thank them both.

All of our collaborators have been exceptional as well. Thank you to Marco Colonna, Yaming Wang and Susan Gilfillan at Washington University in St. Louis for their assistance in acquiring and maintaining the Trem2 knockout mouse line. Thank you also to Hynek Wichterle, Oleg Butovksy, Jessica Hamerman, Plexxikon, Inc. and Nippon Chemipar for their time, effort and resources. The staff at the Columbia Genome Center was also integral to the success of our RNA sequencing experiment early on so I must thank them for their contribution to this work as well.

I also have to thank all of our old neighbors at the Columbia Stem Cell Core, Barbara Corneo, Alejandro Diaz, Kate Oliver, Dario Sirabella and Achchhe Patel. They are all great scientists, but more importantly, exceptional people who made coming to work enjoyable. They always greeted the members of our lab with arms wide open and for that I'm very grateful.

As most would agree, success in the lab and at work also relies heavily on a structurally sound support system at home and elsewhere. The friendships I have cultivated during my time at Columbia have changed my life in more ways than I can count. These people have supported and encouraged me at some of the most difficult moments of my life and there is simply no way for

me to ever repay them. Mina Lee is and has always been the best friend anyone on this planet could ever hope for and I would simply not be here without her. Kyrie Pappas and Roshan Ahmed are two of the best people I know and their friendship and support during graduate school have made me a better scientist and a better feminist. Together, we will bring down the patriarchy. Giang Luc, Kiyanna Williams, Emily Harned and Jess Choi continue to be some of the most brilliant and brilliantly hilarious human beings I have ever known; they never fail to make me laugh or put me in my place and they quite simply deserve the best this world has to offer. Kevin Lee Yi has taught me more about myself and what it means to navigate the absurdity of this world than I ever thought possible. He has challenged me in more ways than I can articulate, encouraged me at my most insufferable and, more than anyone I have met in New York, made me who I am today.

Finally, I must thank my family. Words will never be capable of expressing how grateful I am to have the family that I do. My brilliant mother has motivated me to be the best possible version of myself for as long as I can remember. My father has relentlessly inspired me to wholeheartedly embrace my inner nerd and to never miss an opportunity to laugh as long and as frequently as possible. My brother has taught me that there is no hope more promising than that of the next generation. Seeing him grow into the man that he is today has been one of the greatest privileges of my life and I am so genuinely excited to see what the future holds for him.

In this life, we are nothing if not the quality of the company that we keep. And so, to everyone that has made this possible, thank you.

DEDICATION

This dissertation is dedicated first and foremost to my parents and my brother.

As easily the most difficult member of the family, I would be remiss in thinking that this body of work represents anything more substantial than the collective efforts of 3 people who have demonstrated unfathomable strength of character by simply tolerating my existence.

I would also like to dedicate this to my Uncle John.

I know he would have wanted to be here…most of all, for the celebration.
But his life and the loving openness with which he lived it will forever be an inspiration.

Cheers to you, John.

CHAPTER 1

Introduction

Neuropathic Pain

Our ability to detect potentially harmful and damaging stimuli is essential to human survival. The sensation of pain, transmitted from somatosensory nerve fibers to the dorsal horn of the spinal cord and then propagated to sensory processing centers in our brain, alerts us to the presence of noxious stimuli in internal organs or our surrounding environment. Dysfunction or damage to this tightly regulated system of nociception can have severe consequences that fundamentally alter the way we experience pain and even normally painless sensations like light touch.

Neuropathic pain is caused by a lesion or disease affecting the somatosensory nervous system (Finnerup et al, 2016) and affects 7-10% of the general population (Bennett et al, 2012; van Hecke et al, 2014; DiBonaventura et al, 2017). Common causes include diabetic polyneuropathy, herpes zoster and postherpetic neuralgia, trigeminal and other cranial neuralgias, cancer chemotherapy, degenerative changes of the spine leading to lumbar radiculopathy and nerve trauma. Clinical manifestations of neuropathic pain involve hyperalgesia (heightened or exaggerated pain in response to something that is typically only mildly painful) and allodynia (pain in response to a normally innocuous stimulus). Neuropathic pain is difficult to address. The number of patients needed to be treated (NNT) before one experiences a reduction in pain by at least 50% ranges from about 3.6 to 10.6 for the commonly prescribed therapies (see Table 1 from Binder et al, 2016).

	Number of trials	Number of patients	Number needed to treat [95% CI]
Tricyclic antidepressants	15	948	3.6 [3.0; 4.4]
Serotonin-norepinephrine reuptake inhibitors	10	2541	6.4 [5.2; 8.4]
Pregabalin	25	5940	7.7 [6.5; 9.4]
Gabapentin	14	3503	7.2 [5.9; 9.1]
Tramadol	6	741	4.7 [3.6; 6.7]
High-potency opioids	7	838	4.3 [3.4; 5.8]
Capsaicin 8% patch*	6	2073	10.6 [7.4; 18.8]

Table 1. Efficacy of commonly used pharmacotherapies for the treatment of neuropathic pain (adapted from Binder et al, 2016).

Experimental models of neuropathic pain

A number of experimental models have been established to better assess the mechanisms that lead to neuropathic pain-like behavior. Rodent models of nerve injury-induced neuropathic pain are most often utilized, typically involving loose constriction, tight ligation or transection of a nerve.

While most injury models provoke at least some neuropathic pain-like behaviors that mimic clinical symptoms (such as mechanical allodynia or painful hypersensitivity to cold stimuli), those involving nerve constriction or ligation may not produce long-lasting pain reminiscent of the typically chronic disorders seen in patients (Decosterd and Woolf, 2000). We used the spared nerve injury (SNI) model, which involves a combination of ligating and transecting the peroneal and tibial branches of the sciatic nerve, leaving the innervation territory of the sural

nerve intact for behavioral testing (Fig 1.1). This model consistently produces persistent hypersensitivity in both the rat and mouse (Decosterd and Woolf, 2000; Bourquin et al, 2006). Other models have been developed to study the neurotoxic effects of chemotherapy, neuropathies associated with type 1 and type 2 diabetes and perineural inflammation.

The translational validity of these models is determined by the reproduction of clinically relevant pain hypersensitivity. Specific behavioral tests aid in the experimental evaluation of neuropathic pain-like behavior. Cold hypersensitivity, a common symptom of patients with neuropathic pain, is often tested for using acetone, a chemical that evaporates rapidly off the skin and in the process, produces a cooling sensation. Paw withdrawal is interpreted as a behavior equivalent to cold allodynia in humans. Feeling physical pain from typically innocuous mechanical stimuli (mechanical allodynia) is often measured using von Frey filaments. The filaments range in strength and are applied to the affected hindlimb. In uninjured mice, the filaments are generally innocuous until a threshold of approximately 1 g. Filaments applying greater force induce withdrawal of the hind paw. Mechanical allodynia manifests as a much lower withdrawal threshold. Other behavioral paradigms focus on heat sensitivity, which is more relevant to models of nociceptive pain, including pain after inflammation.

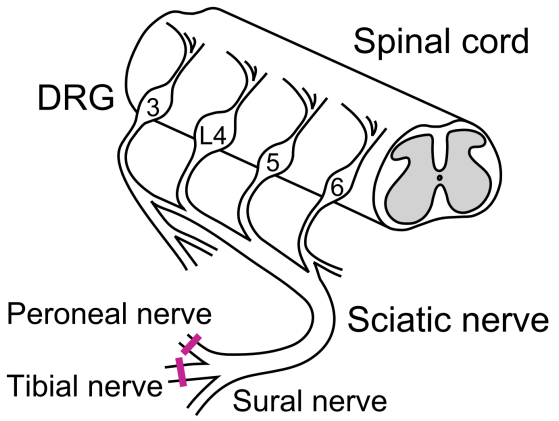

Figure 1.1: Schematic of the spared nerve injury (SNI) model of neuropathic pain. The tibial and peroneal branches of the sciatic nerve are ligated together and transected, leaving the sural nerve intact (or "spared"). Adapted from Inquimbert et al, 2018.

The immune response to peripheral nerve injury

Nerve injury induces profound changes in the excitability and connectivity of neurons both in the periphery and CNS (Woolf and Salter, 2000). Damaged nerve terminals are exposed to inflammatory mediators released by local immune cells that sensitize the neuronal membrane to nociceptive stimuli (Schäfers et al, 2003; Wolf et al, 2006). Increased firing and spontaneous activity of primary somatosensory neurons can induce activity-dependent enhancement of excitatory neurotransmission at the central terminals of damaged primary afferents, not unlike mechanisms of long term potentiation (LTP) observed in the hippocampus (Li et al, 1999; Stubhaug et al, 1997). Augmentation of nociceptive transmission is further enhanced by a reorganization of central synapses and the extension of newly formed axon terminal collaterals in superficial layers of the spinal dorsal horn (Woolf et al, 1992; Kohama et al, 2000). Immune cells, both in the damaged peripheral nerve and in the spinal cord, contribute to this process of sensitization (Scholz and Woolf, 2007). Elucidating the exact role of glia in the pathological amplification of nociceptive sensory information after nerve injury is important for developing more efficient pharmacotherapies to treat neuropathic pain.

A vivid innate immune response in the ipsilateral dorsal horn of the spinal cord is indeed a remarkably conserved phenomenon across models of peripheral nerve lesion. Topically limited to the spinal projection territory of damaged afferent nerve fibers, this pattern of neuroinflammation in commonly used models of sciatic nerve injury is concentrated in the superficial layers of the dorsal horn in lumbar segments L4 and L5. The immune response to peripheral nerve injury involves proliferation and activation of local microglia, which are considered the resident macrophages of the central nervous system (Tsuda et al, 2005; Watkins and Maier, 2003; DeLeo and Yezierski, 2001). Characterized by a sudden upregulation of key microglial activation markers

like ionized calcium-binding adaptor molecule 1 (Iba1) and cluster of differentiation 11b (Cd11b), these cells shift from their morphologically ramified "resting" state to a more amoeboid, pro-inflammatory phenotype (Fig. 1.2).

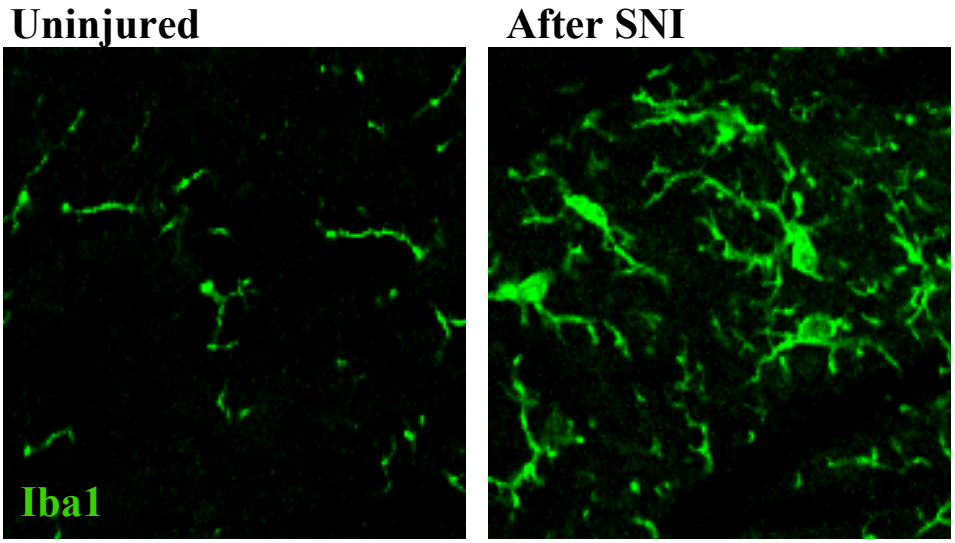

Figure 1.2: Nerve injury-induced microglial activation in the mouse spinal cord. Ipsilateral dorsal horn of the lumbar spinal cord (segment L4). Upregulation of microglial cell markers like Iba1 is accompanied by a shift in cellular morphology and transition to a pro-inflammatory phenotype (unpublished images).

The exact molecular mechanisms regulating the immune response remain incompletely understood. Toll-like receptors (Tlrs) as well as chemokines (Cx3cl1, Ccl2) and purinergic signaling have all been suggested as critical modulators of the response. Nerve injury also induces significant upregulation of colony stimulating factor 1 (Csf1), an essential microglial growth factor, in the injured afferent nerve fibers (Guan et al, 2016). Csf1 is believed to be subsequently transported centrally and released into the spinal dorsal horn (Guan et al, 2016). Studies using transgenic mice engineered to selectively prevent the injury-induced influx of Csf1 into the spinal cord show no increased microglial proliferation or immunoreactivity after nerve injury and exhibit

largely reduced neuropathic pain-like behavior (Guan et al, 2016). This Csf1-mediated immune response also comprises an upregulation of genes implicated in the development of neuropathic pain, including *Ctss*, *Irf8* and the purinergic receptor, *P2rx4* (Guan et al, 2016).

One mechanism illustrating the potential of microglia to modulate pain processing involves the release of brain-derived neurotrophic factor (Bdnf). Stimulation of microglial P2x4 receptors by ATP after peripheral nerve injury drives the increased expression and secretion of Bdnf (Tsuda et al, 2003; Ulmann et al, 2008). Bdnf activates tyrosine receptor kinase B (TrkB) on dorsal horn neurons, leading to the downregulation of potassium-chloride cotransporter 2 or Kcc2 (Coull et al, 2005). Kcc2 function is essential for spinal neurons to maintain a low intracellular concentration

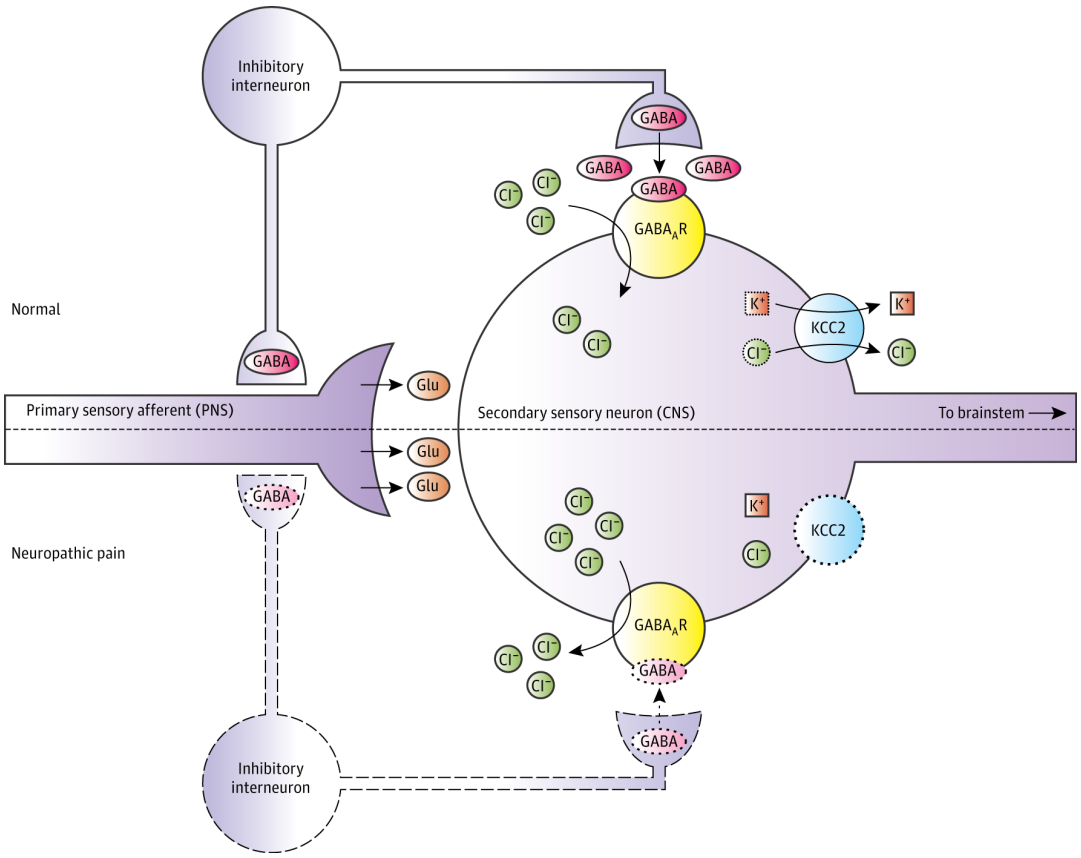

Figure 1.3: Impact of decreased Kcc2 expression on neuronal inhibition. TrkB-mediated downregulation of Kcc2 leads to an increased intracellular concentration of chloride ions. Consequently, $GABA_A$ receptor-mediated hyperpolarization, reliant on chloride ion influx, is less effective (scheme from Kahle et al, 2014).

of chloride ions (Coull et al, 2005; Rivera et al, 2002). Downregulation of Kcc2 leads to a depolarizing shift in the anion reversal potential of spinal neurons, compromising the effect of inhibitory neurotransmitters GABA and glycine. $GABA_A$ and glycine receptor activation typically allows for chloride ion influx, hyperpolarization and fast synaptic inhibition of neurons involved in pain pathways of the dorsal horn (Coull et al, 2005; see Figure 1.3). These findings have led to the development of Kcc2 enhancers as potential analgesics (Kahle et al, 2014; see Figure 1.4).

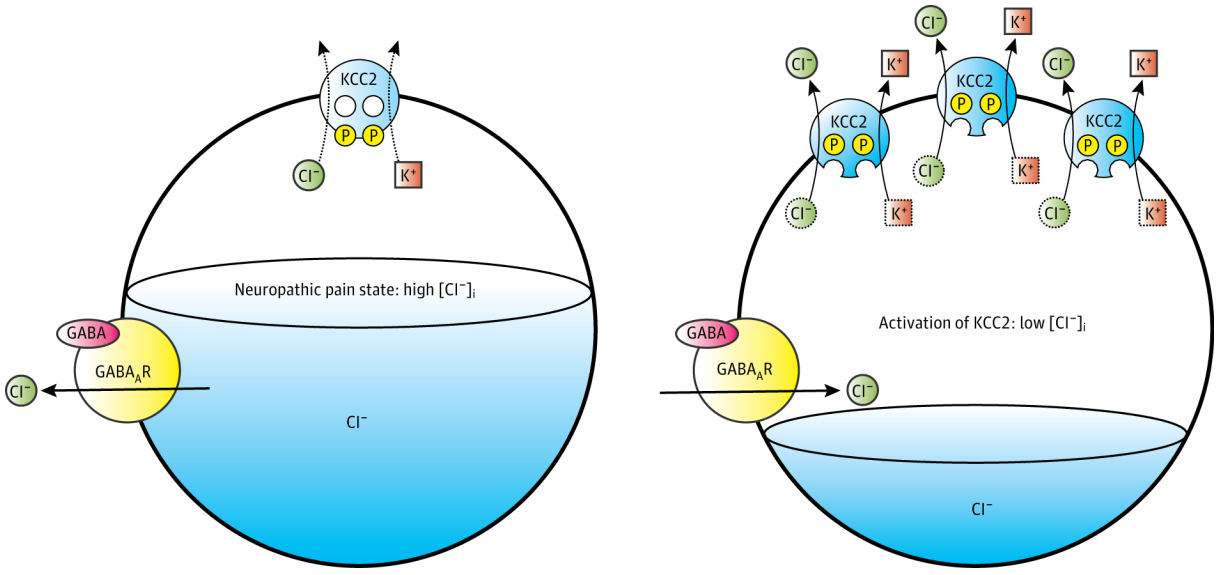

Figure 1.4: Proposed mechanism of enhanced Kcc2-mediated chloride extrusion. Enhancing neuronal chloride extrusion by increasing the expression of Kcc2 in dorsal horn neurons has the potential to restore spinal inhibition and reduce neuropathic pain (scheme from Kahle et al, 2014).

In addition to Bdnf, pro-inflammatory cytokines including interleukin (IL)-1β are known to enhance excitatory neurotransmission in dorsal horn neurons (Liu et al, 2013). Tumor necrosis factor (TNF)-α has also been shown to increase spontaneous excitatory post-synaptic currents (sEPSCs) in dorsal horn neurons (Park et al, 2011).

While traditional approaches to treating neuropathic pain have directly targeted the injury-induced changes in neuronal processing of nociceptive information, mounting evidence of neuroglial interaction suggests the spinal immune response to peripheral nerve injury may in fact play a key role in the induction of neuropathic pain. A more thorough understanding of the biological function(s) of nerve injury-induced spinal inflammation as well as the molecular mechanisms regulating the spatiotemporal dynamics and physiological impact of the response are crucial to the development of therapies targeting this process.

CHAPTER 2

Trem2-mediated phagocytosis in the spinal cord after peripheral nerve injury

Background and Significance

Inflammatory pathways regulating the spinal immune response to peripheral nerve injury are known to recognize damage-associated molecular patterns (DAMPs). Toll-like receptors, for example, bind high mobility group box 1 or Hmgb1 (Park et al, 2004; Yu et al, 2006; Yang et al, 2018) and heat shock proteins (Vabulas et al, 2002; Dybdahl et al, 2002; Asea et al, 2002).

In the context of neuropathic pain, the Tlrs identified as key regulators of nerve injury-induced microglial reactivity include Tlr2 (Kim et al, 2007), Tlr4 (Sorge et al, 2011; Bettoni et al, 2008; Piao et al, 2018) and Tlr5 (Stokes et al, 2013; Ji et al, 2018). Genetic deletion of these Tlrs provides partial reduction in both the spinal immune response and nerve injury-induced mechanical allodynia. All members of the Tlr superfamily recruit the myeloid differentiation primary response 88 (MyD88) intracellular adaptor protein to transduce their signal, except for Tlr3 which signals instead through the TIR-domain-containing adaptor-inducing interferon-β (TRIF) pathway (Yamamoto et al, 2002; Oshiumi et al, 2003; Hoebe et al, 2003; Yamamoto et al, 2003). Activation of Tlrs has been shown to induce the downstream p38 mitogen-activated protein kinase (MAPK)- and nuclear factor κB (NF-κB)-mediated transcriptional upregulation and release of numerous pro-inflammatory cytokines (Gorina et al, 2011).

Consistent with the involvement of Tlr2, Tlr4 and Tlr5, silencing MyD88 signaling (effectively targeting most Tlrs simultaneously) also decreases neuropathic pain-like behavior after peripheral nerve injury (Stokes et al, 2013; Liu et al, 2016). These findings have led

investigators to consider both endogenous and exogenous inhibition of MyD88-induced immune cell activation as a potential focus in the development of novel analgesics. In this context, the triggering receptor expressed on myeloid cells 2 (Trem2) pathway, extensively studied in macrophages as directly inhibiting lipopolysaccharide (LPS)-induced Tlr4-MyD88 signaling (Turnbull et al, 2006; Hamerman et al, 2006; Zhong et al, 2015; Zhang et al, 2017; Zhong et al, 2017), has recently emerged as a potential therapeutic target in neuropathic pain.

Trem2 is a 40 kDa transmembrane receptor containing an extracellular immunoglobulin variable (IgV) domain, a transmembrane domain and a short cytoplasmic tail devoid of any substantive signaling motifs (Paradowska-Gorycka et al, 2013). Trem2 signaling thus depends on the formation of a complex at the inner surface of the plasma membrane with its primary adaptor protein DNAX-activating protein of 12 kDa (Dap12). Upon activation of Trem2, the immunoreceptor tyrosine activation motif (ITAM) on the intracellular region of Dap12 is phosphorylated by Src family kinases (Mason et al, 2006). This phosphorylation triggers recruitment of downstream signaling proteins, including spleen tyrosine kinase or Syk (Yao et al, 2016), to regulate immune cell function (Fig. 2.1).

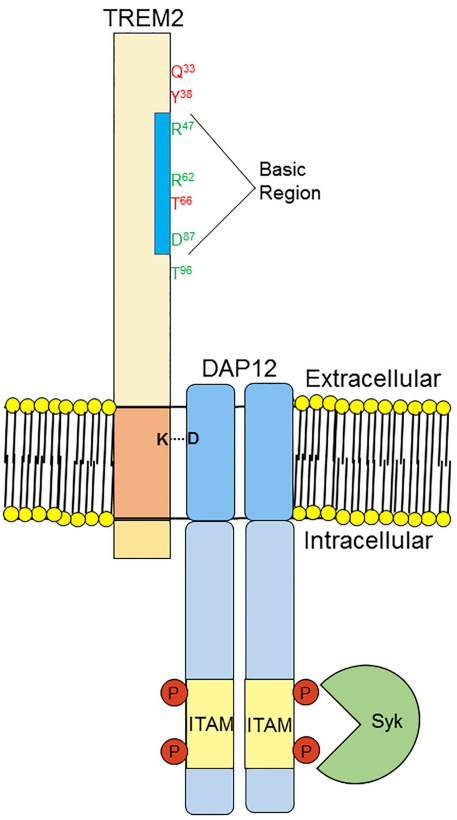

Figure 2.1: **Trem2 forms a signaling complex with Dap12 at the plasma membrane** (Ulrich et al, 2017).

Myd88-dependent activation of macrophages by Tlr agonists and the subsequent production of inflammatory cytokines is augmented in cells lacking Trem2-Dap12 signaling components (Turnbull et al, 2006; Zhong et al, 2017). Similarly, overexpression of Trem2 and

stabilization of the Trem2 signaling complex have been shown to significantly attenuate Tlr-Myd88-induced cytokine production (Zhang et al, 2017; Ren et al, 2018; Zhong et al, 2015). These findings demonstrate the ability of the Trem2-Dap12 pathway to regulate inflammatory immune responses in macrophages and microglia. Consequently, the pathway is considered, in part, a negative regulator of immune cell activation (Fig. 2.2).

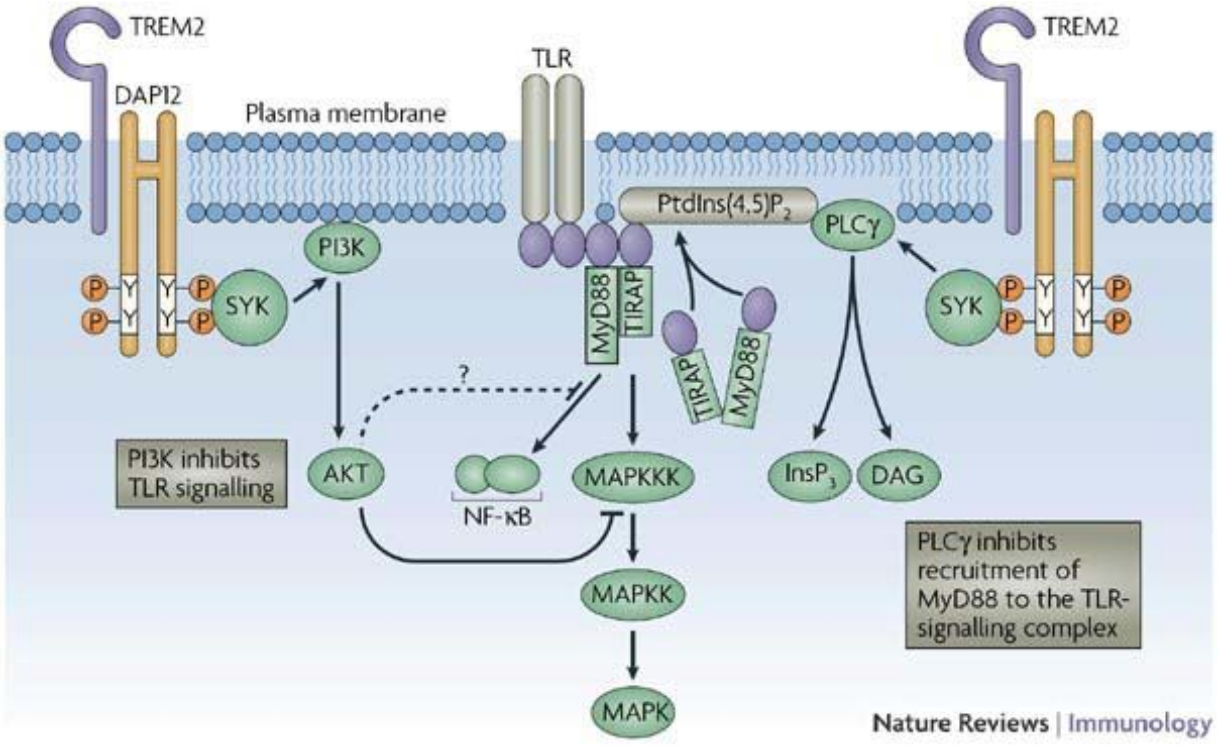

Figure 2.2: **Trem2-Dap12-mediated inhibition of Tlr signaling.** Phosphorylated Dap12 recruits Syk to the Trem2-Dap12 signaling complex, leading to the downstream disruption of MyD88-mediated Tlr signaling (Turnbull and Colonna, 2007).

Several studies have examined the role of different Tlrs in regulating the spinal immune response to peripheral nerve injury, however, the exact function of microglial Trem2 signaling as it pertains to nerve injury-induced spinal inflammation and neuropathic pain-like behavior remains unclear.

Nerve injury-induced apoptosis in the spinal cord

In the days and weeks after nerve lesion, apoptotic cell profiles also appear in the ipsilateral dorsal horn of the spinal cord (Azkue et al, 1998; Moore et al, 2002; Scholz et al, 2005). Initially considered a manifestation of microglial cell turnover (Polgár et al, 2005), it is now clear that the induction of apoptosis in fact reflects nerve injury-induced neurodegeneration (Scholz et al, 2005; Yowtak et al, 2013). I was actually involved with a study recently published by my research group which identified the underlying mechanism of neuronal cell death and determined the functional significance for the development of neuropathic pain (Inquimbert et al, 2018). We demonstrated that neurons in the ipsilateral dorsal horn undergo excitotoxic cell death after SNI and that elimination of functional NMDA receptors through conditional deletion of the essential receptor subunit *Grin1* (GluN1) prevents this loss of neurons (Figure 2.3).

Interestingly, the temporal pattern for the emergence of apoptotic profiles after SNI follows a remarkably similar time course to the spinal immune response to nerve injury (see Figure 2.3c and Figure 2.5). Furthermore, the involvement of inhibitory interneurons in this neuronal apoptosis leads to a decrease in GABAergic inhibition of pain pathways and promotes the transition from acute to chronic pain after nerve injury (Figure 2.4).

Figure 2.3

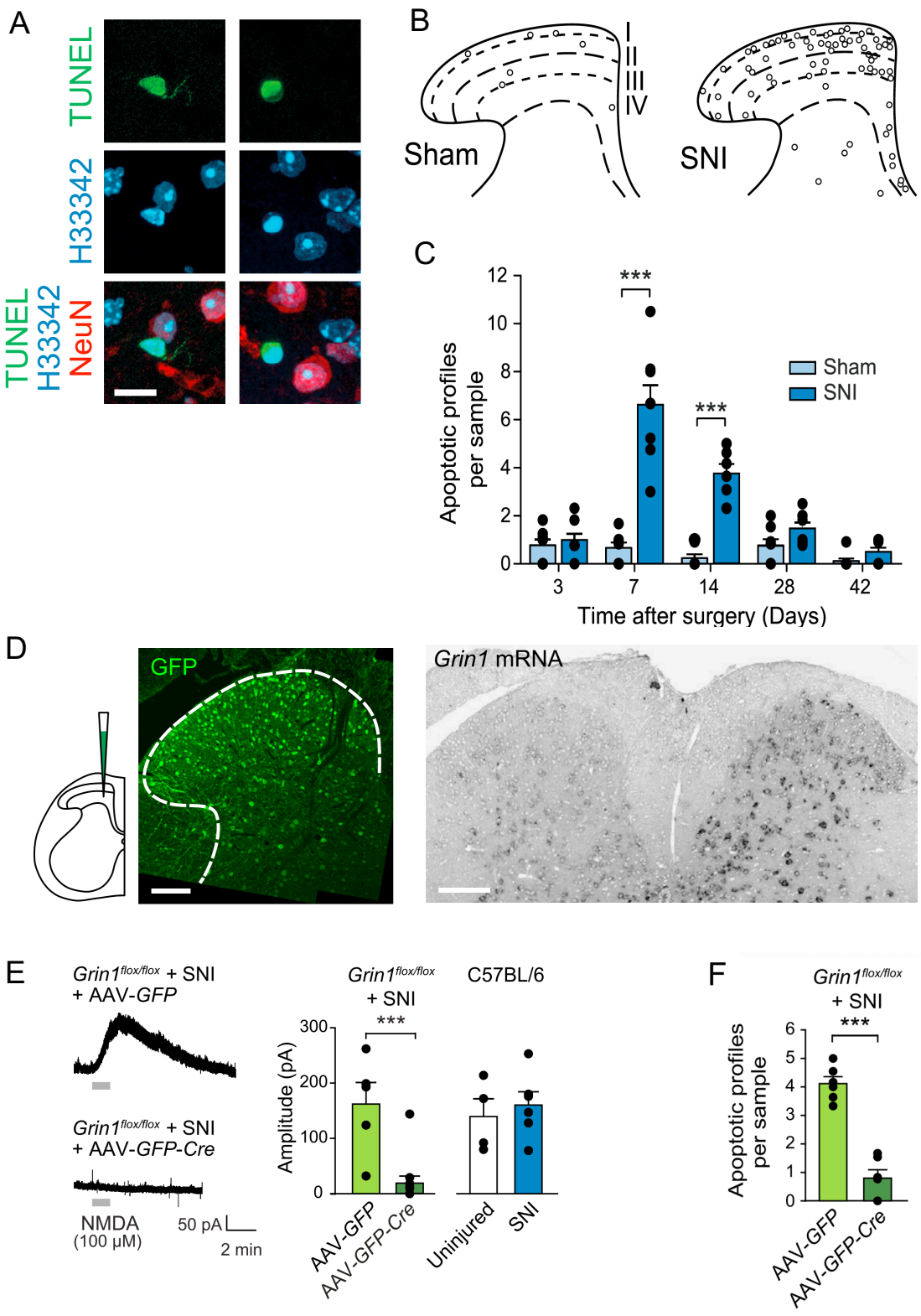
A
TUNEL
H33342
TUNEL
H33342
NeuN
B
I
II
III
IV
Sham
SNI
C
Apoptotic profiles per sample
***
***
Sham
SNI
Time after surgery (Days)
D
GFP
Grin1 mRNA
E
Grin1flox/flox + SNI + AAV-GFP
Grin1flox/flox + SNI + AAV-GFP-Cre
NMDA (100 µM)
50 pA
2 min
Grin1flox/flox + SNI
C57BL/6
Amplitude (pA)
AAV-GFP
AAV-GFP-Cre
Uninjured
SNI
F
Grin1flox/flox + SNI
Apoptotic profiles per sample
AAV-GFP
AAV-GFP-Cre

Figure 2.3: NMDAR-mediated glutamatergic transmission causes nerve injury-induced apoptosis.

(A) Apoptotic cell profiles 7 days after SNI. H33342, Hoechst 33342 (bisbenzimide). Scale bar, 10 μm.

(B) Distribution of apoptotic profiles within the dorsal horn, shown in overlays of 10 sections per Mouse (n=8 mice).

(C) Time course of apoptosis induction. Apoptotic profiles were counted in 10 sections per mouse (n=8). $p<0.001$ for surgery and time in a two-way ANOVA. ***$p<0.001$ in Sidak's test following the ANOVA.

(D) GFP expression (left) and *in situ* hybridization of *Grin1* mRNA (right) 3 weeks after injection of the vector into the left dorsal horn of the lumbar (L4) spinal cord of $Grin1^{flox/flox}$ mice eliminated NMDAR function.

(E) Excitatory currents evoked by NMDA (100 μM) in $Grin1^{flox/flox}$ mice injected with AAV8-*GFP* or AAV8-*GFP*-*Cre*. SNI was performed 2 or 3 weeks after the vector injection. Two weeks after the nerve injury, we compared current amplitudes in the dorsal horn of mice injected with AAV8-*GFP* (n=5 neurons) or AAV8-*GFP*-*Cre* (n=11). ***$p<0.001$ in Student's t test. Currents recorded in $Grin1^{flox/flox}$ mice injected with AAV8-*GFP* did not differ from those in injured C57Bl/6 mice (n=4) or C57Bl/6 mice after SNI (n=6).

(F) Apoptotic profiles 7 days after SNI in the dorsal horn of $Grin1^{flox/flox}$ mice injected with AAV8-*GFP* or AAV8-*GFP*-*Cre* (n=6 mice). ***$p<0.001$ in Student's t test.

Note: Figure components and legend adapted from Inquimbert et al, 2018.

Figure 2.4

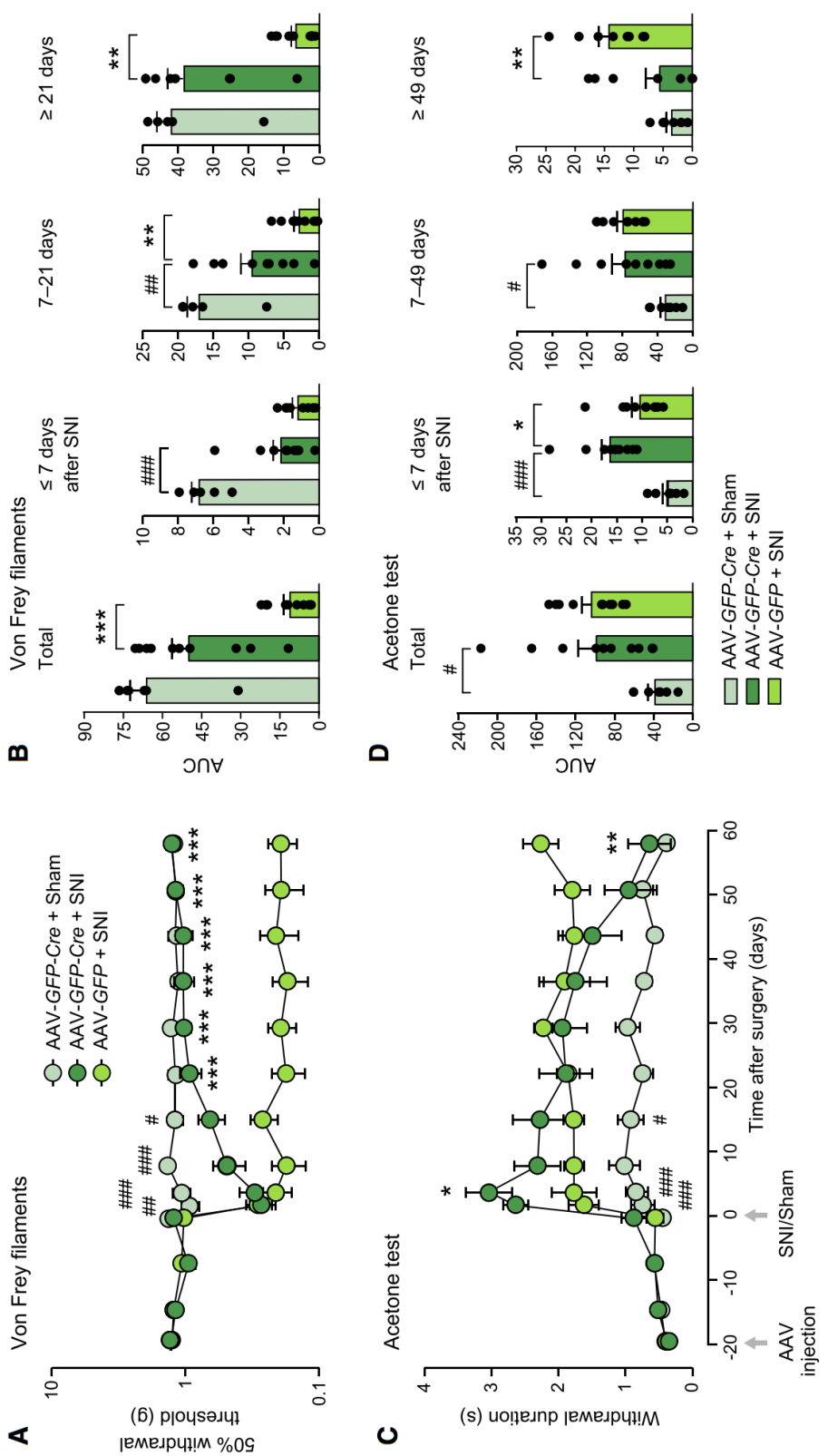
A
Von Frey filaments
50% withdrawal threshold (g)
AAV-GFP-Cre + Sham
AAV-GFP-Cre + SNI
AAV-GFP + SNI
B
Von Frey filaments
Total
≤ 7 days after SNI
7–21 days
≥ 21 days
AUC
C
Acetone test
Withdrawal duration (s)
AAV injection
SNI/Sham
Time after surgery (days)
D
Acetone test
Total
≤ 7 days after SNI
7–49 days
≥ 49 days
AUC

Figure 2.4: Eliminating functional NMDARs in the dorsal horn blocks the transition from acute to chronic neuropathic pain.

(A and C) Withdrawal responses to (A) mechanical (von Frey filaments) or (C) cold stimulation (acetone evaporation) after sham surgery (n=7 mice) or SNI (n=10) in *Grin1*$^{flox/flox}$ mice injected with AAV8-*GFP*-*Cre*, and SNI in *Grin1*$^{flox/flox}$ mice injected with AAV8-*GFP* (n=10). Behavioral outcomes were compared using two-way ANOVAs. $p<0.001$ for treatment and time in the responses to stimulation with von Frey filaments; $p<0.01$ for treatment and $p<0.001$ for time in the acetone test. Asterisks and pound signs indicate the results of Bonferroni's tests following the ANOVAs.

(B and D) Areas under the curve (AUCs) were first compared for the total test duration after SNI ($p<0.001$ for von Frey filaments, B, and acetone test, D, in one-way ANOVAs). Separately, we compared AUCs in the acute phase of the first 7 days after SNI ($p<0.001$ for both test modalities), during the transition from acute to persistent pain ($p<0.001$ for the stimulation with von Frey filaments and $p<0.05$ for the acetone test), and for persistent pain after 21 or 49 days, respectively ($p<0.001$ for von Frey filaments and $p<0.01$ for the acetone test). Asterisks and pound signs indicate the results of Tukey's tests following the ANOVAs.

*$p<0.05$, **$p<0.01$ and ***$p<0.001$ for the comparison of AAV8-*GFP*-*Cre* + SNI and AAV8-*GFP* + SNI; #$p<0.05$, ##$p<0.01$ and ###$p<0.001$ for the comparison of AAV8-*GFP*-*Cre* + Sham and AAV8-*GFP*-*Cre* + SNI. Error bars indicate SEM.

Note: Figure and legend from Inquimbert et al, 2018.

The exact relationship between this neuronal apoptosis and the spinal immune response to SNI has yet to be fully elucidated. However, microglia are the primary phagocytes responsible for the clearance of cellular debris and apoptotic cells in the CNS (Hu et al, 2015). Thus, the increase in apoptosis observed in the dorsal horn after SNI may play a role in the activation of local microglia. Trem2, in addition to its suggested immunoregulatory ability, has been implicated as a key mechanism by which microglial cells recognize and initiate phagocytosis of apoptotic neurons in the CNS (Painter et al, 2015).

Trem2 in neurodegenerative disease

Although the endogenous ligand(s) of Trem2 have yet to be precisely identified, a number of lipid and lipid-containing molecules linked to cell death, including apolipoprotein E or ApoE

(Atagi et al, 2015; Bailey et al, 2015; Krasemann et al, 2017) and phosphotidyl serine (Wang et al, 2015), have been suggested as potential binding partners. In mouse models of Alzheimer's Disease (AD), deficient recognition and clearance of amyloid beta (Aβ) fibers by microglia have been directly linked to loss-of-function mutations in microglial Trem2 (Kleinberger et al, 2014; Wang et al, 2015; Kim et al, 2017; Kober et al, 2016; Zhao et al, 2018; Zhong et al, 2018). Evidence from other disease models involving neurodegeneration including stroke (Kawabori et al, 2015) and Parkinson's Disease (Ren et al, 2018) have shown that microglial phagocytosis of apoptotic neurons is significantly attenuated when Trem2 signaling is disrupted or compromised.

Overexpression of Trem2 has been shown to simultaneously increase microglial phagocytosis and decrease the transcription of proinflammatory cytokines (Takahashi et al, 2005). Indeed, this dual ability of the Trem2 pathway to aid in the clearance of apoptotic cells and extracellular protein aggregates while suppressing inflammation has led investigators to suggest that Trem2 activation confers a neuroprotective function of microglia in the context of neurodegeneration (Jiang et al, 2016; Zhai et al, 2017; Ren et al, 2018).

The neuroprotective or homeostatic functions of spinal microglia responding to nerve injury have not been previously investigated. Hypothesizing that the spinal immune response may involve physiological components in addition to the conventionally observed inflammatory effects, we examined the regulation of Trem2 and its signaling partners after SNI. Following our recently published finding that neuronal apoptosis is a key mechanism implicated in SNI-induced persistent pain, we focused on the role that microglial Trem2 may play in the clearance of nerve injury-induced apoptotic cells in the ipsilateral dorsal horn of the spinal cord.

Results

To determine the time course of the spinal immune response to SNI, we stained spinal cord sections from lumbar segment L4 at multiple intervals after SNI for Iba1, a classical marker of microglial activation known to participate in actin bundling and membrane ruffling in activated microglia and macrophages. L4 represents the region of the spinal cord to which the lesioned afferent nerve fibers in the SNI model project and injury-induced inflammation is most pronounced. A semi-quantitative analysis of the Iba1 staining intensity showed induction of the immune response within 3 days of nerve injury (FC above uninjured controls: 1.8), a peak at 7 days after SNI (FC: 2.8) and the reversal beginning by day 14 (FC: 2.3). Sections stained at 28 days after SNI demonstrated no difference in Iba1 immunoreactivity when compared with uninjured samples (not pictured).

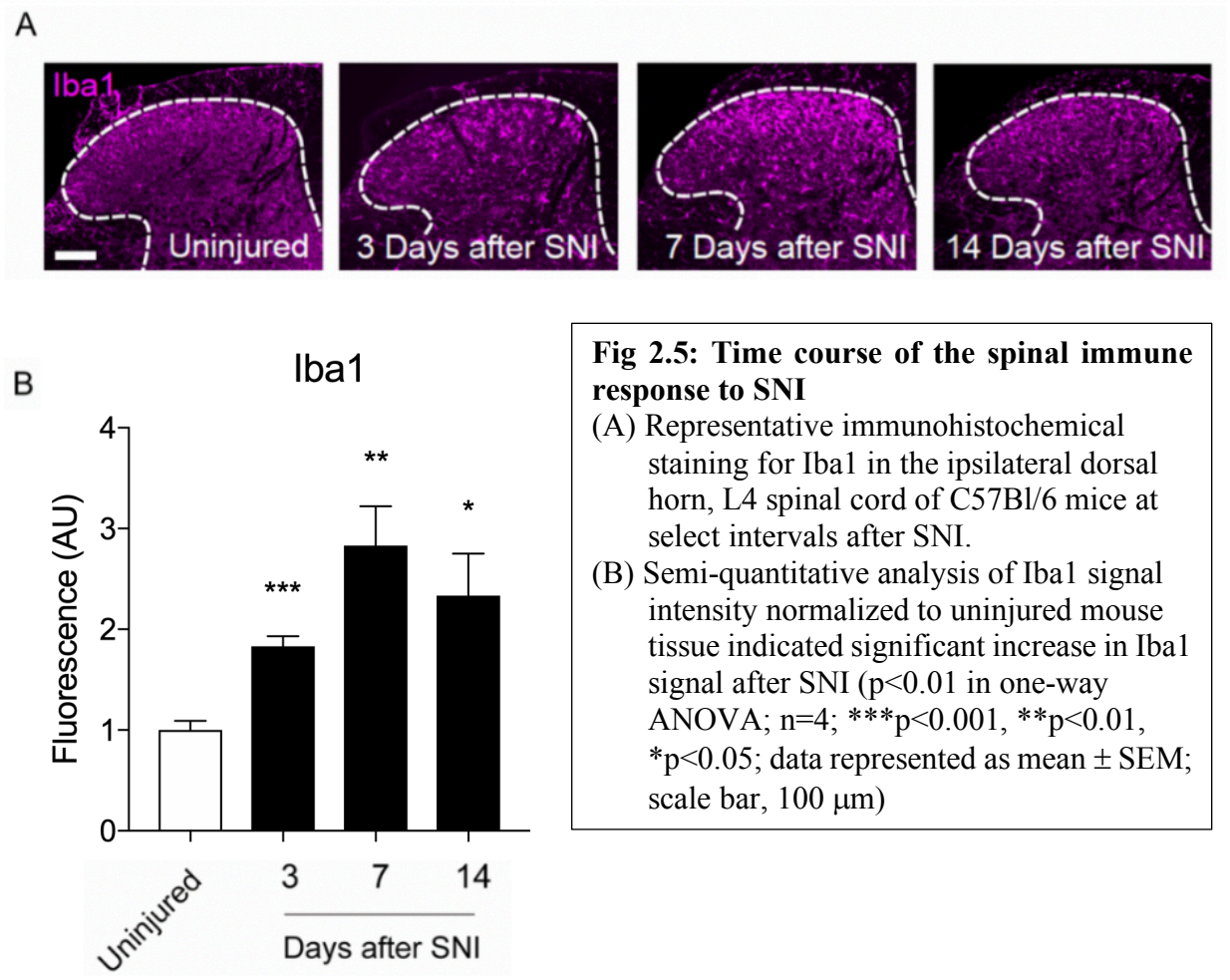

Fig 2.5: Time course of the spinal immune response to SNI

(A) Representative immunohistochemical staining for Iba1 in the ipsilateral dorsal horn, L4 spinal cord of C57Bl/6 mice at select intervals after SNI.

(B) Semi-quantitative analysis of Iba1 signal intensity normalized to uninjured mouse tissue indicated significant increase in Iba1 signal after SNI ($p<0.01$ in one-way ANOVA; n=4; ***$p<0.001$, **$p<0.01$, *$p<0.05$; data represented as mean ± SEM; scale bar, 100 μm)

To better understand the signaling pathways involved in this immune response, we conducted an unbiased transcriptome analysis at the peak of the inflammation after SNI. To this end, we sequenced mRNA isolated from the L4-L5 ipsilateral dorsal horn of the spinal cord. In collaboration with the Columbia Genome Center, we compared the transcripts of C57Bl/6 mice at 7 days after SNI with those of uninjured controls. Many of the most significantly upregulated genes ($p<0.01$) were established markers of microglial activity (Fig. 2.6), including *Itgam* (Cd11b; FC: 3.9), *Aif1* (Iba1; FC: 3.1), *Cx3cr1* (FC: 2.5) and *P2ry12* (FC: 2.2).

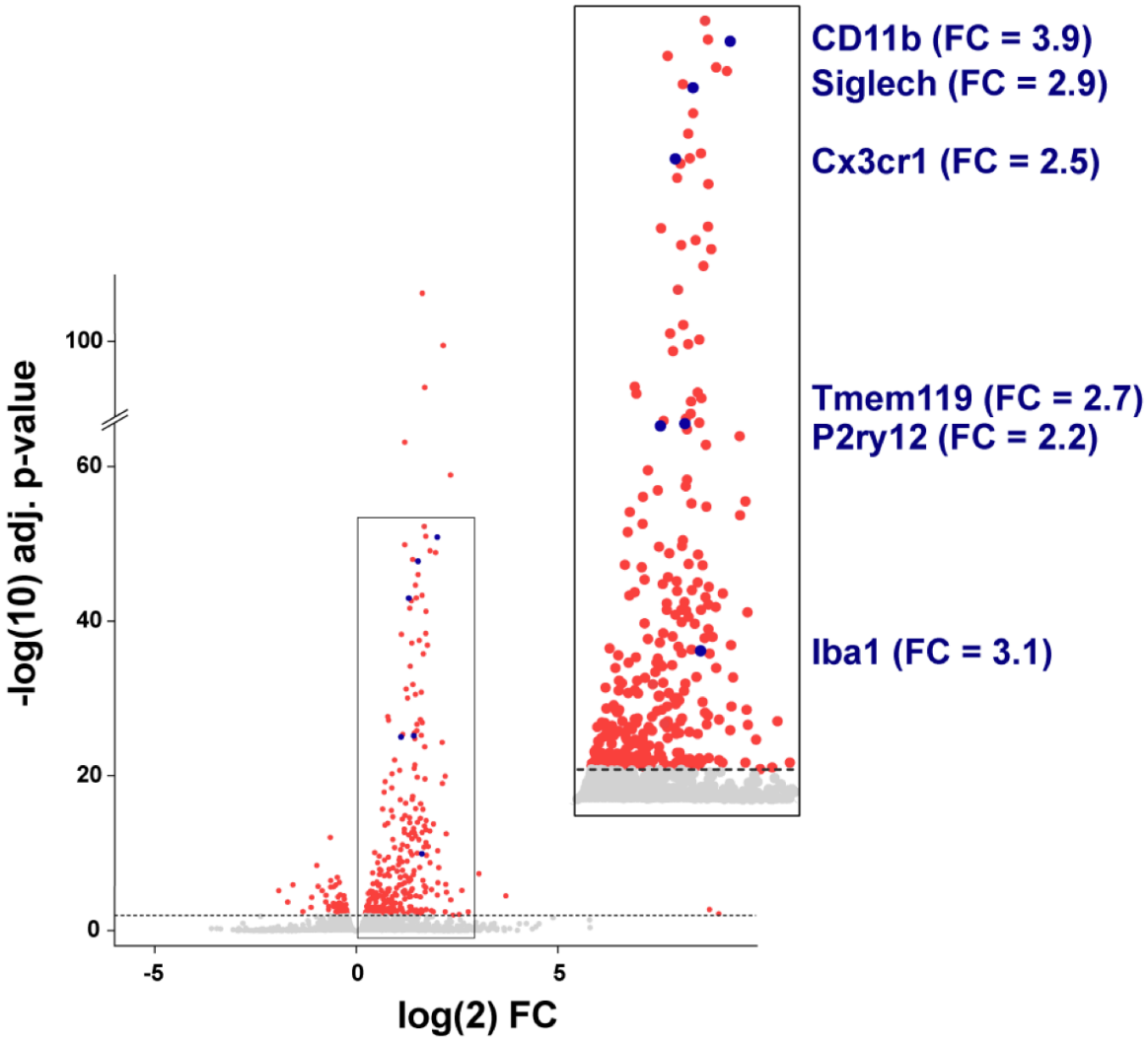

Fig. 2.6: SNI induces a marked upregulation of genes associated with microglial activity. Differential expression analysis of transcripts isolated from the ipsilateral dorsal horn (L4, L5) 7 days after SNI and uninjured controls. Volcano plots shows significantly regulated genes ($p<0.01$) represented by red dots. Boxed inset identifies selected activity-associated genes in blue (n=4).

We subjected the complete list of significantly regulated genes ($p<0.01$) to a gene function and pathway analysis using the Database for Annotation, Visualization and Integrated Discovery (DAVID; Huang da W et al., 2009). We determined the most prominent gene ontology (GO) terms, functions and signaling pathways implicated in the SNI-induced transcriptional changes. Innate immune and inflammatory responses including toll-like receptor signaling (all $p<0.001$) were among the key biological processes and signaling pathways we identified (Fig. 2.7).

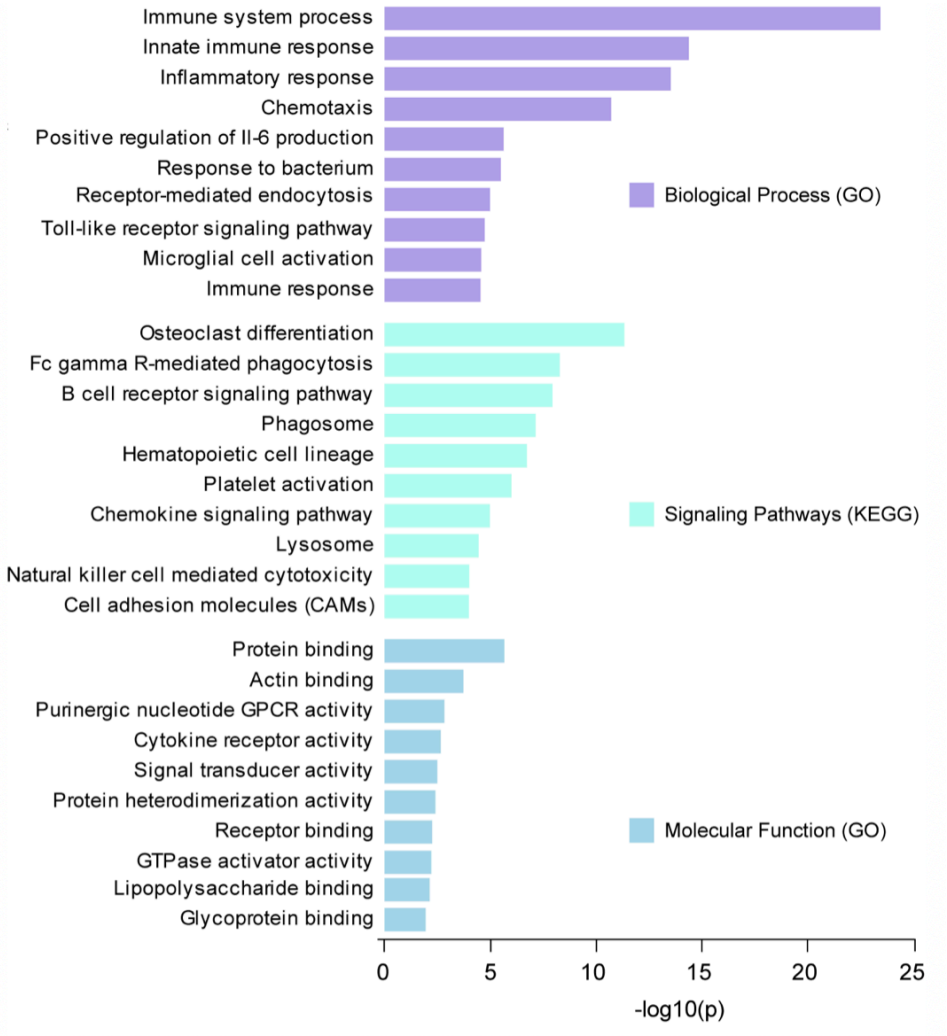

Fig. 2.7: Pathway analysis of SNI-induced transcriptional changes. Signaling pathways and gene ontology (GO) terms for biological processes and molecular functions for significantly regulated genes ($p<0.01$).

Indicators of cell damage and phagocytosis

Multiple Tlrs and associated signaling molecules were upregulated after SNI between 1.6-fold (Tlr2; $p<0.01$) and 4.6-fold (Tlr1; $p<0.001$) (Figure 2.8). These data support previously published work describing the involvement of toll-like receptor signaling in the spinal cord after peripheral nerve injury.

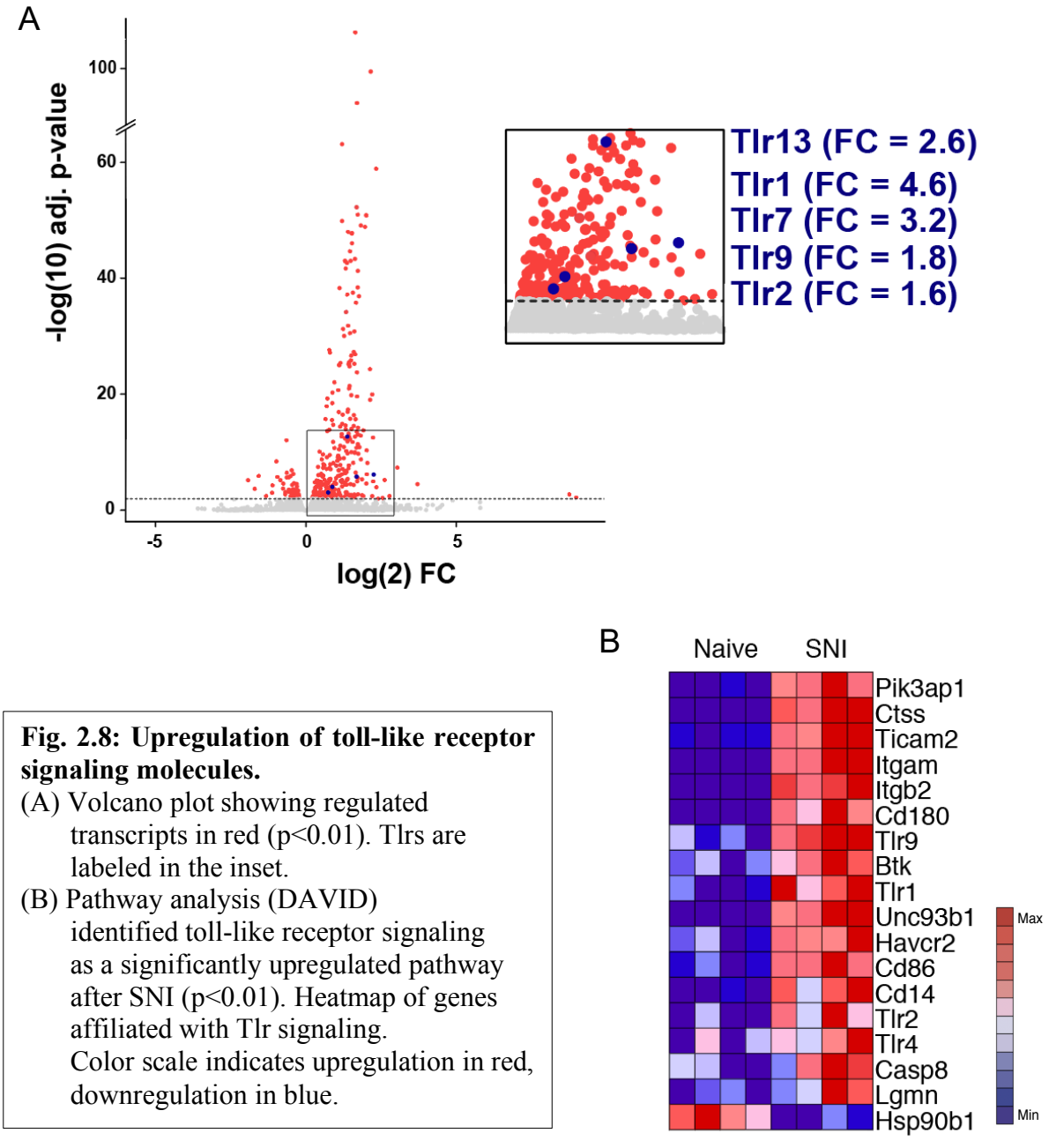

Fig. 2.8: Upregulation of toll-like receptor signaling molecules.
(A) Volcano plot showing regulated transcripts in red ($p<0.01$). Tlrs are labeled in the inset.
(B) Pathway analysis (DAVID) identified toll-like receptor signaling as a significantly upregulated pathway after SNI ($p<0.01$). Heatmap of genes affiliated with Tlr signaling. Color scale indicates upregulation in red, downregulation in blue.

Several Tlrs are known to recognize molecular signals associated with cellular damage (DAMPs), many of which emerge in the context of neurodegeneration. Other upregulated gene transcripts implicated in the immune response to neuronal apoptosis that we identified included *Anxa3* (FC: 1.7), *Hck* (FC: 2.5) and *Trem2* (FC: 3.2). Interestingly, the increase in *Trem2* transcription was accompanied by the upregulation of multiple genes associated with Trem2 signaling, including the intracellular adaptor molecule Dap12 (*Tyrobp*; FC: 2.5) and the key Trem2-Dap12-associated signaling kinase *Syk* (FC: 2.0). The transcriptional upregulation of Trem2 signaling partners was independently verified using quantitative real-time PCR (qRT-PCR; *Trem2* FC: 3.0, *Tyrobp* FC: 2.5, *Syk* FC: 2.2). To further validate the upregulation of *Trem2*, we examined its expression at the protein level. Western blot analysis of protein lysates from the ipsilateral L4-L5 dorsal horn showed that, compared with uninjured controls, Trem2 protein expression after nerve injury increased 2.4-fold at 3 days after SNI, 3.5-fold at the peak of the immune response 7 days after SNI and 2.7-fold 14 days after SNI (Fig. 2.9).

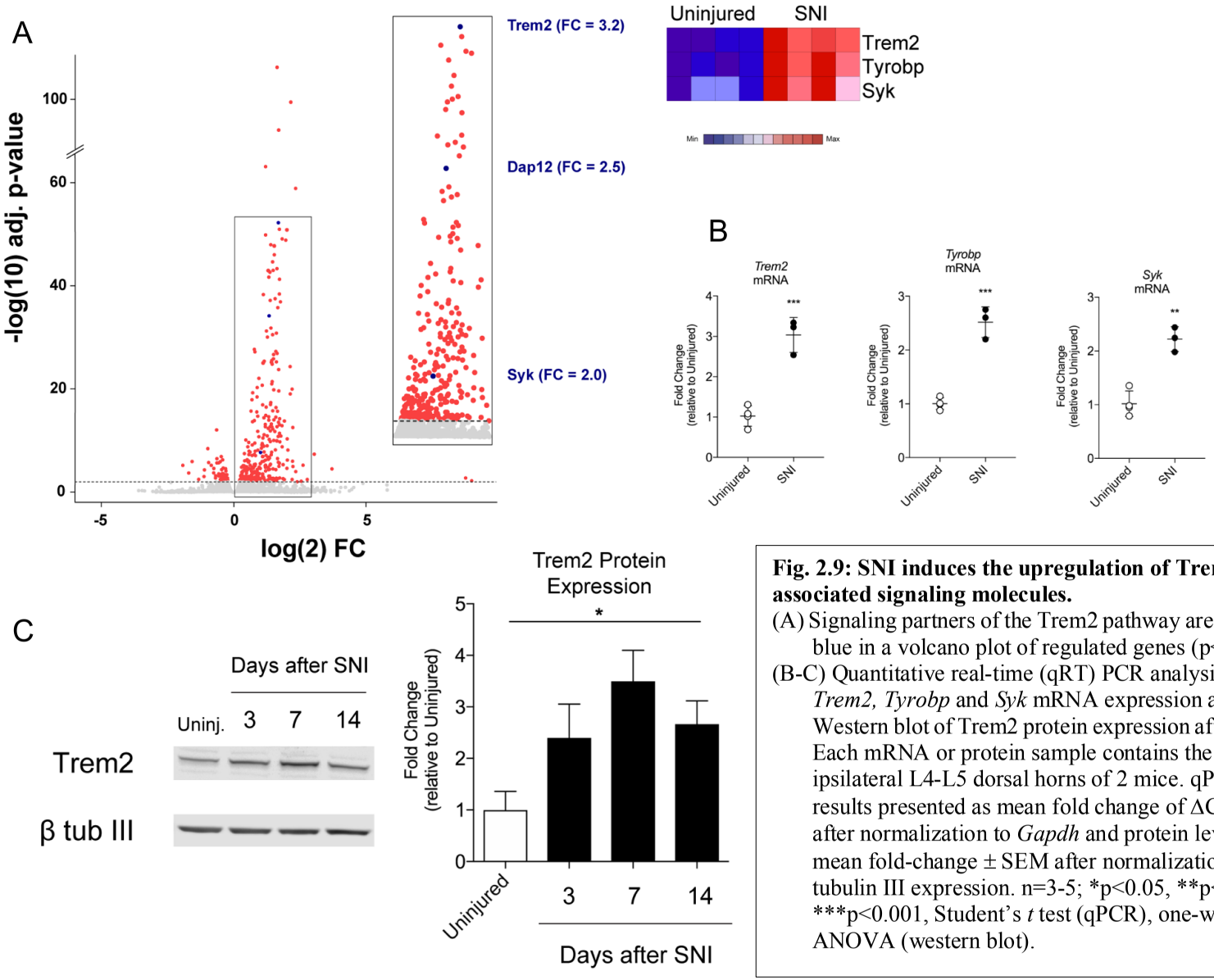

Fig. 2.9: SNI induces the upregulation of Trem2 and associated signaling molecules.
(A) Signaling partners of the Trem2 pathway are labeled blue in a volcano plot of regulated genes ($p<0.01$).
(B-C) Quantitative real-time (qRT) PCR analysis of *Trem2, Tyrobp* and *Syk* mRNA expression and Western blot of Trem2 protein expression after SNI. Each mRNA or protein sample contains the pooled ipsilateral L4-L5 dorsal horns of 2 mice. qPCR results presented as mean fold change of $\Delta C_T \pm$ SD after normalization to *Gapdh* and protein levels as mean fold-change ± SEM after normalization to β-tubulin III expression. n=3-5; *$p<0.05$, **$p<0.01$, ***$p<0.001$, Student's *t* test (qPCR), one-way ANOVA (western blot).

To determine the identity of cells expressing Trem2, we utilized flow cytometry. We isolated live cells from L4-L5 dorsal spinal cord and stained them for Trem2 as well as Cd11b and Cx3cr1, cell-surface markers exclusively expressed in microglia in the CNS (Fig. 2.10). We found that >90% of $Trem2^+$ cells were both $Cd11b^+$ and $Cx3cr1^+$. Control samples counterstained for astroglial and neuronal surface markers did not indicate relevant expression levels of Trem2 (not shown).

We additionally conducted immunocytochemical staining on isolated primary microglial cells grown in vitro and found that Trem2 colocalized with cells stained for Iba1 (Fig. 2.10), confirming microglial expression of the protein in culture. Collectively, these data demonstrate that $Trem2^+$ cells are $Cd11b^+/Cx3cr1^+$ in vivo and coexpress Iba1 in vitro, effectively localizing the observed Trem2 expression to microglia.

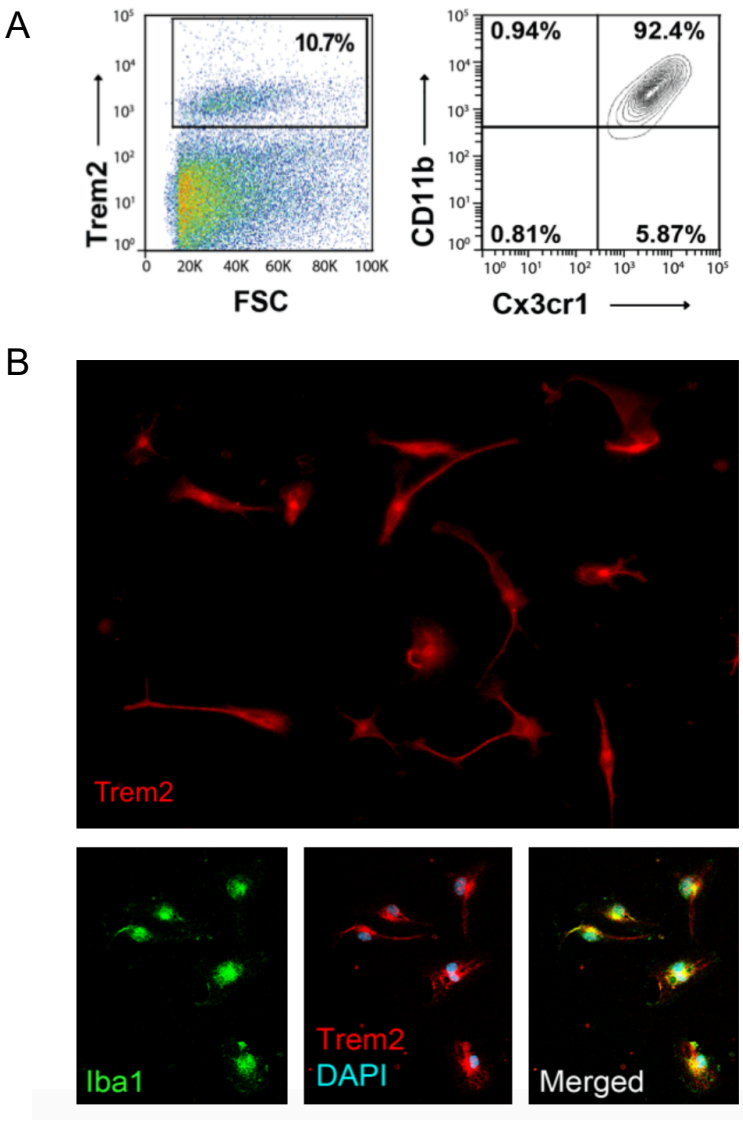

Fig. 2.10: Trem2 is expressed in microglia

(A) Flow cytometric analysis showed that >90% of Trem2^{+} cells isolated from the mouse spinal cord also express the myeloid specific markers Cd11b and Cx3cr1 (n=4)

(B) Representative immunocytochemical stains of primary microglial cultures. More than 90% of cells that stained positive for Trem2 also expressed Iba1, indicating the signal was localized to microglia. DAPI was used to stain for cell nuclei. Images are representative of 4 independent immunocytochemistry experiments.

Trem2-dependent clearance of apoptotic cells after SNI

Facilitating the phagocytosis of apoptotic neurons and cellular debris is a major function of the Trem2 signaling pathway in microglia. GO terms and pathway analysis of the most significantly regulated genes in our RNA sequencing assay also indicated that phagocytosis is a biological process in the spinal cord significantly associated with nerve injury ($p=0.011$). We therefore examined the effect of Trem2 on the clearance of apoptotic cell profiles in the ipsilateral dorsal horn after SNI. For this purpose, we utilized $Trem2^{-/-}$ mice kindly provided by Marco Colonna at Washington University in St. Louis, MO.

Using L4 spinal cord sections harvested at 3 and 7 days after SNI, we stained for apoptotic cell profiles using TUNEL. TUNEL-positive cells that also demonstrated chromatin changes indicative of apoptosis (specifically pyknosis, marginalization or fragmentation) were considered apoptotic. We compared apoptosis in $Trem2^{-/-}$ animals and wild-type controls (Fig. 2.11). We found a significantly higher number of apoptotic profiles in the ipsilateral, but not contralateral dorsal horn of $Trem2^{-/-}$ mice versus wild-type controls. These results demonstrate a critical role for microglial Trem2 in the recognition and clearance of these SNI-induced apoptotic cells in the spinal cord.

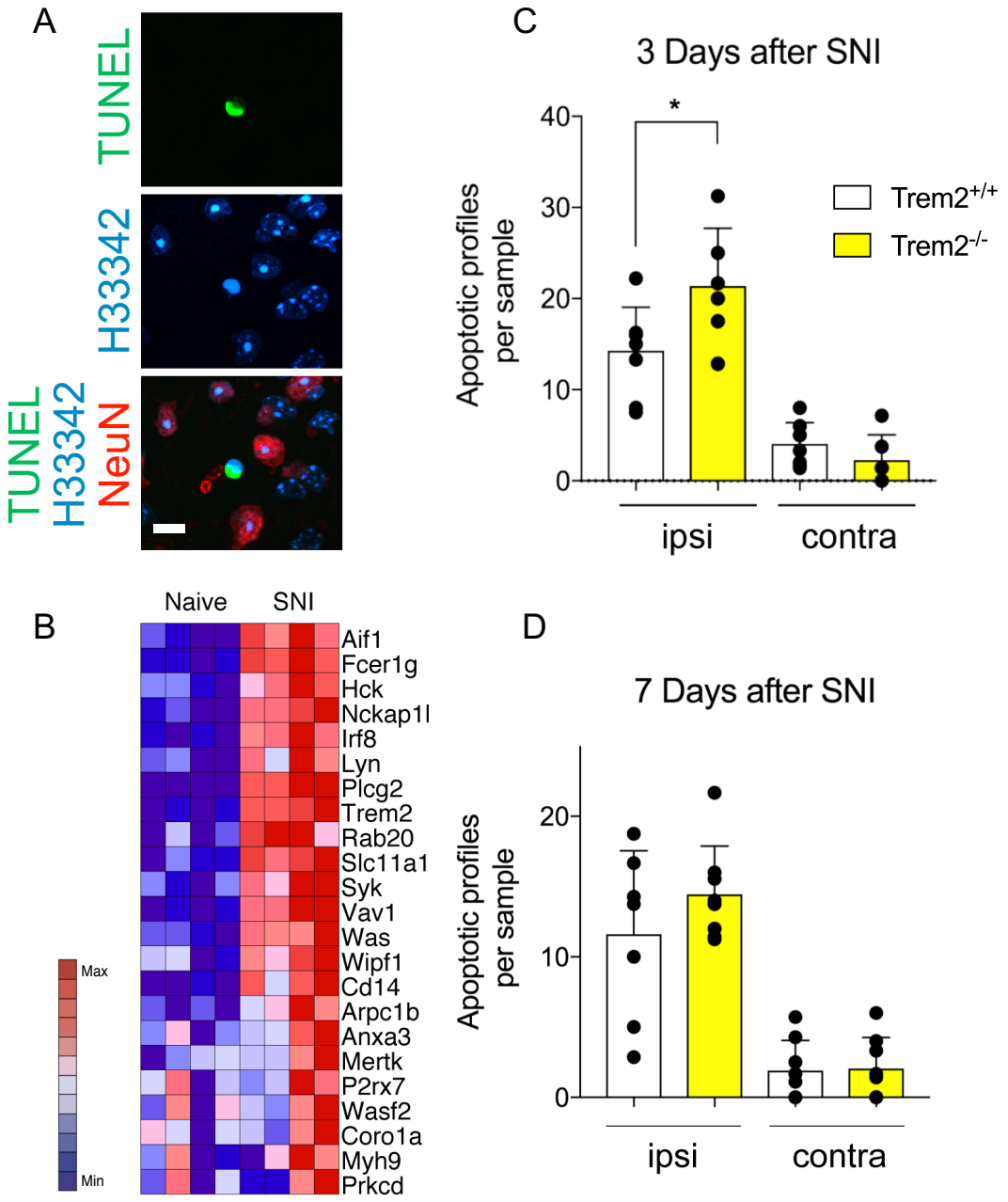

Fig. 2.11: Trem2 mediates the clearance of apoptotic cell profiles

(A) Representative image of apoptotic cell profile 7 days after SNI. H33342 (Hoechst 33342). Scale bar, 10 µm.

(B) Gene ontology analysis with DAVID identified phagocytosis as a biological process associated with transcriptional changes in the ipsilateral dorsal horn after SNI. Heatmap of significantly ($p<0.01$) regulated genes associated with phagocytosis.

(C and D) Quantification of apoptotic profiles 3 (n=6) and 7 days (n=8) after SNI in the dorsal horn of *Trem2*$^{-/-}$ mice or wild-type littermates. *$p<0.05$ in Student's *t* test. Data is represented as mean ± SD.

Trem2 activation does not modulate neuropathic pain-like behavior

Considering the previously reported function of Trem2 as a suppressor of inflammation, we investigated whether its upregulation on day 7, the peak of microglial activity after SNI, has a similar function. We hypothesized that the elimination of Trem2-dependent signaling would lead to an increase in Iba1 immunoreactivity. To test this hypothesis, we stained L4 spinal cord tissue of $Trem2^{-/-}$ mice for Iba1 at several time points after SNI (Fig. 2.12). We found no significant difference in the intensity of Iba1 immunoreactivity at any of the selected time points after SNI when compared with wild-type controls.

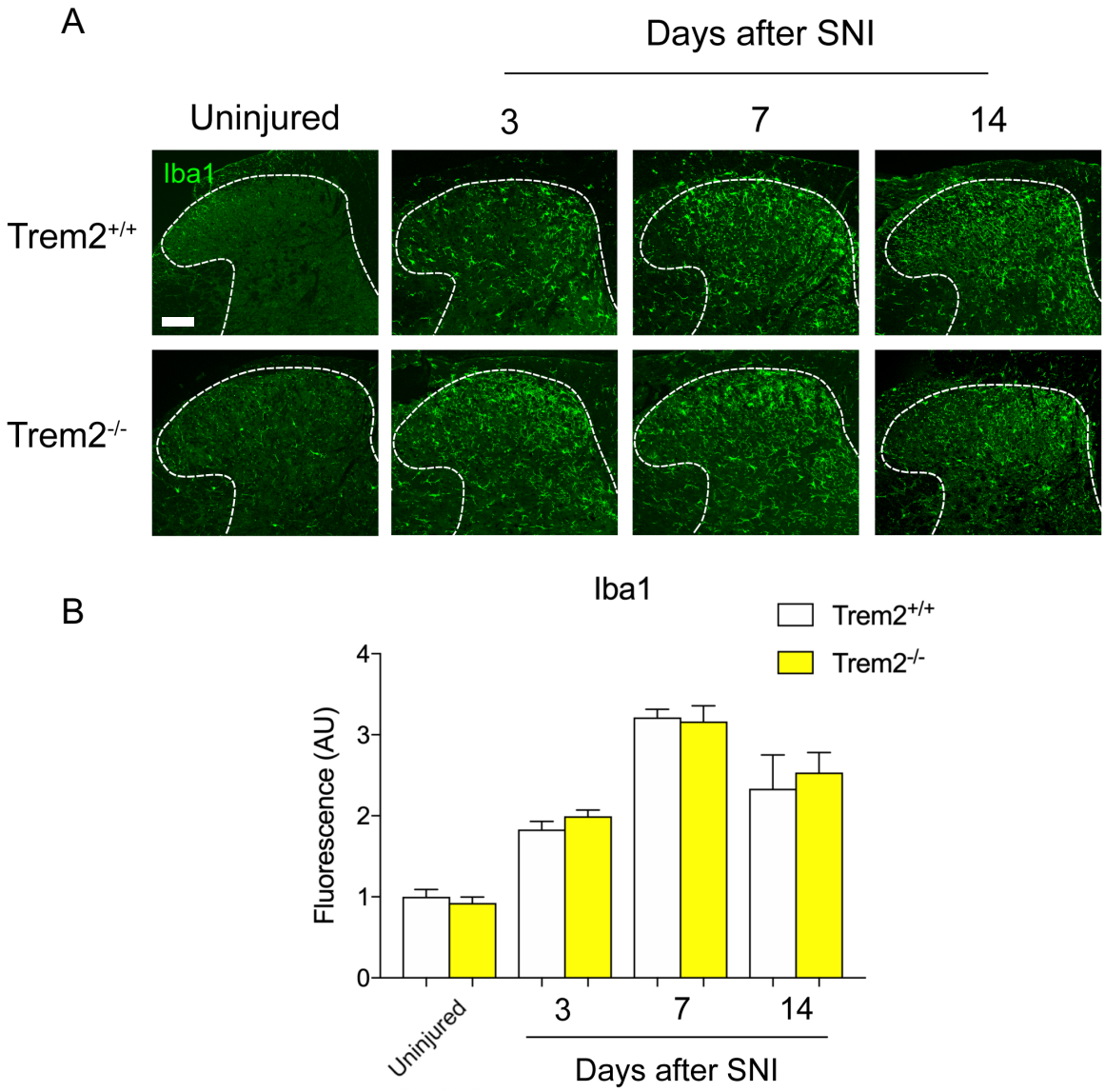

Fig. 2.12: Time course of the spinal immune response to SNI in Trem2$^{-/-}$ mice
(A) Representative immunohistochemical staining for Iba1 in the ipsilateral dorsal horn, L4 spinal cord of Trem2$^{-/-}$ and wild-type littermates after SNI (scale bar, 100 μm)
(B) Semi-quantitative analysis of Iba1 signal intensity normalized to uninjured controls indicated a significant increase in microglial activity after SNI, but no significant difference in signal intensity between genotypes. ($p<0.0001$ for time in a two-way ANOVA; n=3-4; data represented as mean ± SEM)

In addition to assessing the impact that removal of Trem2 signaling has on the spinal immune response to SNI, we also wanted to determine the extent to which Trem2 modulates the development of neuropathic pain-like behavior. To assess pain hypersensitivity after SNI, we established the withdrawal threshold to mechanical stimulation of the hind paw with calibrated von Frey filaments. Neuropathic pain-like behavior in rodents is characterized by a marked decrease in the threshold to normally painless levels of stimulation, equivalent to mechanical allodynia in humans. Both Trem2$^{-/-}$ mice and wild-type littermates exhibited a rapid decrease in the mechanical force eliciting withdrawal responses when applied to the affected hind paw. Slope and extent of the threshold change did not differ between Trem2$^{-/-}$ and Trem2$^{+/+}$ mice, suggesting that the removal of Trem2 signaling does not affect the development of neuropathic-pain like behavior after SNI (Fig. 2.13).

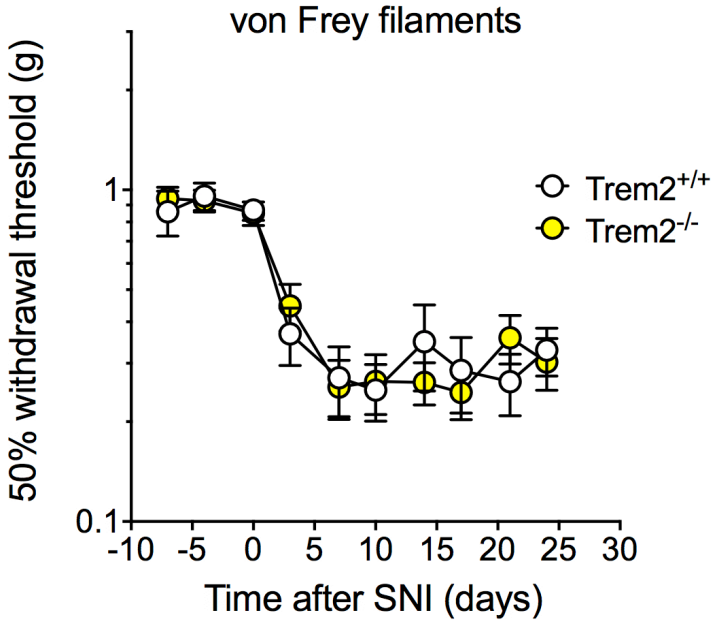

Fig. 2.13: Trem2 deletion does not affect SNI-induced mechanical allodynia.
Withdrawal responses to mechanical stimulation with von Frey filaments after SNI in Trem2$^{-/-}$ mice and wild-type littermates. No difference between genotypes was observed in the development of neuropathic pain-like behavior when compared using a two-way ANOVA (n=5; data are represented as mean ± SEM).

Our results demonstrated that upregulation of endogenous Trem2 regulates the clearance of apoptotic cells, but not the spinal immune response or mechanical allodynia arising in the days and weeks after SNI. We also aimed to determine whether exogenous activation of the Trem2 pathway provides any analgesic effect. Because of Trem2's functional antagonism to Tlr-MyD88 signal transduction, we hypothesized that enhanced Trem2 signaling has the capacity to reduce SNI-induced mechanical allodynia. To induce Trem2-mediated signaling, we took advantage of a Trem2-activating antibody (Bio-Rad).

Trem2-specific antibodies with demonstrated agonistic properties have been used previously to induce Trem2 signaling in microglia (Takahashi et al, 2005). Starting on the day of SNI, we intrathecally administered the Trem2 antibody or a control IgG of matching isotype once a day for 7 days. The effect on mechanical pain hypersensitivity was measured with von Frey filaments. We found no significant difference in the development of neuropathic pain-like behavior after SNI between treatments. These findings suggest that exogenous activation of Trem2 is not sufficient to mitigate the development of pain hypersensitivity after nerve injury.

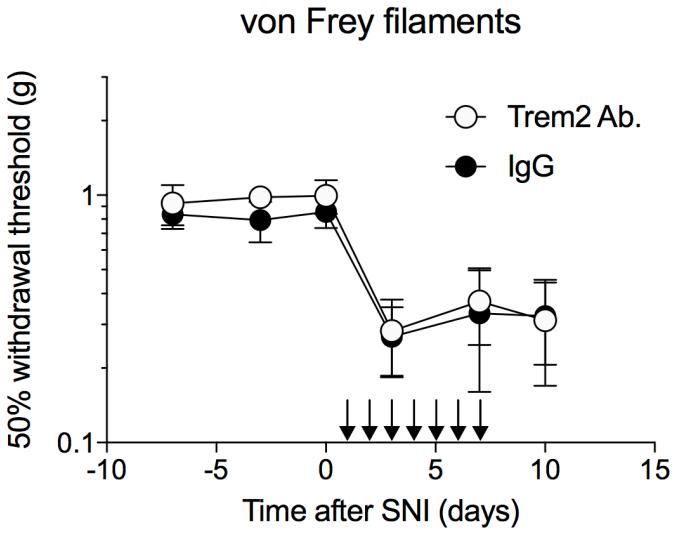

Fig. 2.14: Trem2 activation does not prevent the development of neuropathic pain-like behavior after SNI.
Withdrawal responses to mechanical stimulation with von Frey filaments after SNI in C57Bl/6 mice treated with a Trem2 activating antibody or IgG control (injections indicated with arrows). No difference in neuropathic pain-like behavior was observed when treatments were compared using a two-way ANOVA (n=8; data are represented as mean ± SEM).

Discussion

In this chapter, we first established the time course for the spinal immune response in the ipsilateral dorsal horn of the spinal cord after SNI. Using RNA sequencing, we discovered upregulation of numerous markers of microglial activation. Additionally, we identified increases in multiple gene transcripts associated with the Trem2 signaling pathway, previously implicated both in the regulation of Tlr-mediated immune responses and microglial phagocytosis. We examined the contribution of the Trem2 pathway in spinal microglia to several key aspects of peripheral nerve injury-induced neuropathic pain and found a role for microglial Trem2 in the phagocytosis of apoptotic cells in the ipsilateral dorsal horn after SNI. However, neither removal nor augmentation of Trem2 signaling in the spinal cord affected the overall inflammatory response to SNI or the development of mechanical allodynia.

Our findings challenge the conclusions of a recent study investigating the role of Trem2-Dap12 signaling in neuropathic pain. Kobayashi et al (2016) suggested that activation of Trem2 exacerbates pain by eliciting a proinflammatory response. Nevertheless, evidence provided in this study seems better suited to characterize the role of the adaptor protein Dap12 rather than Trem2. The investigators showed that $Dap12^{-/-}$ animals exhibit significantly less inflammatory cytokine expression and mechanical allodynia after L4 spinal nerve transection when compared with wild-type controls. However, as they acknowledge, Dap12 is a molecular adaptor known to partner with numerous cell surface receptors, including Trem1 and macrophage C-type lectin receptor Clec5a. The link to Trem2 relied on intrathecal administration of a Trem2 agonist antibody in uninjured animals which subsequently provoked mechanical allodynia. However, our results demonstrate in a model of peripheral nerve injury that removal of Trem2 signaling does not affect the spinal immune response nor development of neuropathic pain-like behavior. Although we cannot rule

out the notion that Trem2 activation in the spinal cord of uninjured mice evokes pain, we did not find any additional increase in pain hypersensitivity in nerve lesioned mice that we injected with a Trem2-activating antibody. Based on our findings, we conclude that the role of Trem2 in spinal microglia after nerve injury corresponds to the main function identified in other disease models, namely the clearance of apoptotic cells.

Considering earlier reports of Trem2's potential to suppress inflammation (Zhang et al, 2017; Ren et al, 2018; Zhong et al, 2015), we expected intrathecal administration of a Trem2-activating antibody to reduce microglial activity and indeed, alleviate pain. Our findings do not support such a treatment. On the other hand, we did not have direct information regarding molecular target engagement in the spinal cord. A more efficient method of Trem2 activation may be required to tap into the homeostatic potential of Trem2-Dap12 signaling. Overexpression of Trem2 in spinal microglia would be another way of evaluating the treatment potential of augmented Trem2 signaling in SNI-induced spinal inflammation.

The major function that we determined for microglial Trem2 after SNI corresponds to its previously reported association with microglia-mediated phagocytosis (Takahashi et al, 2005; Hsieh et al, 2009; Kleinberger et al, 2014; Kawabori et al, 2015). As we have recently shown, degeneration of dorsal horn neurons contributes to the transition from acute to chronic neuropathic pain after nerve injury (Inquimbert et al, 2018). Although modulating the clearance of apoptotic cells through Trem2 deletion or activation did not impact the functional outcome in our studies, neuronal apoptosis in the spinal cord is notably slow after nerve injury, likely inducing only a mild, local inflammatory response. In contrast, the widespread nature of Aβ deposits in AD, for example, would alternatively suggest that modulation of microglia-mediated phagocytosis in such a context may provoke a more severe impact on the course of the disease.

Our transcriptome analysis highlighted the magnitude of the inflammatory response in the spinal cord to SNI. To better understand the molecular regulation of this response, we needed to look more closely at other microglial signaling components, several of which we examine in the following chapter.

CHAPTER 3

Cellular components and chemokine regulation of the spinal immune response to SNI

Background and Significance

Animal models of experimental autoimmune encephalitis (Yamasaki et al, 2014) and spinal cord injury (Stirling et al, 2008) have revealed that neuroinflammation in the central nervous system may involve immune cells from the peripheral circulation. Mononuclear cells have been shown to invade the site of inflammation within the CNS and contribute to the immune response. This raises the question of whether immune cells from the periphery invade the dorsal spinal cord following nerve injury and, alongside resident microglia, modulate spinal neuroinflammation. Microglia are known to expand markedly in the days following peripheral nerve lesion (Suter et al, 2009; Calvo et al, 2011; Guan et al, 2016; Okubo et al, 2016; Gu et al, 2016); whether this is due solely to proliferation of resident microglia, invasion of peripheral immune cells or both remains unclear.

Recent findings make an invasion of T-cells very unlikely (Gattlen et al, 2016). However, earlier studies in bone marrow chimeric mice suggest that circulating monocytes cross the blood-spinal cord barrier (BSCB) and play a major role in the injury-induced immune response (Zhang et al, 2007). Although peripheral nerve injury is known to weaken the BSCB (Echeverry et al, 2011; Beggs et al, 2010), independent investigations have also demonstrated that the full body irradiation used in studies of bone marrow transplants also compromise the integrity of the blood-spinal cord barrier (Li et al, 2003; Li et al, 2004). Any analgesic therapy targeting the spinal immune response to peripheral nerve injury would necessarily need to account for the potential

contribution of peripheral immune cells, thus requiring a thorough elucidation of this particular investigative question.

Examining the cellular composition of the spinal immune response would also be relevant for the interpretation of our Trem2-Dap12 findings discussed in Chapter 2. The biochemical markers (Cd11b and Cx3cr1) used to identify the cell population expressing Trem2 do not differentiate peripheral and central myeloid cells. It is conceivable that peripheral monocytes are recruited to the spinal cord after SNI in order to support the clearance of apoptotic cells.

In this chapter, we use multiple experimental approaches to first determine whether or not monocytes from the peripheral circulation invade the dorsal horn after SNI and integrate into the observed immune response. We additionally examine the relative contribution of multiple immune response pathways using a combination of genetic and pharmacological tools to assess the extent to which targeting chemokine and growth factor signaling individually and simultaneously can impact the spinal immune response to SNI and the ensuing behavioral pain phenotype.

Peripheral and central myeloid cells possess different expression patterns of chemokine receptors. The role of chemokines in regulating the spinal immune response to peripheral nerve injury has been intensely studied, because targeting these receptors may lead to the discovery of treatment approaches directed at the recruitment of these immune cells. Early investigations into the spinal immune response explored a possible link between neuronal signaling and the spinal immune cells reacting to the injury. Fractalkine signaling is a prime example of direct neuroimmune crosstalk, because within the central nervous system, fractalkine is primarily expressed by neurons and its only known receptor, Cx3cr1, is present primarily in microglia (Harrison et al, 1998; Jung et al, 2000).

Fractalkine has in fact been linked to one integral component of purinergic signaling in the dorsal spinal cord. ATP emanating from damaged afferent nerve fibers activates the P2x7 receptor on spinal microglia, causing the downstream secretion of cathepsin S (Clark et al, 2010). A lysosomal protease, CatS cleaves the chemokine fragment of membrane-bound fractalkine from the surface of neighboring spinal neurons (Fig. 3.1; Clark et al, 2007; Clark et al, 2009). Once enzymatically released, soluble fractalkine (sFKN) binds to Cx3cr1 on microglia. Activation of Cx3cr1 induces phosphorylation of p38 MAPK and the subsequent release of pro-inflammatory factors like nitric oxide (NO) and interleukins 1β and 6 (IL-1β and IL-6) (Clark et al, 2007).

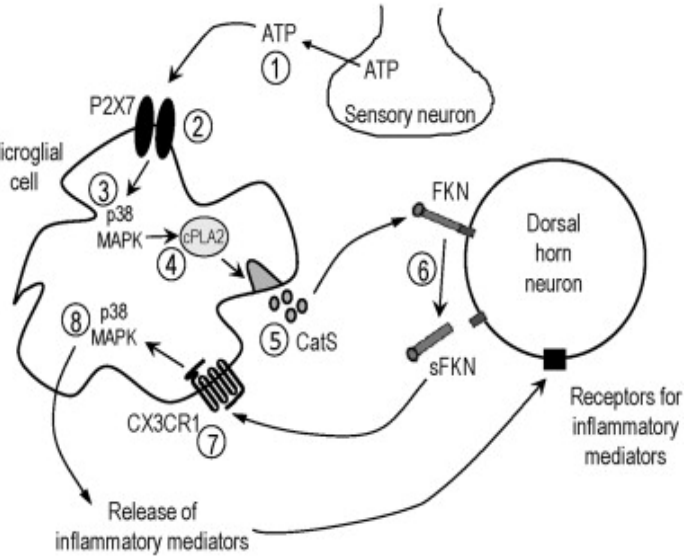

Figure 3.1: Schematic representation of ATP-induced CatS release, resulting in the cleavage of membrane-bound FKN (Clark et al, 2012).

Peripheral nerve injury models cause an increase in sFKN in the dorsal horn of the spinal cord (Clark et al, 2009; Staniland et al, 2010). These findings, combined with experimental results showing that intrathecal administration of FKN- or Cx3cr1-neutralizing antibodies can reduce neuropathic pain-like behavior, suggest that fractalkine signaling in the dorsal horn after nerve injury is a pro-nociceptive process (Milligan et al, 2004; Clark et al, 2007). This hypothesis is further supported by a partial decrease in microglial reactivity after partial nerve ligation (PNL) in mice lacking the Cx3cr1 receptor and a deficit in neuropathic pain-like behavior in these same knockout animals (Staniland et al, 2010).

We decided to examine the contribution of fractalkine signaling to the spinal immune response induced by SNI. Although fractalkine is an established downstream effector of P2x7 receptor activation, ATP stimulation of P2x4 receptor signaling is a key mechanism contributing to neuropathic pain-like behavior, as previously described (see Figures 1.3 and 1.4). To also investigate the possibility of P2x4r-mediated effects of ATP, we utilized NP-1815-PX, a newly developed P2x4r-specific antagonist provided by Nippon Chemiphar.

Additionally, peripheral nerve injury is known to induce significant upregulation and release of Csf1 from injured afferent nerve fibers, as described in Chapter 1 (Guan et al, 2016). Both proliferation and activation of the resident microglia population is affected by this influx of Csf1 (Guan et al, 2016). Within the CNS, the Csf1 receptor is exclusively expressed by microglia and is in fact upregulated in the ipsilateral dorsal horn after peripheral nerve injury (Guan et al, 2016). These data, in combination with the established impact of Csf1 on neuroinflammation and neuropathic pain-like behavior after nerve injury, suggest that preventing increased spinal immunoreactivity in the days following nerve lesion by disrupting Csf1r signaling can prevent the induction of neuropathic pain. Indeed, previous studies have demonstrated that prolonged blockade or removal of Csf1r signaling severely depletes myeloid cell populations, including microglia (Erblich et al, 2011; Rice et al, 2015). To this end, Plexxikon, Inc. has developed several formulations of Csf1r antagonists. In this chapter, we utilize one of these compounds to selectively deplete myeloid cell populations as a way to also examine the impact of microglial depletion on SNI-induced neuropathic pain-like behavior.

Results

The spinal immune response consists primarily of resident microglia

To clarify whether monocytes from the peripheral circulation invade the dorsal horn of the spinal cord after SNI, we used several technical approaches. We first generated a transgenic mouse line that expresses green fluorescent protein (GFP) under the control of the *Cx3cr1* promoter and red fluorescent protein (RFP) under the control of the *Ccr2* promoter by cross-breeding homozygous mice from two commercially available transgenic lines (*Cx3cr1*$^{GFP/GFP}$ and *Ccr2*$^{RFP/RFP}$ respectively). The gene encoding the fractalkine receptor (*Cx3cr1*) is expressed in both microglia and monocyte populations, while Ccr2 is a cell surface receptor predominately expressed in monocytes. These *Cx3cr1*$^{+/GFP}$-*Ccr2*$^{+/RFP}$ mice thus express GFP in both monocytes and microglia, but express RFP exclusively in monocytes. We examined the immunoreactivity for both signals in L4 spinal cord tissue from these transgenic mice 7 days after SNI compared to uninjured controls. While we saw robust induction of Iba1 immunoreactivity in the ipsilateral dorsal horn, we found no RFP signal, suggesting that blood monocytes did not invade the spinal cord (Fig 3.2).

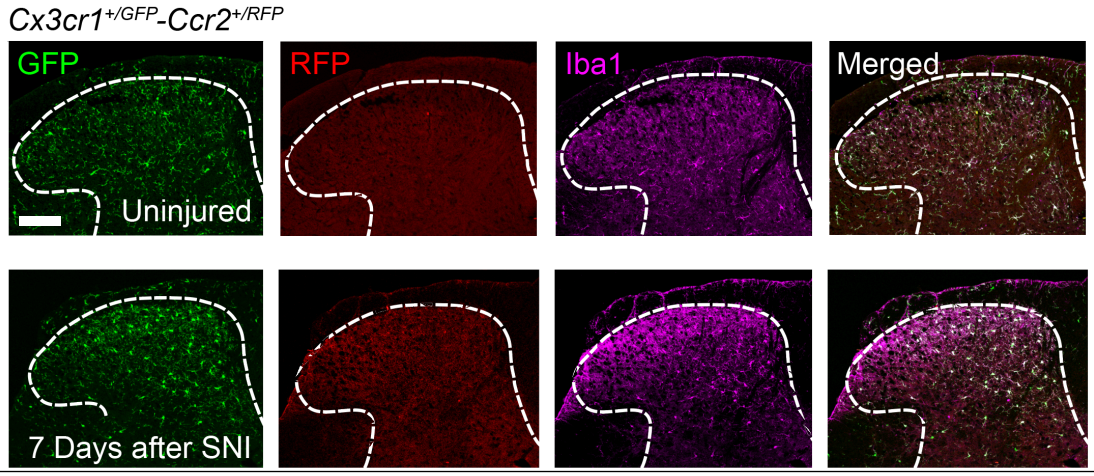

Fig. 3.2: SNI does not lead to invasion of Ccr2+ monocytes into the ipsilateral dorsal horn in *Cx3cr1*$^{+/GFP}$-*Ccr2*$^{+/RFP}$ mice.
Representative immunohistochemical staining of the L4 spinal cord from *Cx3cr1*$^{+/GFP}$-*Ccr2*$^{+/RFP}$ mice. Tissue from mice 7 days after SNI was compared with uninjured controls. No RFP^{+} monocytes were found in the ipsilateral dorsal horn after SNI (n=5; scale bar, 100 μm).

Next, we isolated immune cells from ipsilateral spinal segments L4-L5 and stained for surface markers that distinguish between resident microglia and monocytes to enable the differentiation of these populations by flow cytometry. For this purpose, we stained for Cd11b (a cell surface receptor expressed across all myeloid cells), Cx3cr1 and Ccr2. We examined levels of Ccr2 expression in $Cd11b^{+}/Cx3cr1^{+}$ cells isolated from mice 7 days after SNI, the timepoint we previously determined to be the peak of the immune response, compared with uninjured mice. We found no significant difference in the expression levels of Ccr2 within this cell population when compared to uninjured controls (Fig 3.3). Taken together, our findings suggest that monocytes likely do not invade the dorsal horn of the spinal cord after SNI.

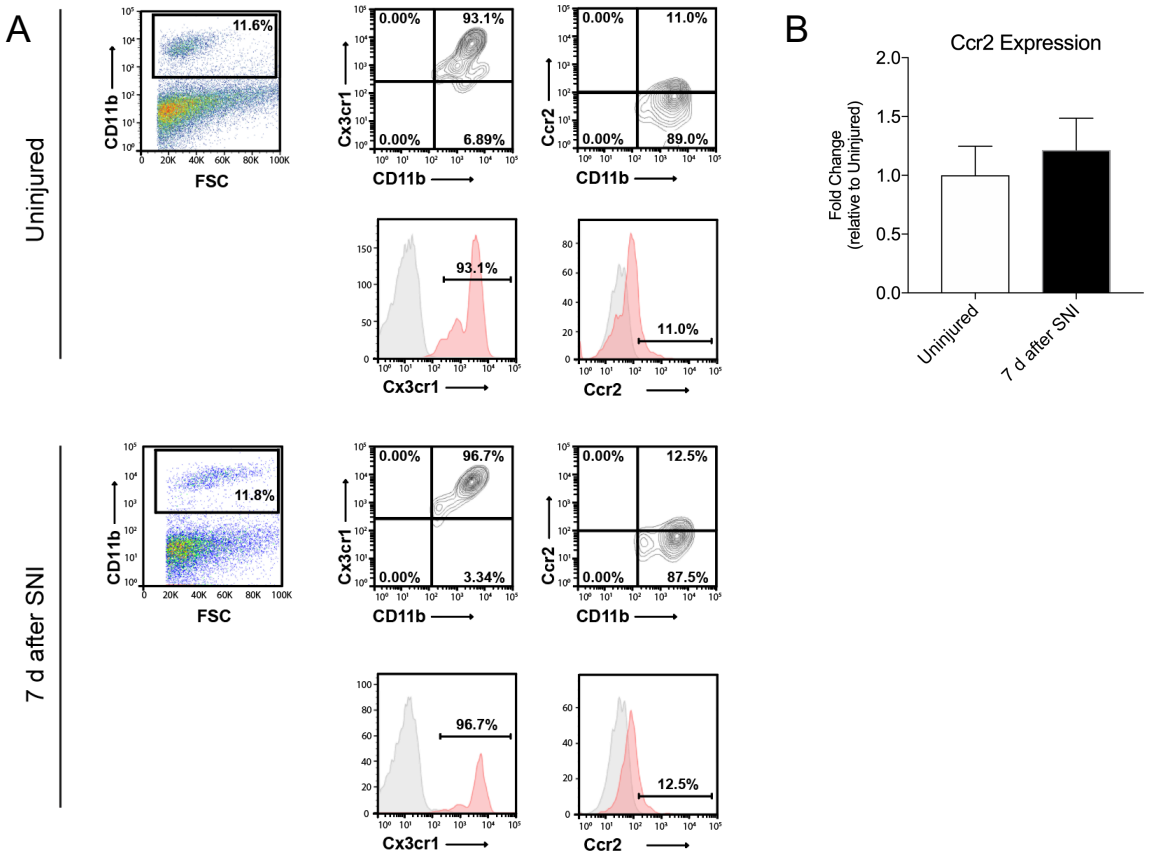

Fig. 3.3: Differentiation of spinal immune cells by flow cytometry

(A) Flow cytometry analysis of uninjured (upper) and 7 days after SNI (lower) ipsilateral L4 spinal cord.

(B) SNI did not induce significant change in the proportion of $Ccr2^{+}$ cells within the $Cd11b^{+}/Cx3cr1^{+}$ population in ipsilateral spinal cord when compared with uninjured controls using Student's *t* test (tissue from 2 mice was pooled per sample; n=4; data represented by mean ± SEM).

Fractalkine signaling is not a critical modulator of neuropathic pain

Using DAVID (see Fig. 2.7), we identified an upregulation of several chemokine signaling pathways ($p<0.001$) at the peak of the immune response 7 days after SNI. Notably, the gene encoding the fractalkine receptor (*Cx3cr1*) increased 2.9-fold ($p<0.001$) 7 days after SNI, suggesting a potential involvement of the fractalkine signaling pathway in the spinal immune response (Fig. 3.4).

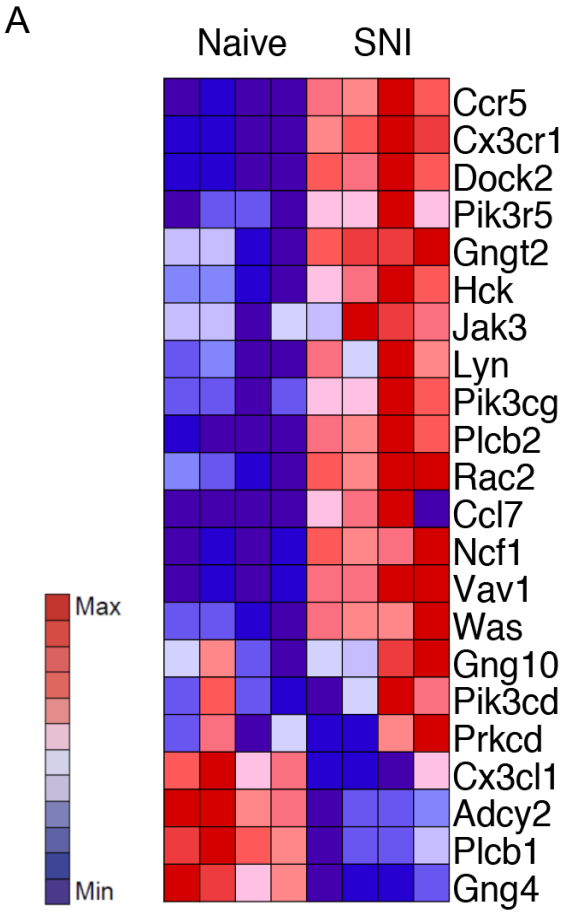

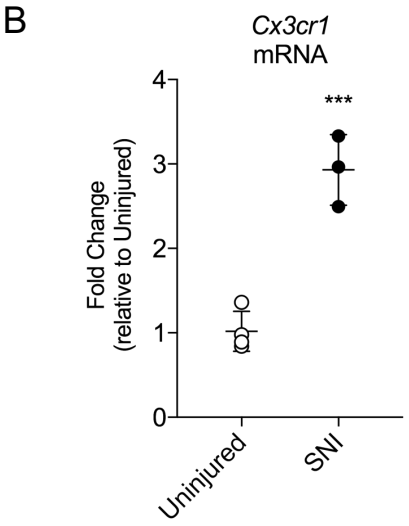

Fig. 3.4: **Upregulation of chemokine signaling molecules.**
(A) Pathway analysis (DAVID) of chemokine signaling after SNI ($p<0.01$). Heatmap of genes associated with chemokine signaling (all $p<0.01$).
(B) SNI induces a marked upregulation of the gene encoding the fractalkine receptor (*Cx3cr1*) as determined by quantitative real-time (qRT) PCR analysis (n=3-4; ***$p<0.001$ in Student's *t* test). qPCR results presented as mean fold change of $\Delta C_T \pm$ SD after normalization to *Gapdh*, relative to uninjured control samples.

We assessed the impact of this pathway on both the spinal immune response and mechanical allodynia induced by SNI. We first harvested spinal cord tissue from animals either heterozygous or homozygous for a deletion of the *Cx3cr1* gene 7 days after SNI. In these mice, GFP is expressed in place of the endogenous *Cx3cr1* gene. We stained L4 spinal cord tissue for Iba1 immunoreactivity to determine any changes in the microglial response. A semiquantitative analysis of the immunofluorescent signal did not indicate a difference in the intensity of the immune response of either genotype when compared with wild-type controls (Fig. 3.5). These results suggest that disrupting fractalkine signaling in spinal microglia does not change the level of SNI-induced microglial activation in the ipsilateral dorsal horn 7 days after SNI.

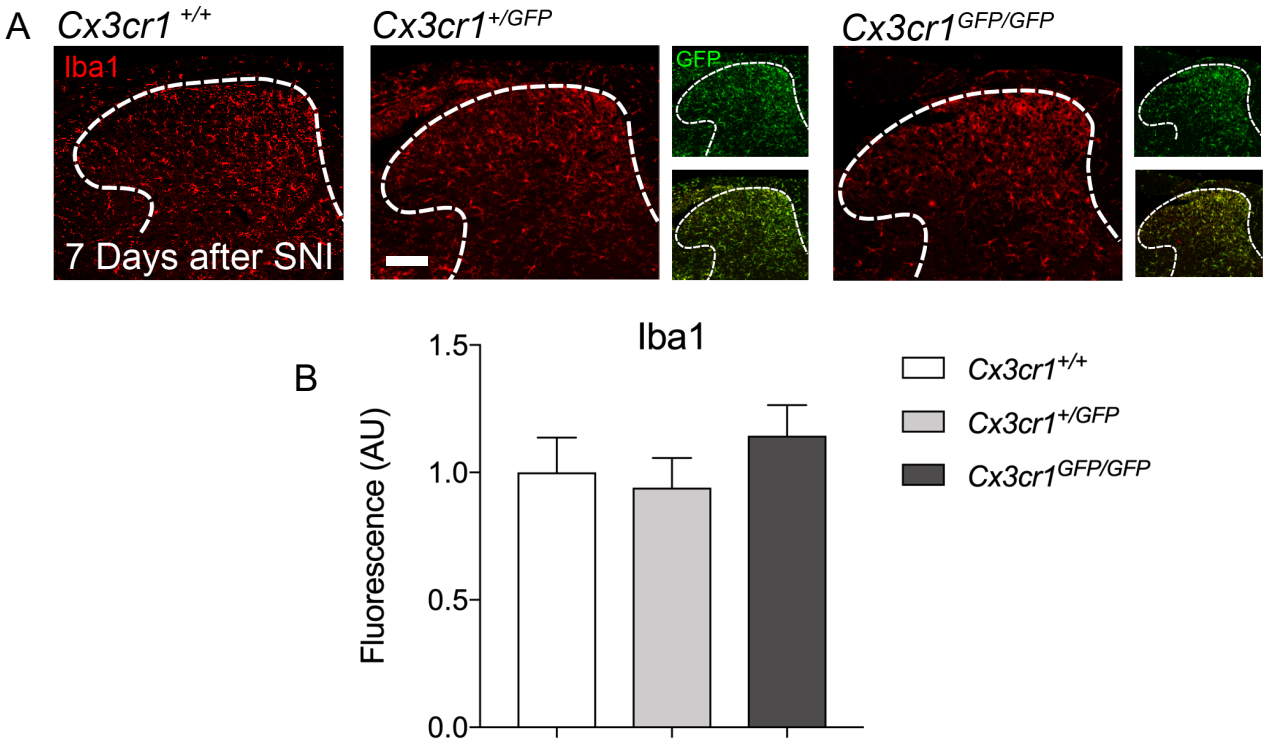

Fig. 3.5: **Disruption of fractalkine signaling does not alter the spinal immune response to SNI**

(A) Representative immunohistochemical staining for Iba1 in the ipsilateral dorsal horn, L4 spinal cord of *Cx3cr1*$^{GFP/GFP}$, *Cx3cr1*$^{+/GFP}$ and *Cx3cr1*$^{+/+}$ mice 7 days after SNI (scale bar, 100 μm).

(B) Semi-quantitative analysis of Iba1 signal intensity normalized to wild-type mouse signal indicated no significant difference in Iba1 fluorescence between genotypes when compared using a one-way ANOVA (n=4; data represented as mean ± SEM).

We then assessed pain hypersensitivity in these animals after nerve injury. After establishing a baseline withdrawal threshold to mechanical stimulation with calibrated von Frey filaments, *Cx3cr1*$^{GFP/GFP}$ and *Cx3cr1*$^{+/GFP}$ mice were tested at multiple intervals after SNI to compare the development of neuropathic pain-like behavior with wild-type littermates. Homozygous, heterozygous and wild-type mice all demonstrated a rapid decrease after SNI in the mechanical force eliciting withdrawal responses when von Frey filaments were applied to the affected hind paw (Fig. 3.6). Slope and extent of the threshold change did not differ between genotypes. Contrary to previous reports, fractalkine signaling did not appear to regulate the development of neuropathic pain-like behavior after peripheral nerve injury.

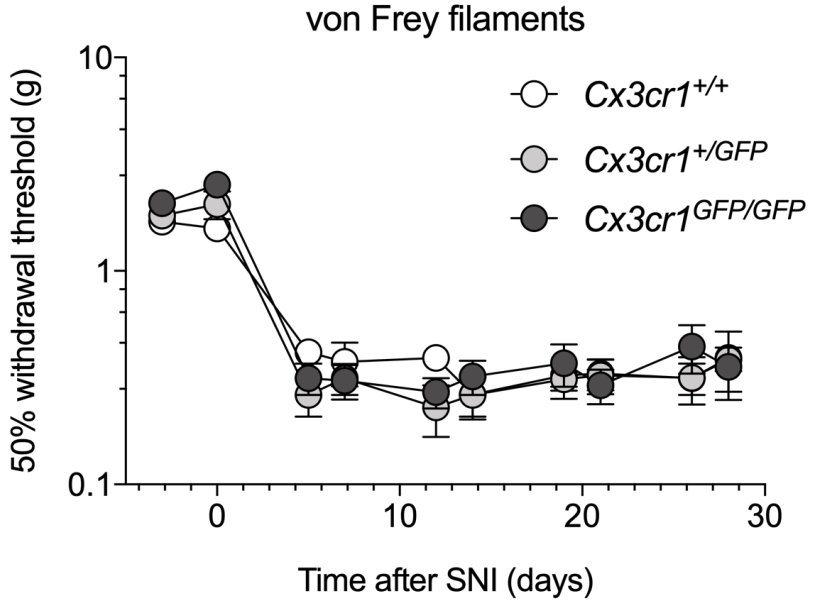

Fig. 3.6: Mechanical allodynia after SNI develops independently of fractalkine signaling.
Withdrawal responses to mechanical stimulation with von Frey filaments after SNI in *Cx3cr1*$^{GFP/GFP}$, *Cx3cr1*$^{+/GFP}$ and *Cx3cr1*$^{+/+}$ mice. No significant difference between genotypes was found in the development of pain-like behavior when compared using a two-way ANOVA (n=10; data are represented as mean ± SEM).

Reducing microglia does not prevent the development of neuropathic pain

Csf1 is an essential growth factor necessary for microglial viability and survival within the CNS. Blockade of Csf1r signaling in microglia has been shown to induce cell death and, in vivo, leads to the large-scale depletion of the resident microglial cell population (Erblich et al, 2011; Rice et al, 2015). After determining a 2.9-fold upregulation of *Csf1r* mRNA in the ipsilateral dorsal horn after SNI using qRT-PCR (suggesting a role for Csf1 signaling in the spinal immune response), we utilized PLX5622, a recently developed Csf1r antagonist, to disrupt Csf1r-mediated signaling in vivo. Mice were fed chow formulated with PLX5622 (or control chow) for 3 weeks prior to behavioral testing and SNI to allow for full depletion of microglia. Treatment continued until the experimental endpoint. Mice on PLX5622 for 3 weeks showed a near complete depletion of $Iba1^+$ cells in the spinal cord (Fig. 3.7).

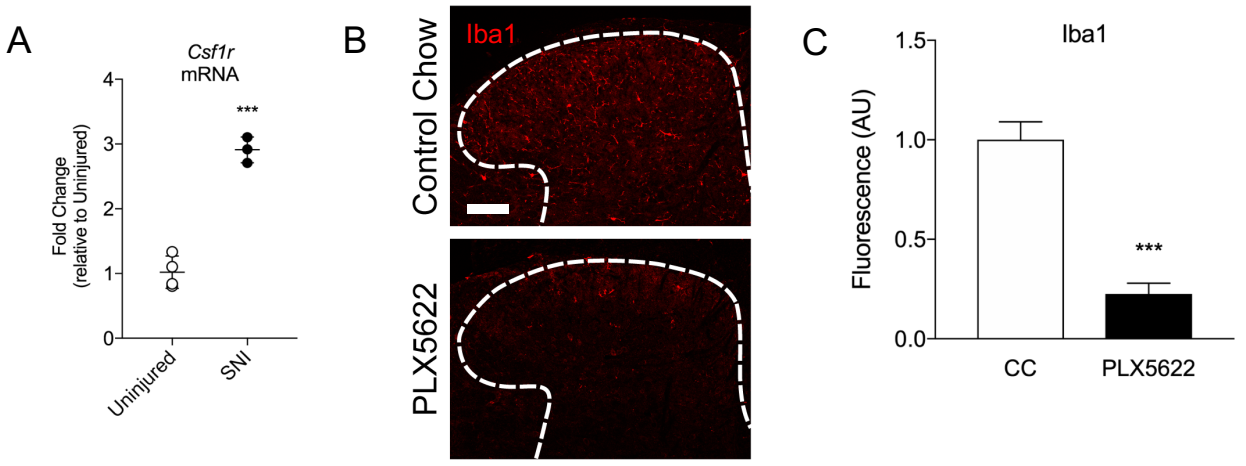

Fig. 3.7: PLX5622 depletes resident microglia in the spinal cord of uninjured mice
(A) SNI induces a marked upregulation of the gene encoding the Csf1 receptor (*Csf1r*) as determined by quantitative real-time (qRT) PCR analysis (n=3-4; ***p<0.001 in Student's *t* test). qPCR results presented as mean fold change of $\Delta C_T \pm$ SD after normalization to *Gapdh*, relative to uninjured control samples.
(B) Representative immunohistochemical staining for Iba1 in the ipsilateral dorsal horn, L4 spinal cord of uninjured C57Bl/6 mice treated with PLX5622 or control chow (scale bar, 100 μm).
(C) Semi-quantitative analysis of Iba1 signal intensity demonstrated a marked decrease in Iba1 immunoreactivity following PLX5622 treatment in a Student's *t* test (n=4; ***p<0.001; data represented as mean ± SEM).

To assess the efficacy of microglial depletion, we stained for Iba1 in L4 spinal cord sections from mice 7 days after SNI. We found a slight activation of remnant microglial cells relative to uninjured mice on PLX5622. However, reactivity 7 days after SNI was vastly diminished when compared with animals receiving control chow (Fig. 3.8).

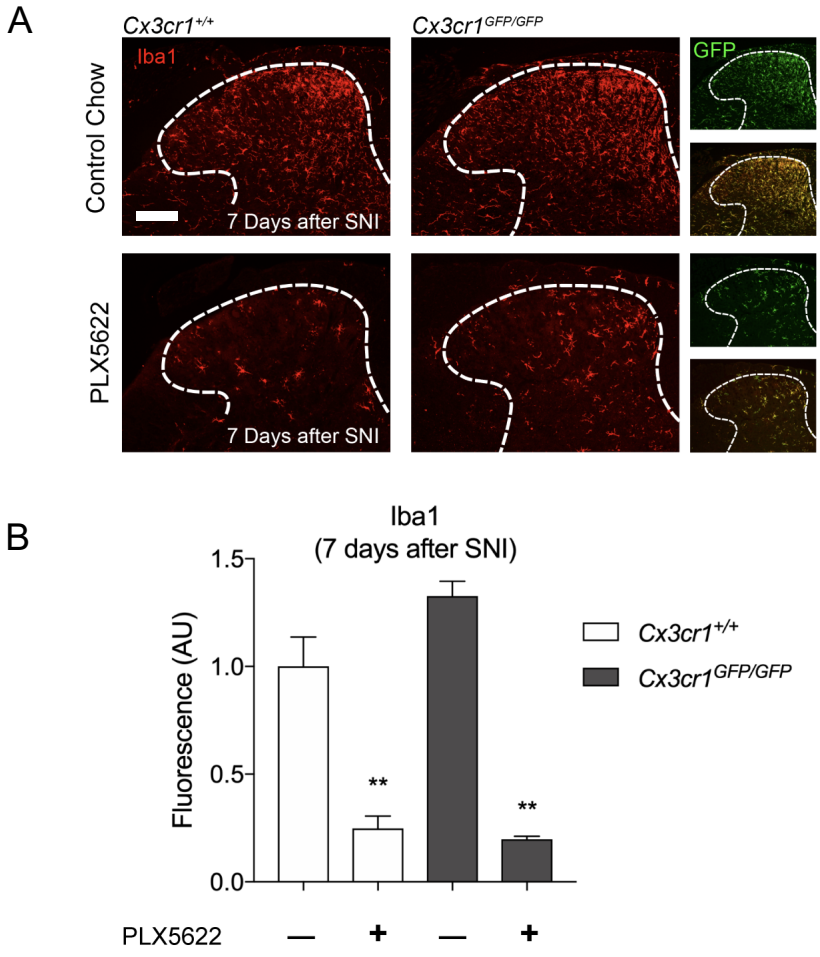

Fig. 3.8: PLX5622 prevents microglial activation after SNI

(A) Representative immunohistochemical staining for Iba1 in the ipsilateral dorsal horn, L4 spinal cord of *Cx3cr1*$^{GFP/GFP}$ and *Cx3cr1*$^{+/+}$ mice fed PLX5622 or control chow, 7 days after SNI (scale bar, 100 μm).

(B) Semi-quantitative analysis of Iba1 signal intensity normalized to signal in wild-type mice on control chow indicated significantly less Iba1 fluorescence in both genotypes when treated with PLX5622, but not control chow, as determined by two-way ANOVA (n=3-4; ***p<0.001 for treatment effect, genotype had no significant effect; data represented as mean ± SEM).

We also treated *Cx3cr1*$^{GFP/GFP}$ mice with PLX5622 to determine if combined disruption of microglial recruitment would alter the development of neuropathic pain-like behavior. *Cx3cr1*$^{GFP/GFP}$ mice on PLX5622 demonstrated similar levels of Iba1 immunoreactivity 7 days after SNI to wild-type controls, a significantly less robust signal than mice on control chow (Fig. 3.8).

Despite clear reduction of the microglial cell population prior to SNI and minimal reactivity by 7 days after nerve injury, testing for mechanical allodynia using von Frey filaments did not demonstrate a difference in the behavioral phenotype between either genotype on PLX5622 and mice on control chow (Fig. 3.9).

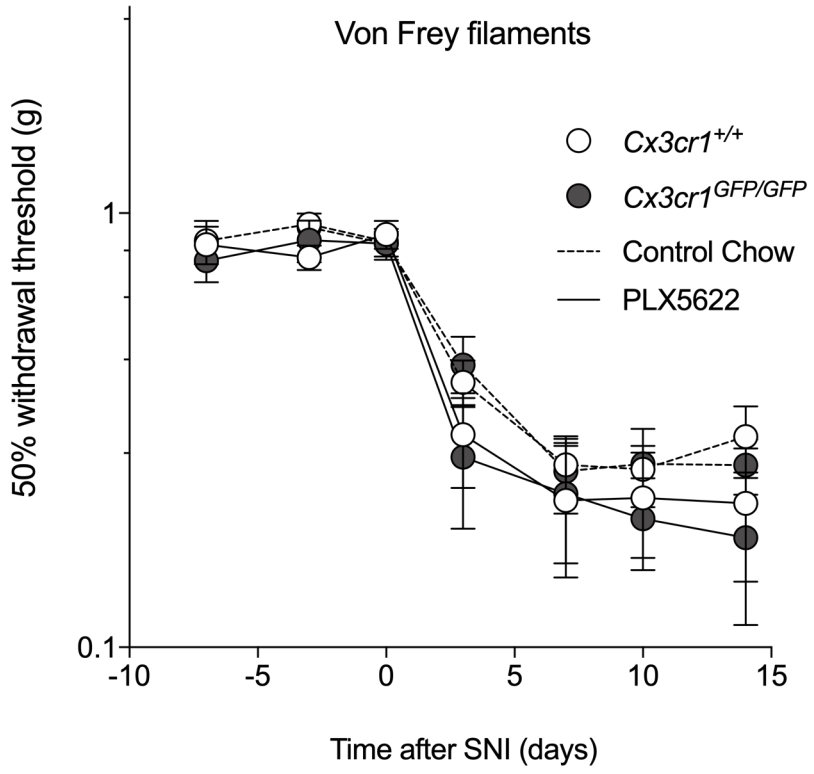

Fig. 3.9: Depletion of microglia via PLX5622 does not reduce mechanical allodynia after SNI.
Withdrawal responses to mechanical stimulation with von Frey filaments after SNI in *Cx3cr1*$^{GFP/GFP}$ mice and wild-type littermates treated with PLX5622 or control chow. No difference between genotypes or treatment regimen was found when compared using a two-way ANOVA (n=5-10; data are represented as mean ± SEM).

Blockade of microglial P2x4r signaling mitigates neuropathic pain

P2x4 receptor signaling has been established as a key regulatory pathway of microglial activity in the spinal cord (Tsuda et al, 2003; Ulmann et al, 2008). To determine whether ATP stimulation of the P2x4 receptor in microglia contributes to SNI-induced mechanical allodynia, we utilized NP-1815-PX, a novel selective antagonist of the P2x4 receptor. Because NP-1815-PX has limited CNS penetrability (Matsumura et al, 2016), we administered the compound intrathecally and examined pain-like behavior within 3 hours of the injection.

We tested for mechanical allodynia using von Frey filaments on days 3, 7 and 10 after SNI. On day 3, we established the neuropathic pain-like phenotype. On day 7, we repeated the stimulation with von Frey filaments following an injection of NP-1815-PX (30 pmol) to test efficacy. Intrathecal administration of NP-1815-PX on day 7 after SNI partially reversed neuropathic pain-like behavior in *Cx3cr1*$^{+/+}$ mice. On day 10, we evaluated the mice again without administering the antagonist and found no sustained effect of NP-1815-PX (Fig. 3.10). The pain phenotype of previously treated mice was indistinguishable from mice injected with vehicle.

To determine whether the analgesic effect of the P2x4r antagonist was mediated by microglia, we conducted our experiment on *Cx3cr1*$^{+/+}$ mice on control chow as well as *Cx3cr1*$^{GFP/GFP}$ mice on PLX5622. We found no significant analgesic effect of NP-1815-PX in microglia-depleted *Cx3cr1*$^{GFP/GFP}$ mice (Fig. 3.10). These findings demonstrate that unlike wild-type mice on control chow, mice with depleted microglia show no reversal of neuropathic pain-like behavior upon administration of the P2x4r antagonist on day 7 after SNI, suggesting that the reduction in mechanical allodynia observed in mice treated with NP-1815-PX is in fact microglia-dependent.

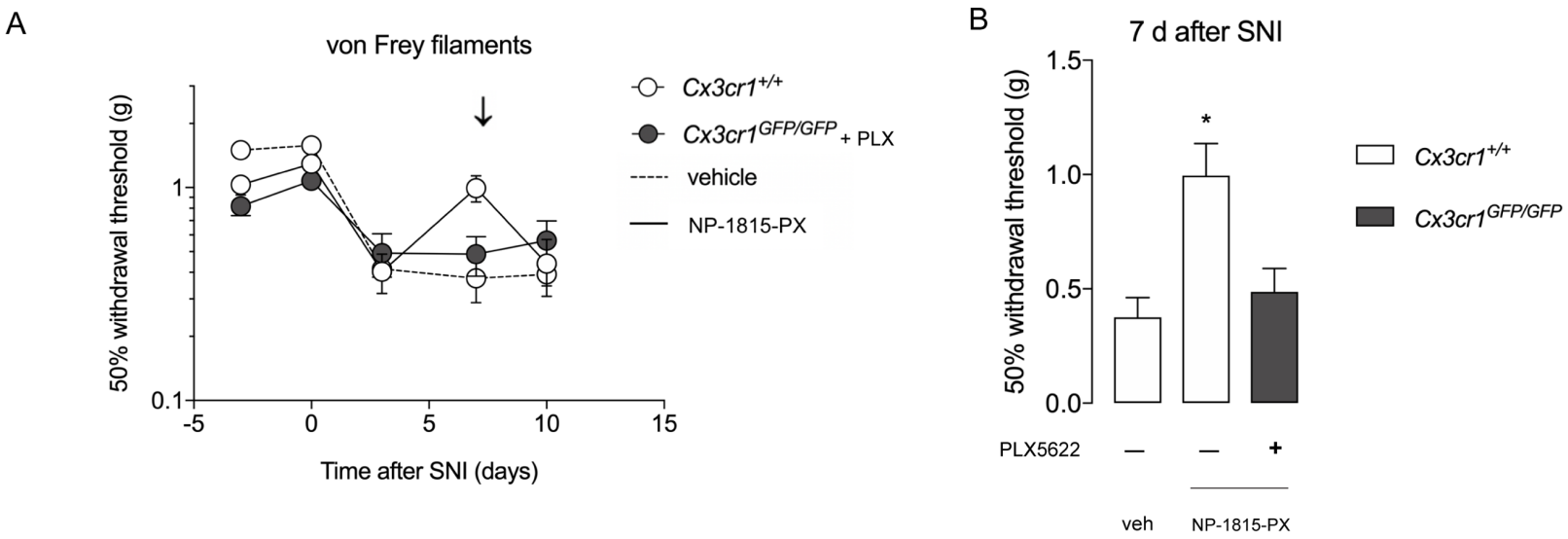

Fig. 3.10: Blocking P2x4r signaling mitigates neuropathic pain-like behavior

(A) Withdrawal responses to mechanical stimulation (von Frey filaments) in *Cx3cr1*$^{GFP/GFP}$ mice or wild-type littermates after SNI. Arrow indicates intrathecal administration of NP-1815-PX or vehicle on day 7 after SNI.

(B) NP-1815-PX treatment partially reversed the withdrawal threshold in wild-type mice on control chow when compared with NP-1815-PX-treated *Cx3cr1*$^{GFP/GFP}$ mice on PLX5622 or wild-type mice on control chow injected with vehicle control (n=9-10; one-way ANOVA; *p<0.01; data represented as mean ± SEM)

Discussion

In this chapter we used a multipronged experimental strategy to examine whether or not monocytes circulating in the blood invade the dorsal horn of the spinal cord after SNI. The complete absence of these cells dismissed the notion that Ccl2, an essential chemokine for peripheral monocyte and macrophage recruitment, is involved in the innate immune reaction to nerve injury. We concluded that resident microglia are solely responsible for the inflammatory response and examined prominent pathways regulating the activity of this innate immune cell population. Using a pharmacogenetic approach, we examined the ability of fractalkine signaling to regulate both the spinal immune response and neuropathic pain-like behavior associated with SNI. We then utilized small molecule inhibitors to selectively disrupt P2x4r signaling and deplete microglia in the CNS. These experiments allowed us to assess the impact of purinergic signaling individually and in combination with myeloid cell depletion on the development of mechanical allodynia after SNI.

The question of monocyte invasion has been addressed in several recent publications involving nerve injury models. A previous transcriptomic analysis of the spinal cord after nerve injury revealed significant upregulation of select microglia-enriched genes, but, similar to our findings, no changes in monocyte-enriched genes after peripheral nerve injury (Guan et al, 2016). Immunohistochemical studies have found aggregation of $Ccr2^{+}$ cells in the L4 dorsal root ganglion after SNT, but no evidence of these cells in the dorsal horn of the spinal cord (Kobayashi et al, 2016). These findings corroborate our immunofluorescent work showing no RFP^{+} monocytes invading the dorsal horn after SNI (see Fig. 3.2). In summary, there now exists strong evidence from several independent investigations suggesting that the spinal immune response to nerve injury does not contain or incorporate any immune cells from the peripheral circulation.

However, it is important to acknowledge that monocytes invading local tissue are often difficult to track, because they readily acquire the cellular phenotype of resident macrophages. While we are confident that our results provide a definitive answer, flow cytometric analyses of key monocyte and microglial markers in the dorsal horn at earlier timepoints after nerve injury (in the hours and first few days after SNI) may provide additional means of observing these changes more closely.

Our experiments examining key pathways implicated in the regulation of spinal microglia further expand our collective understanding of the spinal immune response to SNI. Previous reports have shown a partial reduction of microglial activation in the *Cx3cr1*$^{GFP/GFP}$ mouse after peripheral nerve injury (Staniland et al, 2010). In these same studies, no significant differences in mechanical allodynia were observed between sham-operated and PNL-operated KO animals after injury, suggesting that activation of this pathway was essential for the development of injury-induced mechanical allodynia. These results were recently recapitulated in the context of the spinal nerve transection (SNT) model of neuropathic pain (Gu et al, 2016). Although the mouse strain is consistent between our sets of experiments, we have here provided the first reported microglial activity and behavioral analysis of these mice in the SNI model of neuropathic pain. While both models have historically been used to study neuropathic pain, the surgical differences between models may potentially account for some of the discrepancies we observed in the cellular and behavioral phenotypes after SNI, although such differences across neuropathic pain models have not been extensively studied and would thus warrant further investigation.

Interestingly, multiple investigations into the role of fractalkine signaling in other experimental models involving neurodegeneration demonstrate an anti-inflammatory effect of microglial Cx3cr1 stimulation, showing reduced production of inflammatory cytokines (Tang et

al, 2014; Cho et al, 2011; Pabon et al, 2011). That said, our findings overall do not support a major role for fractalkine signaling in spinal microglia after nerve injury.

Fractalkine signaling is but one downstream effect of ATP signaling observed after peripheral nerve injury. Activation of the P2x7 receptor by ATP triggers the phosphorylation of p38 MAPK in microglia which induces the downstream secretion of CatS, the protease responsible for the extracellular cleavage of membrane-bound fractalkine (Clark et al, 2010; Clark et al, 2012). However, phosphorylated p38 MAPK signaling has also been linked to a shift in microglial phenotype attributed to Irf8-mediated transcription (Masuda et al, 2012). Irf8 is known to regulate the transcription of several factors defining the inflammatory phenotype of microglia, including *Cx3cr1*, *Ctss*, *P2rx4*, *Bdnf* and *Csf1r* (Masuda et al, 2012). Intervention targeting higher-level signaling may thus be required to reduce microglial reactivity. To this end, antagonists of the P2x7 receptor are currently being developed (Bhattacharya et al, 2016) and will shed light on the potential function of this receptor as a regulator of microglial reactivity.

The most intriguing result from this series of experiments is the lack of any impact on neuropathic pain-like behavior following the near-complete depletion of spinal microglia. More research will be required to fully understand the pathophysiological consequences of these findings. One explanation for these data would be that the spinal immune response to nerve injury does not actually play a significant role in the development of SNI-induced mechanical allodynia. This interpretation would be counter to a number of previous studies that have linked mitigation of the immune response to less neuropathic pain-like behavior (Guan et al, 2016; Lee et al, 2018; Echeverry et al, 2017). Specifically, a recently published study using a different method of microglial depletion in the context of the SNT model of neuropathic pain is noteworthy (Peng et al, 2016). In their mouse model, Peng et al used tamoxifen (TM)-controlled Cre recombinase

expression to conditionally express the diphtheria toxin receptor (DTR) in $Cx3cr1^{+}$ cells. Subsequent ablation of spinal microglia by treatment with the diphtheria toxin was shown to abolish both mechanical and thermal hypersensitivity after SNT.

Notably, microglial activity was diminished in both of our studies and indeed both methods of microglial depletion induce cell death, which may in turn cause a local inflammatory response. However, depletion of microglia via our PLX5622 treatment paradigm was gradual and took place over the course of 3 weeks prior to nerve injury, whereas diphtheria toxin-induced cell death occurs rapidly, leading to ablation of microglia within 1-3 days. The significance of the different temporal dynamics observed in these ablation paradigms is unknown. Depletion of microglia with PLX5622 over several weeks would potentially allow for prolonged adaptive changes in the spinal microenvironment in contrast to the acute ablation of this cell population. Alterations in the proteomic composition and function of glutamatergic synapses have been previously reported in microglia-depleted mice (Parkhurst et al, 2013), although the relevance to nerve injury has yet to be investigated.

Lower doses of PLX5622 (roughly 300 mg/kg versus the 1200 mg/kg used in our studies) starting only 2 days prior to partial sciatic nerve ligation (PSNL) reduced microglial activation in the ipsilateral dorsal horn and, in contrast to our findings, were associated with a partial decrease in mechanical allodynia (Lee et al, 2018). In this study, investigators intentionally avoided complete depletion of the microglial population and their findings in fact support the idea that disruption of Csf1r signaling can impact the development of neuropathic pain-like behavior after peripheral nerve injury, as previously reported in Guan et al, 2016.

The analgesic effect of the P2x4r antagonist NP-1815-PX supports previous reports that ATP activation of P2x4r plays an important role in neuropathic pain (Tsuda et al, 2003; Coull et

al, 2005; Masuda et al, 2014). As described in Chapter 1 (see Fig. 1.3), activation of P2x4r after peripheral nerve injury induces the secretion of Bdnf from activated microglia, which subsequenty induces a depolarizing shift in the chloride reversal potential of neighboring inhibitory interneurons (Coull et al, 2005). This shift reduces the efficacy of fast synaptic inhibition through $GABA_A$ and glycine receptors, thus altering the carefully controlled balance of neurotransmission in nociceptive signaling pathways of the dorsal horn. Intrathecal administration of NP-1815-PX demonstrated the acute analgesic efficacy of ATP-P2x4r inhibition. Whether this effect is due directly to the Bdnf-mediated impact on inhibitory interneurons has yet to be fully investigated, but our results support P2x4r as a promising therapeutic target for neuropathic pain.

Alternatively, the lack of therapeutic effect in microglia-depleted mice may indicate that spinal microglia serve a supportive physiological role after SNI in addition to the mediation of inflammation. As discussed in Chapter 2, the characterization of microglial activation as neuroprotective or neurotoxic in instances of neurodegeneration has yet to be fully elucidated in the context of peripheral nerve injury. Assessing the contribution of master transcriptional regulators of microglial phenotype, a few of which are discussed in the following chapter, to nerve injury-induced inflammation may provide greater insight into the therapeutic potential of targeting the spinal immune response.

CHAPTER 4

Conclusions and Research Outlook

One pathophysiological hallmark of peripheral nerve injury is the induction of a vivid innate immune response in the dorsal horn of the spinal cord. Although this neuroinflammatory reaction has been extensively studied in recent years, the exact cellular and molecular mechanisms underlying the immune response remain incompletely understood and clinically efficient pharmacotherapies targeting this reaction have yet to be developed. Elucidating key immunoregulatory signaling pathways in spinal microglia is essential for understanding how to properly modulate this immune response as a means of treating neuropathic pain.

We have examined the contribution of microglia to peripheral nerve injury-induced neuroinflammation and mechanical allodynia, one of the key features of neuropathic pain in humans. As described in Chapter 2, we discovered a role for microglial Trem2 in the phagocytic clearance of apoptotic cells after SNI. We recently published a study establishing neuronal apoptosis in the ipsilateral dorsal horn of the spinal cord as a key mechanism driving the transition from acute to chronic pain after nerve injury (Inquimbert et al, 2018). Here we demonstrate that microglial Trem2 signaling is necessary for the removal of these apoptotic cells. In collaboration with Hynek Wichterle from the Department of Pathology and Cell Biology at Columbia University, we are currently establishing an in vitro model to further elucidate the key downstream signaling partners of Trem2 involved in the regulation of microglial phagocytosis. Our model will utilize stem cell-derived inhibitory interneurons and co-cultured primary microglia to study the phagocytosis of apoptotic cells following an excitotoxic challenge. This model will also facilitate

research on the molecular determinants that define the vulnerability of inhibitory interneurons to excitotoxic cell death.

Several recent studies have provided evidence showing that mitigation of the spinal immune response can reduce neuropathic pain-like behavior after nerve injury (Guan et al, 2016; Lee et al, 2018). Here we present new findings that demonstrate the microglial reaction to neurodegeneration is one component of this neuroinflammatory process. In fact, the role of microglia in the context of neurodegenerative disease has become the central topic of much research in recent years. Whether neuroinflammation creates a neurotoxic environment or actually serves a physiological and ultimately neuroprotective role by clearing cellular debris and protein aggregates has been debated in the context of ALS and Alzheimer's disease (Keren-Shaul et al, 2017; Wang et al, 2016; Frakes et al, 2014; Re et al, 2014). Although we established an NMDA receptor-dependent mechanism of excitotoxic cell death in Inquimbert et al, 2018, the possible contribution to this excitotoxicity of inflammatory cytokines secreted by activated microglia has not yet been studied. A thorough understanding of changes induced by neuronal apoptosis to the cellular environment of the spinal dorsal horn will be essential to the future development of neuroprotective therapeutics.

One of our key findings is the lack of impact on the spinal immune response and SNI-induced mechanical allodynia we achieved by individually targeting several key immunoregulatory pathways, including Trem2 and fractalkine signaling. In Chapter 3, we present evidence that suggests the spinal immune response consists primarily of resident microglia. Consequently, we do not expect that targeting the monocyte receptor Ccr2 would affect the functional outcome of nerve injury as has been previously reported in studies relying on whole-body irradiation and bone marrow transplants (Zhang et al, 2007). The increased permeability of

the blood-spinal cord barrier induced by such irradiation means that the involvement of Ccr2 observed in these studies is likely an artifact, a conclusion supported by a recent independent reevaluation of monocyte function in neuropathic pain (Peng et al, 2016). However, neither the disruption of fractalkine signaling nor the inhibition of Csf1r, both established targets for the modulation of microglia (Staniland et al, 2010; Guan et al, 2016), produced analgesia either.

Perhaps our most striking finding in this series of experiments was the lack of consequences on neuropathic pain-like behavior observed after the near-complete depletion of microglia. Considering the significant effects reported by other investigators conducting similar studies (Lee et al, 2018; Peng et al, 2016), we expected to find at least partial pain alleviation after the removal of microglia. One interpretation of our findings would reasonably suggest that the spinal immune response is largely irrelevant to the development of SNI-induced mechanical allodynia. This conclusion would challenge a host of previous studies demonstrating pain relief after the blockade of microglial signaling pathways (Guan et al, 2016; Staniland et al, 2010; Stokes et al, 2013). In fact, we also demonstrated a microglia-dependent analgesic effect of the P2x4r antagonist NP-1815-PX after SNI. Consequently, the immune response may not be necessary for the development of pain, but targeting the neuroinflammatory process that unfolds after nerve injury may still hold therapeutic promise (Watkins and Maier, 2003; Ji et al, 2014). An alternative interpretation would be that microglial activity is required to maintain a homeostatic microenvironment in the days after peripheral nerve injury. In this case, depleting microglia would abolish not only inflammation but also disrupt the protective function exercised by spinal microglia, ultimately failing to prevent the shift of pain-processing pathways in the dorsal horn toward hyperexcitability.

Several studies on the physiological functions of microglia support this hypothesis. Transforming growth factor-β (TGF-β) is a key microglial growth factor known to maintain these cells in a "resting" or homeostatic M0 phenotype (Butovsky et al, 2013; Bohlen et al, 2017). Although microglial activation leads to diminished TGF-β expression (Affram et al, 2017), intrathecal administration of TGF-β reverses nerve injury-induced spinal inflammation and neuropathic pain-like behavior (Echeverry et al, 2009; Chen et al, 2013). In the context of peripheral nerve injury, treatment with TGF-β has been shown to mitigate spinal inflammation by reducing the phosphorylation of extracellular signal related kinase (ERK) and p38 MAPK, two essential kinases linked to the downstream expression of numerous markers of microglial activation (Chen et al, 2016).

Another factor influencing microglial phenotype is PU.1, often considered a master regulator of myeloid cell differentiation and development (Vangala et al, 2003; Perdiguero et al, 2012). Chromatin immunoprecipitation and deep sequencing (ChIP-seq) studies examining direct transcriptional targets of PU.1 have shown binding to the promoter regions of nearly every major target discussed in this dissertation, including *Aif1* (Iba1), *Itgam* (Cd11b), *Csf1, Csf1r, Cx3cr1, Tyrobp* (Dap12) and *Trem2* (Satoh et al, 2014). Other transcriptional modulators of microglial phenotype like *Irf8* and *Runx1* are also subject to PU.1-mediated regulation (Satoh et al, 2014). *Irf8*$^{-/-}$ mice in fact exhibit reduced microglial reactivity and less severe mechanical allodynia after peripheral nerve injury when compared with wild-type littermates (Masuda et al, 2012). Expression of PU.1 is controlled by the transcription factor CCAAT/enhancer-binding protein-α (C/EBP-α). Notably, Csf1 signaling through phosphorylated ERK has been shown to increase expression and activity of both PU.1 and C/EBP-α (Smith et al, 2013; Jack et al, 2009).

Interestingly, members of this regulatory cascade determining microglial phenotype were significantly upregulated after SNI (PU.1: FC=2.7, $p<0.001$; C/EBP-α: FC=1.4, $p<0.05$; *Irf8*: FC=2.7, $p<0.001$; *Runx1*: FC=2.5, $p<0.001$), strongly implying that this broad control mechanism is activated in the days following nerve injury. Targeting individual downstream response pathways, like Trem2 or Cx3cr1, may not produce a sufficient effect on cellular phenotype, possibly due to compensation by simultaneously upregulated alternative pathways.

Mossadegh-Keller and colleagues (2013) have shown that Csf1 directly induces and activates PU.1. Guan and colleagues (2016) have further demonstrated that Csf1 released from the central terminals of an injured nerve promotes the upregulation of genes linked to PU.1-mediated microglial activation. Interestingly, the effects of Csf1 after nerve injury were dependent on Dap12. The exact relationship between Dap12 and Csf1r has yet to be fully elucidated, but a role for Dap12 in microglial activation and nerve injury-induced pain has been confirmed in multiple independent investigations (Guan et al, 2016; Kobayashi et al, 2016).

Another possible molecular target for upstream therapeutic intervention is microRNA-124. An endogenous inhibitor of C/EBP-α, miR-124 has been shown in the context of EAE (Ponomarev et al, 2011), Parkinson's Disease (Yao et al, 2018), intracerebral hemorrhage (Yu et al, 2017) and focal cerebral ischemia (Hamzei Taj et al, 2016) to induce a neuroprotective phenotype in microglia by promoting microglial quiescence. In fact, daily intrathecal administration of miR-124 completely prevented the development of neuropathic pain-like behavior after peripheral nerve injury (Willemen et al, 2012). Activation of spinal microglia was not assessed in this study, but the known effects of miR-124 on C/EBP-α-mediated activation would lead one to hypothesize that microglial activation was likely absent in this model. Interestingly, Ponomarev et al, 2011 also showed that miR-124 is highly enriched in CNS microglia (relative to peripheral macrophages), is

downregulated upon microglial activation and that restoring miR-124 expression results in the increased expression of TGF-β in these cells. Taken altogether, a more thorough examination of the therapeutic potential of miR-124, including its effect on SNI-induced microglial activation, would appear to hold great promise in the treatment of peripheral nerve injury-induced neuropathic pain.

Our results provide new insight into some of the key mechanisms regulating microglial phenotype and function in the spinal cord after peripheral nerve injury. Resolving the complex interaction of pathways regulating microglial activity after nerve injury will require more work however. From a translational perspective, developing safe and effective treatment strategies aimed at mitigating spinal neuroinflammation will require highly specific interventions that nevertheless deliver a broader cellular effect than can be accomplished by inhibiting a single immune response pathway. While our hypothesis that the functional phenotype of microglia can be therapeutically manipulated away from an inflammatory activation state toward homeostatic functions is intriguing, such a comprehensive approach is likely to require targeting a master regulator of the microglial transcriptome. The therapeutic promise of reducing or preventing the development of neuropathic pain should necessarily be balanced against the risks associated with such a profound alteration of microglial physiology.

MATERIALS and METHODS

Animals

All experimental procedures involving the use of animals were carried out in accordance with the National Institutes of Health (NIH) Guide for the Care and Use of Laboratory Animals and approved by the Institutional Animal Care and Use Committee (IACUC) of Columbia University. Mice were housed in a barrier-protected facility with free access to food and water. C57Bl/6J mice, *Cx3cr1*$^{GFP/GFP}$ mice (Jung et al., 2000; strain: B6.129P(Cg)-*Ptprc*^{a} *Cx3cr1*^{tm1Litt}/LittJ; stock number 008451) and *Ccr2*$^{RFP/RFP}$ mice (Saederup et al., 2010; strain: B6.129(Cg)-*Ccr2*$^{tm2.1Ifc}$/J; stock number 017586) were obtained from the Jackson Laboratory. Heterozygous *Cx3cr1*$^{+/GFP}$ mice were generated by cross-breeding homozygous *Cx3cr1*$^{GFP/GFP}$ mice with wild-type C57Bl/6J mice. Heterozygous *Cx3cr1*$^{+/GFP}$-*Ccr2*$^{+/RFP}$ mice were generated by cross-breeding homozygous *Cx3cr1*$^{GFP/GFP}$ mice with homozygous *Ccr2*$^{RFP/RFP}$ mice. *Trem2*$^{-/-}$ mice were generously provided by Marco Colonna of Washington University in St. Louis, MO. These transgenic strains have been bred for >10 generations so that their genetic background was assumed to be equivalent to C57Bl/6. All experiments involved adult (8-13 weeks old) male mice.

Genotyping

DNA for genotyping was extracted from ear punches harvested within the first three weeks of life. Primer sequences used to screen for individual genotypes are as follows:

Cx3cr1

Common: 5'-GGTTCCTAGTGGAGCTAGGG-3'

Reverse 1: 5'-TTCACGTTCGGTCTGGTGGG-3'

Reverse 2: 5'-GATCACTCTCGGCATGGACG-3'

Ccr2

Forward: 5'-TAAACCTGGTCACCACATGC-3'

Reverse 1: 5'-GGAGTAGAGTGGAGGCAGGA-3'

Reverse 2: 5'-CTTGATGACGTCCTCGGAG-3'

Trem2

Forward 1: 5'-CCCTAGGAATTCCTGGATTCTCCC-3'

Forward 2: 5'-TTACACAAGACTGGAGCCCTGAGGA-3'

Reverse: 5'-TCTGACCACAGGTGTTCCCG-3'

Spared Nerve Injury (SNI)

Surgery for spared nerve injury (SNI) was performed as previously described (Decosterd et al., 2000). Under 2.5% isoflurane anesthesia, an incision of < 1 cm in length was made in the left leg to expose the trifurcation of the sciatic nerve into the tibial, common peroneal and sural nerves. The tibial and common peroneal branches were tightly ligated using 6-0 nylon sutures (Ethicon) and transected distal to the site of ligation, leaving the sural branch intact (spared). Connective tissue and muscle were sutured using 5-0 Vicryl monofilament (Ethicon). Wound clips and Vetbond tissue adhesive were used to close skin incisions.

Intrathecal injection

Drugs were intrathecally administered as previously described (Njoo et al., 2014). Under 2.5% isoflurane anesthesia, the mouse was placed on its ventral side with a small gauze cushion under the hips to prop up the lower spine. The L6 spinous process was located through palpation and a 30G needle with beveled tip (BD Microlance) was used to inject 5 µl of the drug solution into the intrathecal space between the L5 and L6 vertebrae. A flick of the tail was used to confirm the entry of the needle through the dura and pia mater.

Tissue dissection, cryopreservation and sectioning

Under deep (5%) isoflurane anesthesia, mice underwent a thoracotomy and transcardiac perfusion with 50 ml of DPBS without divalent cations ($DPBS_{w/o}$, Invitrogen, catalog number 14190-235) containing 2mM EDTA then with 50 ml of 4% paraformaldehyde (PFA). Lumbar segments L4 and L5 of the spinal cord were then dissected, post-fixed in 4% PFA for 2 hours at 4°C and incubated in 30% sucrose overnight at 4°C. The following day, tissue was removed from the 30% sucrose solution, dried to remove any excess sucrose solution, embedded in Tissue-Tek OCT (VWR), flash-frozen over liquid nitrogen and stored in -80°C. Frozen, embedded spinal cord tissue was then cryosectioned into 10 µm thick tissue sections using a Leica CM3050S cryostat and stored at -80°C.

Immunohistochemistry (IHC)

Cryosections of 10 µm thickness from lumbar segment L4 of the mouse spinal cord were gradually brought to room temperature from -80°C before being briefly rinsed with PBS. Nonspecific protein binding sites were blocked for 1 hour at room temperature using 10% goat serum (ThermoFisher

Scientific) in PBS with 0.1% Triton X-100 (Sigma). After blocking, sections were incubated overnight at 4°C with primary antibody (see "Antibodies" for specific dilutions) and subsequently washed 3 times for 5 minutes each in PBS at room temperature (20-25°C) on a shaker set to 55rpm. Sections were incubated for 45 minutes at room temperature with secondary antibody (see "Antibodies" for specific dilutions) and washed again 3 times for 5 minutes each in PBS prior to mounting in either Vectashield (Vector Laboratories) or Prolong Gold (ThermoFisher). All immunohistochemistry presented throughout was generated following this protocol unless otherwise noted.

Immunocytochemistry (ICC)

Immunoselected microglia harvested and isolated as described above were cultured for 7 days on poly-D-lysine coated glass coverslips at a density of 120,000 cells/ml. Cells were then fixed with 4% paraformaldehyde in PBS for 20 minutes at room temperature (20-25°C) and subsequently washed 3 times for 5 minutes each in PBS before being incubated with blocking solution (10% goat serum in PBS with 0.1% Triton X-100) for 1 hour at room temperature. After blocking, cells were then incubated overnight in 4°C with primary antibody (see "Antibodies for specific dilutions) before being washed 3 times for 5 minutes each with PBS. Cells were then incubated for 40 minutes at room temperature with secondary antibody (see "Antibodies" for specific dilutions), washed 3 times for 5 minutes each in PBS and mounted onto glass slides using Vectashield with 4',6-diamidino-2-phenylindole (DAPI; Vector Laboratories).

Terminal deoxynucleotidyl transferase dUTP nick end labeling (TUNEL) assay

L4 segments from mouse spinal cord were cut into 10 μm cryosections, incubated in a pre-chilled (-20°C) mixture of 2:1 ethanol and acetic acid for 5 minutes at -20°C, rinsed twice in pre-chilled PBS (4°C) and probed for TUNEL using the ApopTag In Situ Apoptosis Detection Kit (EMD Millipore, catalog number S7110) according to the manufacturer's instructions. Sections were incubated with bisbenzimide (H33342; Calbiochem) to counterstain for chromatin and mounted using Vectashield (Vector Laboratories) or Prolong Gold (ThermoFisher Scientific). From a random starting location within the first 10 cryosections, we selected every tenth section for staining and counted TUNEL positive cell profiles in the dorsal horn of the spinal cord. Only TUNEL-positive profiles that also demonstrated chromatin changes indicative of apoptosis (specifically pyknosis, marginalization or fragmentation) were counted. The total number of cells counted in the L4 spinal cord of an animal was normalized to 10 sections for the means reported (total counts divided by the number of sections counted multiplied by 10). Within each assay, positive control stains were generated using DNase I (Sigma) and negative control stains were generated by omitting terminal deoxynucleotidyl transferase from the assay of sections treated with DNase I. Immunostaining of TUNEL sections with antibodies against NeuN, Iba1 or both was performed after the incubation with ethanol and acetic acid and before probing for TUNEL, following our standard protocol for immunohistochemistry.

Confocal Microscopy

All images were collected using an A1 confocal system (Nikon) equipped with 405 nm (100mW fiber output) diode laser; 458, 477, 488 and 514 nm (50 mW) multiline laser, 561 nm (20 mW) and 640 nm (100 mW) diode lasers; polarizing beam splitter and 32-channel detector. An Eclipse

Ti-E microscope (Nikon), QuantEM 512SC electron-multiplying CCD (EMCCD) camera (Photometrics) and NiS-Elements C software (Nikon) were used for acquiring all images at a resolution of 1,024 x 1,024 or 2,048 x 2,048 pixels and an image depth of 12 bit. During image acquisition, the gain was adjusted to avoid pixel saturation. Artificial colors were generated using ImageJ software (Schindelin et al., 2015).

Quantification of immunofluorescence

Spinal cord sections from 3-4 animals per experimental condition were imaged at an optical thickness of 1.0 μm on a confocal microscope. The ipsilateral dorsal quadrant of the spinal cord was outlined in ImageJ and the integrated density (fluorescence intensity) of the Iba1 signal within this region of interest (ROI) was measured. The integrated density threshold was standardized across all images to account for background signal.

Isolation of primary mouse microglia

Dissection and purification of primary mouse microglia were adapted for the spinal cord from previously described protocols (Cardona et al., 2006). Under deep (5%) isoflurane anesthesia, mice underwent a thoracotomy and transcardiac perfusion with 50 ml of $DPBS_{w/o}$ containing 2mM EDTA. Brain or spinal cord was dissected, the dura removed and the tissue was transferred to 6 ml of a working enzyme solution containing 0.2% Collagenase Type 4 (Worthington, catalog number LS004188) and 2.5mM calcium chloride in RPMI without phenol red + L-glutamine (Invitrogen, catalog number 11875-093). We intentionally excluded the enzyme dispase from the enzyme solution, because we found that dispase compromises the integrity of some cell surface proteins, e.g. Cd11b. Using a sterile razor blade, the tissue was minced in the enzyme solution then

incubated for 45 minutes at 37°C, with intermittent trituration using a 1 ml pipette every 10 minutes. Fifteen minutes before the end of the 45-minute incubation, 120 µl of 2 mg/ml DNase I was added to the solution. At the end of 45 minutes, one last trituration was performed and 3 ml of DEF solution (5mM EDTA and 1% Fetal Bovine Serum in $DPBS_{w/o}$) was added to the working enzyme solution. An additional 4.5 ml of physiologic Percoll solution [9 parts Percoll (Sigma) and 1 part 10x $DPBS_{w/o}$] was added and the cell suspension transferred to a 15 ml falcon tube and thoroughly mixed. Then 2 ml of $DPBS_{w/o}$ were carefully added on top of the combined enzyme solution creating two distinct layers. The tube was then spun down at 500 g for 30 minutes at 18°C with the brake set to 0. Debris and supernatant were aspirated. The pellet was resuspended in 2 ml of DPBSw/o and spun down again at 500 g for 7 minutes at 18°C. The supernatant was aspirated and the cell pellet was then further processed for cell culture or flow cytometry (see corresponding sections below).

Cell culture of primary microglia

After extraction and enrichment of microglia from the mouse CNS (see above), the cell pellet was resuspended in 90 µl of MACS buffer [0.5% Bovine Serum Albumin (Sigma) and 2mM EDTA (ThermoFisher Scientific) in $DPBS_{w/o}$]. Ten µl of anti-Cd11b microbeads (Miltenyi, catalog number 130-049-601) were added and mixed. The cells and microbeads-containing suspension was incubated at 4°C for 15 minutes with gentle mixing every 5 minutes. After adding 1 ml of MACS buffer, the suspension was then spun down for 10 minutes at 300 g at 18°C. After aspirating the supernatant, the resulting cell pellet was resuspended in 500 µl of MACS buffer. Using a MiniMACS Starting Kit (Miltenyi, catalog number 130-090-312), an MS column was set up in the MiniMACS separator attached to the MultiStand and rinsed with 500 µl of MACS buffer. The 500

μl of the cells-microbeads suspension were applied through a pre-separation filter (Miltenyi, catalog number 130-101-812) to the pre-rinsed column and allowed to flow through completely. The column was then rinsed 3 more times with 500 μl of MACS buffer. After removing the column from the magnetic holder and out of the magnetic field entirely, 1 ml of MACS buffer was added to the column and pushed through forcibly using a column plunger. The cells were spun down for 10 minutes at 300 g at 18°C. The resulting cell pellet was resuspended in microglia culturing medium or MCM [10% FBS (Sigma), 1% Penicillin/Streptomycin (ThermoFisher Scientific), 1% Microglia Growth Supplement (ScienCell) in DMEM/F-12 + Glutamax (ThermoFisher Scientific) supplemented with 10 ng/ml of recombinant mouse colony stimulating factor 1 (Csf1, R&D Systems) and 50 ng/ml of recombinant transforming growth factor-beta (Tgfβ, Miltenyi)]. Cells were grown on poly-D-lysine-coated 6- or 24-well plates at a density of 120,000 cells/ml.

Flow cytometry

After extraction of microglia from the mouse CNS (see above), the cell pellet was resuspended in 100 μl of Cell Staining Buffer (Biolegend, catalog number 420201). TruStain fcX anti-mouse CD16/32 (Biolegend, catalog number 101319) was added in a 1:100 dilution as a blocking reagent and the suspension was incubated in the dark on ice for 20 minutes. The suspension was subsequently diluted in Cell Staining Buffer to obtain aliquots 100 μl per staining condition, including IgG control stains. The suspensions were incubated with corresponding conjugated antibodies (see "Antibodies" for specific dilutions) in the dark on ice for 30 minutes. When using unconjugated primary antibodies, suspensions were further diluted with 1 ml of Cell Staining Buffer, centrifuged at 300 g at 4°C for 10 minutes, resuspended in 100 μl of Cell Staining Buffer and incubated with fluorescently conjugated secondary antibodies (see "Antibodies" for specific

dilutions) in the dark on ice for 20 minutes. After incubation with the respective antibodies, all cell suspension samples were diluted with 1 ml of Cell Staining Buffer and centrifuged at 300 g at 4°C for 10 minutes. Cell pellets were resuspended in 100 μl of Cell Staining Buffer containing 0.1 μg of DAPI and gently mixed. All samples were analyzed on a Beckman Coulter MoFlo Astrios FACS machine using Summit software for processing of data. Raw data files were subsequently processed in FlowJo software version 10.

Western Blotting

Protein lysate was extracted from harvested tissue by homogenization using a Potter-Elvehjem tissue grinder and a saponin-based lysis buffer consisting of 5 mM Tris-HCl (pH 8.0), 50 mM sodium chloride, 0.01% sodium azide, 0.05% saponin, 0.25% triton, 0.25% sodium deoxycholate, 25mM Tris base, 0.5% Igepal, 0.5mM EDTA in ultrapure milli-Q water containing phosphatase inhibitor cocktails 2 and 3 (Sigma, catalog numbers P5726 and P0044) and mini EDTA-free protease inhibitor tablet (Roche). Homogenized tissue was incubated in lysis buffer on ice for 30 minutes, spun down at 4000 g for 30 minutes at 4°C and supernatant containing the protein lysate was saved. Protein concentration was determined using the Pierce protein assay and samples were prepared with LDS sample buffer and reducing agent (both from ThermoFisher Scientific), such that 10 μg of protein were loaded (after denaturation for 5 minutes at 95°C) into each well of a NuPAGE 4-12% Bis-Tris protein gel (ThermoFisher Scientific). The electrophoresis chamber was filled with MOPS running buffer (ThermoFisher Scientific) and antioxidant added to the buffer solution in the inner chamber of the gel box. Samples were run at 170V for 60 minutes before being transferred to a polyvinylidene fluoride membrane (EMD Millipore). NuPAGE transfer buffer (ThermoFisher Scientific) containing 10% methanol and 0.1% antioxidant was used for the

transfer performed at 30V for 60 minutes. Membranes were briefly rinsed in tris-buffered saline (TBS) before being incubated with Odyssey blocking buffer (Li-Cor, catalog number 927-40100) for 1 hour at room temperature (20-25°C) on a shaker set to 60 rpm. After blocking, membranes were incubated in primary antibody diluted in TBS with 0.1% Tween-20 for 2 hours at room temperature (see "Antibodies" for specific dilutions) and washed 3 times for 5 minutes each in TBS with 0.1% Tween-20. Membranes were then incubated in secondary antibody diluted in TBS with 0.1% Tween-20 and 0.02% SDS (see "Antibodies" for specific dilutions) before being washed 3 times for 5 minutes each in TBS with 0.1% Tween-20. The membranes were imaged using an Odyssey CLx system (Li-Cor) and ImageStudioLite software.

RNA extraction and analysis

Tissue harvested from lumbar segments L4 and L5 of the mouse spinal cord was homogenized in QIAzol lysis reagent (Qiagen, catalog number 79306) using a PowerGen 125 tissue homogenizer. RNA was extracted and purified using an RNeasy Mini Kit (Qiagen, catalog number 74104) according to the manufacturer's instructions. Tissue from the ipsilateral dorsal horns of L4 and L5 lumbar spinal cord segments from 2 mice were pooled for each RNA sample. Purity and integrity of RNA were verified using the Agilent Bioanalyzer Chip (Columbia Genome Center). RNA samples were sequenced by the Columbia Genome Center using a HiSeq2000 system (Illumina). The Columbia Genome Center employed the TopHat 2.0.4 algorithm to map reads to the mouse genome and the Cufflinks 2.0.2 software program to infer expression level and examine differential expression. Functional gene annotations and pathway analyses were performed and identified using the Database for Annotation, Visualization and Integrated Discovery or DAVID (Huang da W et al., 2009). Figures and graphical representations of RNA sequencing data were

generated using GraphPad Prism as well as the GenePattern software (Broad Institute). For quantitative real-time (qRT-)PCR analysis, the Applied Biosystems 7500 Quantitative Realtime PCR System was used in accordance with the manufacturer's instructions using Fast SYBR Green Master Mix (ThermoFisher Scientific, catalog number 4385612). All qRT-PCR values were normalized to *Gapdh* for analysis. Primers used for qPCR analysis include:

Trem2

Forward: 5'-CGAGAGGCTGAGGTCCTGCAGAAA-3'

Reverse 1: 5'-TGTGTTCCACTTGGGCACCCTCGAAA-3'

Tyrobp

Forward: 5'-GATTGCCCTGGCTGTGTACTCTCT-3'

Reverse: 5'-GCCTCTGTGTGTTGAGGTCACTGTATACTT-3'

Syk

Forward: 5'-GAGCAGACGGTCCTCATAGGGTCAAAGA-3'

Reverse: 5'-TCCCTGTCAATGCGGTAGTGCAATACTT-3'

Csf1r

Forward: 5'-CGAGGGAGACTCCAGCTACAAGAACAT-3'

Reverse: 5'-ACTTGAAGAAGTCGAGACAGGCCTCAT-3'

Cx3cr1

Forward: 5'-GGTGAGTGACTGGCACTTCCTGCAGAA-3'

Reverse: 5'-CCCAAATAACAGGCCTCAGCAGAATCGTCATA-3'

Gapdh

Forward: 5'-CACAATTTCCATCCCAGACC-3'

Reverse: 5'-GTGGGTGCAAACTTTAT-3'

Antibodies

Listed below are antibodies used for IHC, ICC, Western blotting and flow cytometry:

IHC

Cd11b (Bio-Rad, catalog number MCA74G) – 1:500

Iba1 (Wako, catalog number 016-26721) – 1:500

NeuN (EMD Millipore, catalog number MAB377) – 1:5000

Goat anti-rabbit Alexa Fluor 488 (ThermoFisher, catalog number A11008) – 1:500

Goat anti-rabbit Alexa Fluor 594 (ThermoFisher, catalog number A11012) – 1:500

Goat anti-mouse Alexa Fluor 594 (ThermoFisher, catalog number A11005) – 1:500

Donkey anti-rat Alexa Fluor 594 (ThermoFisher, catalog number A21209) – 1:500

ICC

Iba1 (Wako, catalog number 016-26721) – 1:200

Trem2 (R&D Systems, catalog number MAB17291) – 1:200

Goat anti-rabbit Alexa Fluor 488 (ThermoFisher, catalog number A11008) – 1:400

Donkey anti-rat Alexa Fluor 594 (ThermoFisher, catalog number A21209) – 1:400

Western Blotting

Trem2 (Santa Cruz, catalog number sc-48765) – 1:1000

β-tubulin III (Sigma, catalog number T8578) – 1:5000

Goat anti-mouse 680RD (Odyssey, catalog number 925-68070) – 1:10,000

Goat anti-rabbit 800CW (Odyssey, catalog number 925-32211) – 1:10,000

Flow cytometry

TruStain fcX anti-mouse CD16/32 (Biolegend, catalog number 101319) – 1:100

APC anti-Cd11b (Biolegend, catalog number 101212) – 1:100

PE anti-Cx3cr1 (Biolegend, catalog number 149005) – 1:100

AF647 anti-Ccr2 (Biolegend, catalog number 150603) – 1:100

PE anti-CD39 (Biolegend, catalog number 143803) – 1:100

PECy7 anti-CD45 (Biolegend, catalog number 103113) – 1:100

FITC anti-Ly6c (Biolegend, catalog number 128005) – 1:100

Trem2 (R&D Systems, catalog number MAB17291) – 1:200

PECy7 goat anti-rat IgG (Biolegend, catalog number 405413) – 1:100

APC rat IgG2c isotype control (Biolegend, catalog number 400713) – 1:100

PE rat IgG2a isotype control (Biolegend, catalog number 400507) – 1:100

PECy7 rat IgG2a isotype control (Biolegend, catalog number 400521) – 1:100

FITC mouse IgG2a isotype control (Biolegend, catalog number 400207) – 1:100

The intrathecally administered monoclonal antibody targeting Trem2 (Bio-Rad, catalog number MCA4772) as well as the corresponding isotype control antibody (rat IgG1, Bio-Rad, catalog number MCA1211) were diluted in sterile saline and injected in a volume of 5 μl for a total administration of 1 μg of Ig per injection.

Drugs

PLX5622: The Csf1r antagonist PLX5622 was provided by Plexxikon, Inc. The drug was formulated into AIN-76A irradiated chow at a dose of 1200 mg/kg. To allow for complete depletion of microglia, animals were fed PLX5622 for 21 days prior to SNI. Treatment with PLX5622-containing chow or AIN-76A control chow was continued after SNI until euthanasia to maintain microglial depletion throughout the duration of the study.

NP-1815-PX: The P2x4r antagonist NP-1815-PX was provided by Nippon Chemiphar. The lyophilized powder was reconstituted into a 6 mM stock. Thirty pmol of NP-1815-PX diluted in 5 μl of sterile saline were intrathecally injected and all behavioral studies were carried out within 90-180 minutes of the injection.

Behavioral Tests

In compliance with the ARRIVE guidelines (Kilkenny et al, 2010), mice were randomly allocated to experimental conditions and investigators blinded to the allocation during outcome assessment. Mice examined for pain-like behavior were randomly assigned to test boxes. To assess the mechanical withdrawal threshold of the mice, calibrated von Frey filaments were applied to the plantar surface of the hind paw within the projection territory of the spared sural nerve. The up-down method was applied for the threshold determination as previously described (Chaplan et al, 1994). Cold sensitivity was tested by applying a drop of acetone, which produces a cooling sensation upon evaporation, to the same region of hind paw and recording the duration of withdrawal responses within one minute after the application. Withdrawal responses included shaking, licking or biting the affected paw. Prior to SNI, all animals to be used for behavioral testing underwent habituation to the experimental setting as well as 2 baseline readings for each experimental output.

Statistical analysis

All statistical tests were performed using GraphPad Prism software Version 7.0. Normal distribution of data and equal variances across groups were assumed, but not tested. For comparisons of 2 experimental conditions, an unpaired two-tailed Student's *t* test was used. For

comparisons of > 2 experimental conditions, a one-way analysis of variance (ANOVA) was used, followed by Dunnett's or Tukey's test for multiple comparisons. To compare different experimental conditions over time, a two-way ANOVA was used, followed by Sidak's or Bonferroni's test for multiple comparisons. Specific details of each statistical analysis can be found within the associated results section and corresponding figure legends.

REFERENCES

Affram KO, Mitchell K, and Symes AJ (2017). Microglial activation results in inhibition of TGF-β-regulated gene expression. *J Mol Neurosci* 63(3-4):308-319.

Asea A, Rehli M, Kabingu E, Boch JA, Baré O, Auron PE, Stevenson MA, and Calderwood SK. (2002). Novel signal transduction pathway utilized by extracellular Hsp70: Role of toll like receptor (Tlr) 2 and Tlr4. *J Biol Chem* 277: 15028-15034.

Atagi Y, Liu, CC, Painter MM, Chen XF, Verbeeck C, Zheng H, Li X, Rademakers R, Kang SS, Xu H, Younkin S, Das P, Fryer JD, and Bu G. (2015). Apolipoprotein E is a ligand for triggering receptor expressed on myeloid cells 2 (Trem2). *J Biol Chem* 290(43): 26043 50.

Azkue JJ, Zimmermann M, Hsieh TF, and Herdegen T. (1998). Peripheral nerve insult induces NMDA receptor-mediated delayed degeneration in spinal neurons. *European J of Neurosci* 10: 2204-2206.

Bailey CC, DeVaux LB, and Farzan M. (2015). The triggering receptor expressed on myeloid cells 2 binds apolipoprotein E. *J Biol Chem* 290(43): 26033-42.

Beggs S, Liu XJ, Kwan C, and Salter MW. (2010). Peripheral nerve injury and TRPV1-expressing primary afferent C-fibers cause opening of the blood-brain barrier. *Mol Pain* 6: 74.

Bennett MI, Rayment C, Hjermstad M, Aass N, Caraceni A, and Kaasa S. (2012). Prevalence and aetiology of neuropathic pain in cancer patients: a systematic review. *Pain* 153(2): 359-65.

Bettoni I, Comelli F, Rossini C, Granucci F, Giagnoni G, Peri F, and Costa B. (2008). Glial Tlr4 receptor as new target to treat neuropathic pain: efficacy of a new receptor antagonist in a model of peripheral nerve injury in mice. *Glia* 56(12): 1312-9.

Bhattacharya A and Biber K. (2016). The microglial ATP-gated ion channel P2X7 as a CNS drug target. *Glia* 64: 1772-1787.

Binder A and Baron R. (2016). The pharmacological therapy of chronic neuropathic pain. *Dtsch Atztebl Int* 113(37): 616-625.

Bohlen CJ, Bennett FC, Tucker AF, Collins HY, Mulinyawe SB, and Barres BA. (2017). Diverse requirements for microglial survival, specification and function revealed by defined-medium cultures. *Neuron* 94(4): 759-773.e8.

Bourquin AF, Süveges M, Pertin N, Gilliard N, Sardy S, Davison AC, Spahn DR, and Decosterd I. (2006). Assessment and analysis of mechanical allodynia-like behavior induced by spared nerve injury (SNI) in the mouse. *Pain* 122(1-2): 14.e1-14.

Butovsky O, Jedrychowski MP, Moore CS, Cialic R, Lanser AJ, Gabriely G, Koeglsperger T, Dake B, Wu PM, Doykan CE, Fanek Z, Liu L, Chen Z, Rothstein JD, Ransohoff RM, Gygi SP, Antel JP, and Weiner HL. (2014). Identification of a unique TGF-β-dependent molecular and functional signature in microglia. *Nat Neurosci* 17(1):131-43.

Calvo M, Zhu N, Grist J, Ma Z, Loeb JA, and Bennett DLH. (2011) Following nerve injury neuregulin-1 drives microglial proliferation and neuropathic pain via the MEK-ERK pathway. *Glia* 59(4): 554-568.

Cardona AE, Huang D, Sasse ME, and Ransohoff RM. (2006). Isolation of murine microglial cells for RNA analysis or flow cytometry. *Nat Protoc* 1(4):1947-51.

Chaplan SR, Bach FW, Pogrel JW, Chung JM, and Yaksh TL. Quantitative assessment of tactile allodynia in the rat paw. *J Neurosci Methods* 53:55-63.

Chen NF, Huang SY, Chen WF, Chen CH, Lu CH, Chen CL, Yang SN, Wang HM, and Wen ZH. (2013). TGF-β1 attenuates spinal neuroinflammation and the excitatory amino acid system in rats with neuropathic pain. *Pain* 14(12): 1671-1685.

Chen NF, Chen WF, Sun CS, Lu CH, Chen CL, Hung HC, Feng CW, Chen CH, Tsui KH, Kuo HM, Wang HM, Wen ZH, and Huang SY. (2016) Contributions of p38 and ERK to the antinociceptive effects of TGF-β1 in chronic constriction injury-induced neuropathic rats. *J Headache Pain* 17(1): 72.

Cho SH, Sun B, Zhou Y, Kauppinen TM, Halabisky B, Wes P, Ransohoff RM, and Gan L. (2011). Cx3cr1 protein signaling modulates microglial activation and protects against plaque independent cognitive deficits in a mouse model of alzheimer's disease. *J Biol Chem* 286: 32713-32722.

Clark AK, Yip PK, Grist J, Gentry C, Staniland AA, Marchand F, Dehvari M, Wotherspoon G, Winter J, Ullah J, Bevan S, and Malcangio M. (2007). Inhibition of spinal microglial cathepsin S for the reversal of neuropathic pain. *Proc Natl Acad Sci U S A* 104(25):10655 60.

Clark AK, Yip PK, and Malcangio M. (2009). The liberation of fractalkine in the dorsal horn requires microglial cathepsin S. *J Neurosci* 29(21): 6945-54.

Clark AK, Wodarski R, Guida F, Sasso, and Malcangio M. (2010). Cathepsin S release from primary cultured microglia is regulated by the P2x7 receptor. *Glia* 58(14) 1710-26.

Clark AK and Malcangio M. (2012). Microglia signalling mechanisms: Cathepsin S and fractalkine. *Exp Neurol* 234(2): 283-92.

Coull JA, Beggs S, Boudreau D, Boivin D, Tsuda M, Inoue K, Gravel C, Salter MW, and De Koninck Y. (2005). BDNF from microglia causes the shift in neuronal anion gradient underlying neuropathic pain. *Nature* 438(7070): 1017-21.

Decosterd I and Woolf CJ. (2000). Spared nerve injury: an animal model of persistent peripheral neuropathic pain. *Pain* 87(2): 149-58.

DeLeo JA and Yezierski RP. (2001). The role of neuroinflammation and neuroimmune activation in persistent pain. *Pain* 90(1-2): 1-6.

DiBonaventura MD, Sadosky A, Concialdi K, Hopps M, Kudel I, Parsons B, Cappelleri JC, Hlavacek P, Alexander AH, Stacey BR, Markman JD, and Farrar JT. (2017). The prevalence of probably neuropathic pain in the US: results from a multimodal general population health survey. *J Pain Res* 10: 2525-2538.

Dybdahl B, Wahba A, Lien E, Flo TH, Waage A, Qureshi N, Sellevold OF, Espevik T, and Sundan A. (2002). Inflammatory response after open heart surgery: release of heat-shock protein 70 and signaling through toll-like receptor-4. *Circulation* 105(6):685-90.

Echeverry S, Shi XQ, Haw A, Liu H, Zhang ZW, and Zhang J. (2009). Transforming growth factor-beta1 impairs neuropathic pain through pleiotropic effects. *Mol Pain* 5:16.

Echeverry S, Shi XQ, Rivest S, and Zhang J. (2011). Peripheral nerve injury alters blood-spinal cord barrier functional and molecular integrity through a selective inflammatory pathway. *J Neurosci* 31(30):10819-28.

Echeverry S, Shi XQ, Yang M, Huang H, Wu Y, Lorenzo LE, Perez-Sanchez J, Bonin RP, De Koninck Y, and Zhang J. (2017). Spinal microglia are required for long-term maintenance of neuropathic pain. *Pain* 158(9): 1792-1801.

Erblich B, Zhu L, Etgen AM, Dobrenis K, and Pollard JW. (2011) Absence of colony stimulating factor-1 receptor results in loss of microglia, disrupted brain development and olfactory deficits. *PLoS One* 6(10): e26317.

Finnerup NB, Haroutounian S, Kamerman P, Baron R, Bennett DL, Bouhassira D, Cruccu G, Freeman R, Hansson P, Nurmikko T, Raja SN, Rice AS, Serra J, Smith BH, Treede RD, and Jensen TS. (2016) Neuropathic pain: an updated grading system for research and clinical practice. *Pain* 157(8): 1599-606.

Frakes AE, Ferraiuolo L, Haidet-Phillips AM, Schmelzer L, Braun L, Miranda CJ, Ladner KJ, Bevan AK, Foust KD, Godbout JP, Popovich PG, Guttridge DC, and Kaspar BK. (2014). Microglia induce motor neuron death via the classical NF-κB pathway in amyotrophic lateral sclerosis. *Neuron* 81(5): 1009-1023.

Gattlen C, Clarke CB, Piller N, Kirschmann G, Pertin M, Decosterd I, Gosselin RD, and Suter MR. (2016). Spinal cord T-cell infiltration in the rat spared nerve injury model: a time course study. *Int J Mol Sci* 17(3): 352.

Gorina R, Font-Nieves M, Márquenz-Kisinousky L, Santalucia T, and Planas AM. (2011). Astrocyte TLR4 activation induces a proinflammatory environment through the interplay between MyD88-dependent NFκB signaling, MAPK, and Jak1/Stat1 pathways. *Glia* 59(2) 242-55.

Gu N, Peng J, Murugan M, Wang X, Eyo UB, Sun D, Ren Y, DiCicco-Bloom E, Young W, Dong H, and Wu LJ. (2016) Spinal microgliosis due to resident microglial proliferation is required for pain hypersensitivity after peripheral nerve injury. *Cell Reports* 16(3): 605-14.

Guan Z, Kuhn JA, Wang X, Colquitt B, Solorzano C, Vaman S, Guan AK, Evans-Reinsch Z, Braz J, Devor M, Abboud-Werner SL, Lanier LL, Lomvardas S, and Basbaum AI. (2016). Injured sensory neuron-derived Csf1 induces microglial proliferation and Dap12-dependent pain. *Nat Neurosci* 19(1): 94-101.

Hamerman JA, Jarjoura JR, Humphrey MB, Nakamura MC, Seaman WE, and Lanier LL. (2006). Cutting Edge: Inhibition of TLR and FcR responses in macrophages by triggering receptor expressed on myeloid cells (Trem)-2 and Dap12. *J Immunol* 177(4):2051-2055.

Hamzei Taj S, Kho W, Riou A, Wiedermann D, and Hoehn M. (2016). MiRNA-124 induces neuroprotection and functional improvement after focal cerebral ischemia. *Biomaterials* 91: 151-165.

Harrison JK, Jiang Y, Chen S, Xia Y, Maciejewski D, McNamara RK, Streit WJ, Salafranca MN, Adhikari S, Thompson DA, Botti P, Bacon KB, and Feng L. (1998) Role for neuronally derived fractalkine in mediating interactions between neurons and Cx3cr1-expressing microglia. *Proc Natl Acad Sci U S A* 95(18): 10896-901.

Hoebe K, Du X, Georgel P, Janssen E, Tabeta K, Kim SO, Goode J, Lin P, Mann N, Mudd S, Crozat K, Sovath S, Han J, and Beutler B. (2003). Identification of Lps2 as a key transducer of MyD88-independent TIR signaling. *Nature* 424(6950): 743-8.

Hsieh CL, Koike M, Spusta SC, Niemi EC, Yenari M, Nakamura MC, and Seaman WE. (2009) A role for Trem2 ligands in the phagocytosis of apoptotic neuronal cells by microglia. *J Neurochem* 109(4): 1144-56.

Hu X, Leak RK, Shi Y, Suenaga J, Gao Y, Zheng P, and Chen J. (2014). Microglial and macrophage polarization – new prospects for brain repair. *Nat Review Neurol* 11: 56-64.

Huang da W, Sherman BT, Zheng X, Yang J, Imamichi T, Stephens R, and Lempicki RA. (2009). Extracting biological meaning from large gene lists with DAVID. *Curr Protoc Bioinformatics* Chapter 13: Unit 13.11.

Inquimbert P, Moll M, Latremoliere A, Tong CK, Whang J, Sheehan GF, Smith BM, Korb E, Athie MCP, Babaniyi O, Ghasemlou N, Yanagawa Y, Allis CD, Hof PR, and Scholz J. (2018). NMDA receptor activation underlies the loss of spinal dorsal horn neurons and the transition to persistent pain after peripheral nerve injury. *Cell Reports* 23: 2678-2689.

Jack GD, Zhang L, and Friedman AD. (2009). M-CSF elevates c-Fos and phosphor-C/EBPalpha(S21) via ERK whereas G-CSF stimulates SHP2 phosphorylation in marrow progenitors to contribute to myeloid lineage specification. *Blood* 114(10): 2172-80.

Ji RR, Berta T, and Nedergaard M. (2014). Glia and pain: Is chronic pain a gliopathy? *Pain* 154(0_1): S10-S28.

Ji LJ, Shi J, Lu JM, and Huang QM. (2018). MiR-150 alleviates neuropathic pain via inhibiting toll-like receptor 5. *J Cell Biochem* 119(1): 1017-1026.

Jiang T, Zhang YD, Chen Q, Gao Q, Zhu XC, Zhou JS, Shi JQ, Lu H, Tan L, and Yu JT. (2016). Trem2 modifies microglial phenotype and provides neuroprotection in P301S tau transgenic mice. *Neuropharmacology* 105: 196-206.

Jung S, Aliberti J, Graemmel P, Sunshine MJ, Kreutzberg GW, Sher A, and Littman DR. (2000). Analysis of fractalkine receptor Cx3cr1 function by targeted deletion and green fluorescent protein reporter gene insertion. *Mol Cell Biol* 20(11): 4106-4114.

Kahle KT, Khanna A, Clapham DE, and Woolf CJ. (2014). Theapeutic restoration of spinal inhibition via druggable enhancement of potassium-chloride cotransporter Kcc2-mediated chloride extrusion in peripheral neuropathic pain. *JAMA Neurol* 71(5): 640-645.

Kawabori M, Kacimi R, Kauppinen T, Calosing C, Kim JY, Hsieh CL, Nakamura MC, and Yenari MA. (2015). Triggering receptor expressed on myeloid cells 2 (Trem2) deficiency attenuates phagocytic activities of microglia and exacerbates ischemic damage in experimental stroke. *J Neurosci* 35(8): 3384-96.

Keren-Shaul H, Spinrad A, Weiner A, Matcovitch-Natan O, Dvir-Szternfeld R, Ulland TK, David E, Baruch K, Lara-Atstaiso D, Toth B, Itzkovitz S, Colonna M, Schwartz M, and Amit I. (2017). A unique microglia type associated with restricting development of Alzheimer's disease. *Cell* 169(7): 1276-1290.e17.

Kilkenny C, Browne W, Cuthill IC, Emerson M, and Altman DG. (2010). Animal research: Reporting in vivo experiments: The ARRIVE guidelines. *Br J Pharmacol* 160(7): 1577 1579.

Kim D, Kim MA, Cho IH, Kim MS, Lee S, Jo EK, Choi SY, Park K, Kim JS, Akira S, Na HS, Oh SB, and Lee SJ. (2007). A critical role of toll-like receptor 2 in nerve injury-induced spinal cord glial cell activation and pain hypersensitivity. *J Biol Chem* 282(20):14975-83.

Kim SM, Mun BR, Lee SJ, Joh Y, Lee HY, Ji KY, Choi HR, Lee EH, Kim EM, Jang JH, Song HW, Mook-Jung I, Choi WS, and Kang HS. (2017). Trem2 promotes Aβ phagocytosis by upregulating C/EBPα-dependent CD36 expression in microglia. *Sci Rep* 7(1): 11118.

Kleinberger G, Yamanishi Y, Suárez-Calvet M, Czirr E, Lohmann E, Cuyvers E, Struyfs H, Pettkus N, Wenninger-Weinzierl A, Mazaheri F, Tahirovic S, Lleó A, Alcolea D, Fortea J, Willem M, Lammich S, Molinuevo JL, Sánchez-Valle R, Antonell A, Ramirez A, Heneka MT, Sleegers K, van der Zee J, Martin JJ, Engelborghs S, Demirtas-Tatlidede A, Zetterberg H, Van Broeckhoven C, Gurvit H, Wyss-Coray T, Hardy J, Colonna M, and Haass C. (2014). Trem2 mutations implicated in neurodegeneration impair cell surface transport and phagocytosis. *Sci Transl Med* 6(243): 243ra86.

Kobayashi M, Konishi H, Sayo A, Takai T, and Kiyana H. (2016). Trem2-Dap12 signal elicits proinflammatory response in microglia and exacerbates neuropathic pain. *J Neurosci* 36(43): 11138-11150.

Kober DL, Alexander-Brett JM, Karch CM, Cruchaga C, Colonna M, Holtzman MJ, and Brett TJ. (2016). Neurodegenerative disease mutations in Trem2 reveal a functional surface and distinct loss-of-function mechanisms. *eLife* 5:e20391.

Kohama I, Ishikawa K, and Kocsis JD. (2000). Synaptic reorganization in the substantia gelatinosa after peripheral nerve neuroma formation: aberrant innervation of lamina II neurons by Aβ afferents. *J Neurosci* 20(4): 1538-1549.

Krasemann S, Madore C, Cialic R, Baufeld C, Calcagno N, El Fatimy R, Beckers L, O'Loughlin E, Xu Y, Fanerk Z, Greco DJ, Smith ST, Tweet G, Humulock Z, Zrzavy T, Conde Sanroman P, Gacias M, Weng Z, Chen H, Tjon E, Mazaheri F, Hartmann K, Madi A, Ulrich JD, Glatzel M, Worthmann A, Heeren J, Budnik B, Lemere C, Ikezu T, Heppner FL, Litvak V, Holtzman DM, Lassmann H, Weiner HL, Ochando J, Haass C, and Butovsky O. (2017). The Trem2-ApoE pathway drives the transcriptional phenotype of dysfunctional microglia in neurodegenerative diseases. *Immunity* 47(3): 566-581.

Lee SH, Shi XQ, Fan A, West B, and Zhang J. (2018). Targeting macrophage and microglia activation with colony stimulating factor 1 receptor inhibitor is an effective strategy to treat injury-triggered neuropathic. *Mol Pain* 14:1744806918764979.

Li J, Simone DA, and Larson AA. (1999). Windup leads to characteristics of central sensitization. *Pain* 79(1): 75-82.

Li YQ, Chen P, Haimovitz-Friedman A, Reilly RM, and Wong CS. (2003). Endothelial apoptosis initiates acute blood-brain barrier disruption after ionizing radiation. *Cancer Res* 63(18): 5950-6.

Li YQ, Chen P, Jain V, Reilly RM, and Wong CS. (2004). Early radiation-induced endothelial cell loss and blood-spinal cord barrier breakdown in the rat spinal cord. *Radiat Res* 161(2): 143-52.

Liu T, Jiang CY, Fujita T, Luo SW, and Kumamoto E. (2013). Enhancement by interleukin-1β of AMPA and NMDA receptor-mediated currents in adult rat spinal superficial dorsal horn neurons. *Mol Pain* 9:16.

Liu XJ, Liu T, Chen G, Wang B, Yu XL, Yin C, and Ji RR. (2016). TLR signaling adaptor protein MyD88 in primary sensory neurons contributes to persistent inflammatory and neuropathic pain and neuroinflammation. *Sci Rep* 6: 28188.

Mason LH, Willette-Brown J, Taylor LS, and McVicar DW. (2006). Regulation of Ly49D/Dap12 signal transduction by Src-family kinases and CD45. *J Immunol* 176(11): 6615-23.

Masuda T, Tsuda M, Yoshinaga R, Tozaki-Saitoh H, Ozato K, Tamura T, and Inoue K. (2012). Irf8 is a critical transcription factor for transforming microglia into a reactive phenotype. *Cell Rep* 1(4): 334-340.

Masuda T, Iwamoto S, Yoshinaga R, Tozaki-Saitoh H, Nishiyama A, Mak TW, Tamura T, Tsuda M, and Inoue K. (2014). Transcription factor IRF5 drives P2x4r+-reactive microglia gating neuropathic pain. *Nat Commun* 5: 3771.

Matsumura Y, Yamashita T, Sasaki A, Nakata E, Kohno K, Masuda T, Tozaki-Saitoh H, Imai T, Kuraishi Y, Tsuda M, and Inoue K. (2016). A novel P2x4 receptor-selective antagonist produces anti-allodynic effect in a mouse model of herpetic pain. *Sci Rep* 6: 32461.

Milligan ED, Zapata V, Chacur M, Schoeniger D, Biedenkapp J, O'Connor KA, Verge GM, Chapman G, Green P, Foster AC, Naeve GS, Maier SF, and Watkins LR. (2004). Evidence that exogenous and endogenous fractalkine can induce spinal nociceptive facilitation in rats. *Eur J Neurosci* 20(9): 2294-302.

Moore KA, Kohno T, Karchewski LA, Scholz J, Baba H, and Woolf CJ. (2002). Partial peripheral nerve injury promotes a selective loss of GABAergic inhibition in the superficial dorsal horn of the spinal cord. *J Neurosci* 22(15): 6724-31.

Mossadegh-Keller N, Sarrazin S, Kandalla PK, Espinosa L, Stanley ER, Nutt SL, Moore J, and Sieweke MH. (2013). M-CSF instructs myeloid lineage fate in single haematopoietic stem cells. *Nature* 497(7448): 239-43.

Njoo C, Heinl C, and Kuner R. (2014). In vivo siRNA transfection and gene knockdown in spinal cord via rapid noninvasive lumbar intrathecal injections in mice. *J Vis Exp* (85).

Okubo M, Yamanaka H, Kobayashi K, Dai Y, Kanda H, Yagi H, and Noguchi K. (2016). Macrophage-colony stimulating factor derived from injured primary afferent induces proliferation of spinal microglia and neuropathic pain in rats. *PLoS One* 11(4): e0153375.

Oshiumi H, Sasai M, Shida K, Fujita T, Matsumoto M, and Seya T. (2003). TIR-containing adapter molecular (TICAM)-2, a bridging adapter recruiting to toll-like receptor 4 TICAM-1 that induces interferon-beta. *J Biol Chem* 278(50): 49751-62.

Pabon MM, Bachstetter AD, Hudson CE, Gemma C, and Bickford PC. (2011). Cx3cl1 reduces neurotoxicity and microglial activation in a rat model of Parkinson's disease. *J Neuroinflammation* 8:9.

Painter MM, Atagi Y, Liu CC, Rademakers R, Xu H, Fryer JD, and Bu G. (2015). Trem2 in CNS homeostasis and neurodegenerative disease. *Mol Neurodegener* 10:43.

Paradowska-Gorycka A and Jurkowska M. (2013). Structure, expression pattern and biological activity of molecular complex Trem2-Dap12. *Hum Immunol* 74(6): 730-7.

Park JS, Svetkauskaite D, He Q, Kim JY, Strassheim D, Ishizaka A, and Abraham E. (2004). Involvement of toll-like receptors 2 and 4 in cellular activation by high mobility group box 1 protein. *J Biol Chem* 279(9): 7370-7.

Park CK, Lü N, Xu ZZ, Liu T, Serhan CN, and Ji RR. (2011). Resolving TRPV1- and TNF-α-mediated spinal cord synaptic plasticity and inflammatory pain with neuroprotection D1. *J Neurosci* 31(42): 15072-85.

Parkhurst CN, Yang G, Ninan I, Savas, JN, Yates, JR, Lafaille JJ, Hempstead BL, Littman DR, and Gan WB. (2013). Microglia promote learning-dependent synapse formation through brain-derived neurotrophic factor. *Cell* 155(7): 1596-1609.

Peng J, Gu N, Zhou L, B Eyo U, Murugan M, Gan WB, and Wu LJ. (2016). Microglia and monocytes synergistically promote the transition from acute to chronic pain after nerve injury. *Nat Commun* 7: 12029.

Perdiguero EG, Schulz C, and Geissmann F. (2012). Development and homeostasis of "resident" myeloid cells: The case of the microglia. *Glia* 61(1): 112-120.

Piao Y, Gwon DH, Kang DW, Hwang TW, Shin N, Kwon HH, Shin HJ, Yin Y, Kim JJ, Hong J, Kim HW, Kim Y, Kim SR, Oh SH, and Kim DW. (2018). Tlr4-mediated autophagic impairment contributes to neuropathic pain in chronic constriction injury mice. *Mol Brain* 11:11.

Polgár E, Hughes DI, Arham AZ, and Todd AJ. (2005). Loss of neurons from laminas I-III of the spinal dorsal horn is not required for development of tactile allodynia in the spared nerve injury model of neuropathic pain. *J Neurosci* 25(28): 6658-6666.

Ponomarev ED, Veremeyko T, Barteneva N, Krichevsky AM, and Weiner HL. (2011). MicroRNA-124 promotes microglia quiescence and suppresses EAE by deactivating macrophages via the C-EBP-α-PU.1 pathway. *Nat Med* 17(1): 64-70.

Re DB, Le Verche V, Yu C, Amoroso MW, Politi KA, Phani S, Ikiz B, Hoffmann L, Koolen M, Nagata T, Papadimitriou D, Nagy P, Mitsumoto H, Kariya S, Wichterle H, Henderson CE, and Przedborski S. (2014) Necroptosis drives motor neuron death in models of both sporadic and familial ALS. *Neuron* 81(5): 1001-1008.

Ren M, Guo Y, Wei X, Yan S, Qin Y, Zhang X, Jiang F, and Lou H. (2018). Trem2 overexpression attenuates neuroinflammation and protects dopaminergic neurons in experimental models of Parkinson's disease. *Exp Neurol* 302: 205-213.

Rice RA, Spangenberg EE, Yamate-Morgan H, Lee RJ, Arora RP, Hernandez MX, Tenner AJ, West BL, and Green KN. (2015). Elimination of microglia improves functional outcomes following extensive neuronal loss in the hippocampus. *J Neurosci* 35(27): 9977-89.

Rivera C, Li H, Thomas-Crusells J, Lahtinen H, Viitanen T, Nanobashvili A, Kokaia Z, Airaksinen MS, Voipio J, Kaila K, and Saarma M. (2002). BDNF-induced TrkB activation down-regulates the K+-Cl- cotransporter KCC2 and impairs neuronal Cl- extrusion. *J Cell Biol* 159(5): 747-52.

Saederup N, Cardona AE, Croft K, Mizutani M, Cotleur AC, Tsou CL, Ransohoff RM, and Charo IF. (2010). Selective chemokine receptor usage by central nervous system myeloid cells in Ccr2-red fluorescent protein knock-in mice. *PLoS One* 12(4): e0176931.

Satoh J, Asahina N, Kitano S, and Kino Y. (2014). A comprehensive profile of ChIP-seq-based PU.1/Spi1 target genes in microglia. *Gene Regul Syst Bio* 8: 127-39.

Schäfers M, Lee DH, Brors D, Yaksh TL, and Sorkin LS. (2003). Increased sensitivity of injured and adjacent uninjured rat primary sensory neurons to exogenous tumor necrosis factor-alpha after spinal nerve ligation. *J Neurosci* 23(7): 3028-38.

Scholz J and Woolf CJ. (2007). The neuropathic pain triad: neurons, immune cells and glia. *Nature Neurosci* 10: 1361-1368.

Scholz J, Broom DC, Youn DH, Mills CD, Kohno T, Suter MR, Moore KA, Decosterd I, Coggeshall RE, and Woolf CJ. (2005). Blocking caspase activity prevents transsynaptic neuronal apoptosis and the loss of inhibition in lamina II of the dorsal horn after peripheral nerve injury. *J Neurosci* 25(32): 7317-23.

Schindelin J, Rueden CT, Hiner MC, and Eliceiri KW. (2015). The ImageJ ecosystem: An open platform for biomedical image analysis. *Mol Reprod Dev* 82(7-8): 518-29.

Smith AM, Gibbons HM, Oldfield RL, Bergin PM, Mee EW, Curtis MA, Faull RLM, and Dragunow M. (2013). M-CSF increases proliferation and phagocytosis while modulating receptor and transcription factor expression in adult human microglia. *J Neuroinflammation* 10: 859.

Sorge RE, LaCroix-Fralish ML, Tuttle AH, Sotocinal SG, Austin JS, Ritchie J, Chanda ML, Graham AC, Topham L, Beggs S, Salter MW, and Mogil JS. (2011). Spinal cord toll-like receptor 4 mediates inflammatory and neuropathic hypersensitivity in male but not female mice. *J Neurosci* 31(43): 15450-15454.

Staniland AA, Clark AK, Wodarski R, Sasso O, Maione F, D'Acquisto F, and Malcangio M. (2010). Reduced inflammatory and neuropathic pain and decreased spinal microglial response in fractalkine receptor (Cx3cr1) knockout mice. *J Neurochem* 114(4): 1143-57.

Stirling DP and Yong VW. (2008). Dynamics of the inflammatory response after murine spinal cord injury revealed by flow cytometry. *J Neurosci Res* 86(9): 1944-58.

Stokes JA, Cheung J, Eddinger K, Corr M, and Yaksh TL. (2013). Toll-like receptor signaling adapter proteins govern spread of neuropathic pain and recovery following nerve injury in male mice. *J Neuroinflammation* 10: 148.

Stubhaug A, Breivik H, Eide PK, Kreunen M, and Foss A. (1997). Mapping of punctuate hyperalgesia around a surgical incision demonstrates that ketamine is a powerful suppressor of central sensitization to pain following surgery. *Acta Anaesthesiol Scand* 41(9): 1124-32.

Suter MR, Berta T, Gao YJ, Decosterd I, and Ji RR. (2009). Large A-fiber activity is required for microglial proliferation and p38 MAPK activation in the spinal cord: different effects of resiniferatoxin and bupivacaine on spinal microglial changes after spared nerve injury. *Mol Pain 5*: 53.

Takahashi K, Rochford CDP, and Neumann H. (2005). Clearance of apoptotic neurons without inflammation by microglial triggering receptor expressed on myeloid cells-2. *J Exp Med* 201(4): 647.

Tang Z, Gan Y, Liu Q, Yin JX, Liu Q, Shi J, and Shi FD. (2014). Cx3cr1 deficiency suppresses activation and neurotoxicity of microglia/macrophage in experimental ischemic stroke. *J Neuroinflammation* 11:26.

Tsuda M, Shigemoto-Mogami Y, Koizumi S, Mizokoshi A, Kohsaka S, Salter MW, and Inoue K. (2003). P2x4 receptors induced in spinal microglia gate tactile allodynia after nerve injury. *Nature* 424: 778-783.

Tsuda M, Inoue K, and Salter MW. (2005). Neuropathic pain and spinal microglia: a big problem from molecules in "small" glia. *Trends Neurosci* 28(2): 101-7.

Turnbull IR and Colonna M. (2007). Activating and inhibitory functions of Dap12. *Nat Rev Immunol* 7(2): 155-61.

Turnbull IR, Gilfillan S, Cella M, Aoshi T, Miller M, Piccio L, Hernandez M, and Colonna M. (2006). Cutting edge: Trem2 attenuates macrophage activation. *J Immunol* 177(6): 3520-4.

Ulmann L, Hatcher JP, Hughes JP, Chaumont S, Green PJ, Conquet F, Buell GN, Reeve AJ, Chessell IP, and Rassendren F. (2008). Up-regulation of P2x4 receptors in spinal microglia after peripheral nerve injury mediates BDNF release and neuropathic pain. *J Neurosci* 28(44): 11263-8.

Ulrich JD, Ulland TK, Colonna M, and Holtzman DM. (2017). Elucidating the role of Trem2 in Alzheimer's Disease. *Neuron* 94(2): 237-248.

Vabulas RM, Wagner H, and Schlid H. (2002). Heat shock proteins as ligands of toll-like receptors. *Curr Top Microbiol Immuno* 270: 169-84.

van Hecke O, Austin SK, Khan RA, Smith BH, and Torrance N. (2014). Neuropathic pain in the general population: a systematic review of epidemiological studies. *Pain* 155(4): 654-62.

Vangala RK, Heiss-Neumann MS, Rangatia JS, Singh SM, Schoch C, Tenen DG, Hiddemann W, and Behre G. (2003). The myeloid master regulator transcription factor PU.1 is inactivated by AML1-ETO in t(8;21) myeloid leukemia. *Blood* 101(1): 270-7.

Wang Y, Ulland TK, Ulrich JD, Song W, Tzaferis JA, Hole JT, Yuan P, Mahan TE Shi Y, Gilfillan S, Cells M, Grutzendler J, DeMattos RB, Cirrito JR, Holtzman DM, and Colonna M. (2016). Trem2-mediated early microglial response limits diffusion and toxicity of amyloid plaques. *J Exp Med* 213(5): 667-75.

Watkins LR and Maier SF. (2003). GLIA: A novel drug discovery target for clinical pain. *Nat Rev Drug Disc* 2: 973-975.

Willemen HLDM, Huo XJ, Mao-Ying QL, Zijlstra J, Heijnen C, and Kavelaars A. (2012). MicroRNA-124 as a novel treatment for persistent hyperalgesia. *J Neuroinflammation* 9: 143.

Wolf G, Gabay E, Tal M, Yirmiya R, and Shavit Y. (2006). Genetic impairment of interleukin-1 signaling attenuates neuropathic pain, autotomy and spontaneous ectopic neuronal activity, following nerve injury in mice. *Pain* 120: 315-324.

Woolf CJ and Salter MW. (2000). Neuronal plasticity: increasing the gain in pain. *Science* 288(5472): 1765-8.

Woolf CJ, Shortland P, and Coggeshall RE. (1992). Peripheral nerve injury triggers central sprouting of myelinated afferents. *Nature* 355(6355): 75-8.

Yamamoto M, Sato S, Mori K, Hoshino K, Takeuchi O, Takeda K, and Akira S. (2002). Cutting edge: a novel Toll-IL-1 receptor domain-containing adapter that preferentially activates the IFN-beta promoter in the Toll-like receptor signaling. *J Immunol* 169(12): 6668-72.

Yamamoto M, Sato S, Hemmi H, Hoshino K, Kaisho T, Sanjo H, Takeuchi O, Sugiyama M, Okabe M, Takeda K, and Akira S. (2003). Role of adaptor TRIF in the MyD88-independent toll-like receptor signaling pathway. *Science* 301(5633): 640-3.

Yamasaki R, Lu H, Butovsky O, Ohno N, Rietsch AM, Cialic R, Wu PM, Doykan CE, Lin J, Cotleur AC Kidd G, Zorlu MM, Sun N, Hu W, Liu L, Lee JC, Taylor SE, Uehlein L, Dixon D, Gu J, Floruta CM, Zhu M, Charo IF, Weiner HL, and Ransohoff RM. (2014). Differential roles of microglia and monocytes in the inflamed central nervous system. *J Exp Med* 211(8): 1533-49.

Yang Y, Han C, Guo L, and Guan Q. (2018). High expression of the Hmgb1-Tlr4 axis and its downstream signaling factors in patients with Parkinson's disease and the relationship of pathological staging. *Brain Behav* 8(4): e00948.

Yao Y, Li H, Chen J, Xu W, Yang G, Bao Z, Xia D, Lu G, Hu S, and Zhou J. (2016). Trem-2 serves as a negative regulator through Syk pathway in an IL-10 dependent manner in lung cancer. *Oncotarget* 7(20): 29620-34.

Yao L, Ye Y, Mao H, Lu F, He X, Lu G, and Zhang S. (2018). MicroRNA-124 regulates the expression of MEKK3 in the inflammatory pathogenesis of Parkinson's disease. *J Neuroinflammation* 15(1): 13.

Yowtak J, Wang J, Kim HY, Lu Y, Chung K, and Chung JM. (2013). Effect of antioxidant treatment on spinal GABA neurons in a neuropathic pain model in the mouse. *Pain* 154(11):10.1016/j.pain.2013.07.024.

Yu M, Wang H, Ding A, Golenbock DT, Latz E, Czura CJ, Fenton MJ, Tracey KJ, and Yang H. (2006). Hmgb1 signals through toll-like receptor (Tlr) 4 and Tlr2. *Shock* 26(2): 174-9.

Yu A, Zhang T, Duan H, Pan Y, Zhang X, Yang G, Wang J, Deng Y, and Yang Z. (2017). MiR-124 contributes to M2 polarization of microglia and confers brain inflammatory protection via the C/EBP-α pathway in intracerebral hemorrhage. *Immuno Lett* 182: 1-11.

Zhai Q, Li F, Chen X, Jia J, Sun S, Zhou D, Ma L, Jiang T, Bai F, Xiong L, and Wang Q. (2017). Triggering receptor expressed on myeloid cells 2, a novel regulator of immunocyte phenotypes, confers neuroprotection by relieving neuroinflammation. *Anesthesiology* 127(1): 98-110.

Zhang J, Shi XQ, Echeverry S, Mogil JS, De Koninck Y, and Rivest S. (2007). Expression of Ccr2 in both resident and bone marrow-derived microglia plays a critical role in neuropathic pain. *J Neurosci* 27(45): 12396-406.

Zhang X, Yan F, Cui J, Wu Y, Luan H, Yin M, Zhao Z, Feng J, and Zhang J. (2017). Triggering receptor expressed on myeloid cells 2 overexpression inhibits proinflammatory cytokines in lipopolysaccharaide-stimulated microglia. *Mediators Inflamm* 2017: 9340610.

Zhao Y, Wu X, Li X, Jiang LL, Gui X, Liu Y, Sun Y, Zhu B, Piña-Crespo JC, Zhang M, Zhang N, Chen X, Bu G, An Z, Huang TY, and Xu H. (2018). Trem2 is a receptor for β-amyloid that mediates microglial function. *Neuron* 97(5): 1023-1031.e7.

Zhong L, Chen XF, Zhang ZL, Wang Z, Shi XZ, Xu K, Zhang YW, Xu H, and Bu G. (2015). Dap12 stabilizes the c-terminal fragment of the triggering receptor expressed on myeloid cells-2 (Trem2) and protects against LPS-induced pro-inflammatory response. *J Biol Chem* 290(25): 15866-77.

Zhong L, Zhang ZL, Li X, Liao C, Mou P, Wang T, Wang Z, Wang Z, Wei M, Xu H, Bu G, and Chen XF. (2017). Trem/Dap12 complex regulates inflammatory responses in microglia via the JNK signaling pathway. *Front Aging Neurosci* 9: 204.

Zhong L, Wang Z, Wang D, Wang Z, Martens YA, Wu L, Xu Y, Wang K, Li J, Huang R, Can D, Xu H, Bu G, and Chen XF. (2018). Amyloid-beta modulates microglial responses by binding to the triggering receptor expressed on myeloid cells 2 (Trem2). *Mol Neurodegener* 13(1): 15.